NAVAL POSTGRADUATE SCHOOL
Monterey, California

THESIS

ANALYSIS OF A SEMI-TAILLESS AIRCRAFT DESIGN

by

Kurt W. Muller

March 2002

Thesis Advisor:	Conrad F. Newberry
Second Reader:	Richard M. Howard

Approved for public release; distribution is unlimited

THIS PAGE INTENTIONALLY LEFT BLANK

REPORT DOCUMENTATION PAGE			Form Approved OMB No. 0704-0188
Public reporting burden for this collection of information is estimated to average 1 hour per response, including the time for reviewing instruction, searching existing data sources, gathering and maintaining the data needed, and completing and reviewing the collection of information. Send comments regarding this burden estimate or any other aspect of this collection of information, including suggestions for reducing this burden, to Washington headquarters Services, Directorate for Information Operations and Reports, 1215 Jefferson Davis Highway, Suite 1204, Arlington, VA 22202-4302, and to the Office of Management and Budget, Paperwork Reduction Project (0704-0188) Washington DC 20503.			
1. AGENCY USE ONLY *(Leave blank)*	**2. REPORT DATE** March 2002	**3. REPORT TYPE AND DATES COVERED** Master's Thesis	
4. TITLE AND SUBTITLE: Title (Mix case letters) Analysis of a Semi-Tailles Aircraft Design			**5. FUNDING NUMBERS**
6. AUTHOR(S) LT Kurt Muller			
7. PERFORMING ORGANIZATION NAME(S) AND ADDRESS(ES) Naval Postgraduate School Monterey, CA 93943-5000			**8. PERFORMING ORGANIZATION REPORT NUMBER**
9. SPONSORING / MONITORING AGENCY NAME(S) AND ADDRESS(ES) N/A			**10. SPONSORING / MONITORING AGENCY REPORT NUMBER**
11. SUPPLEMENTARY NOTES The views expressed in this thesis are those of the author and do not reflect the official policy or position of the Department of Defense or the U.S. Government.			
12a. DISTRIBUTION / AVAILABILITY STATEMENT Approved for public release; distribution is unlimited			**12b. DISTRIBUTION CODE**

13. ABSTRACT ***(maximum 200 words)***

Many unique aircraft configurations came out of Germany in World War II, one of these was the Blohm and Voss BV P 208. By using longitudinal and directional control surfaces located outboard of the wing tips they are removed from the downwash of the main wing. Additionally, the result is fewer component surfaces with less total surface area, thereby reducing both friction and interference drag and manufacturing cost.

The configuration should lend itself well to low-observability, making it a good stealth candidate.

The P 208, provided the author an opportunity to analyze an unconventional configuration with the conceptual NASA design codes RAM, VORVIEW, and ACSYNT. A lack of wind tunnel or flight data prevented the evaluation of the performance of these codes for this configuration. However, results are presented for future comparison and evaluation.

Claims of aerodynamic benefits of the P 208 configuration appear largely to be verified. The P 208 suffers from poor natural short-period longitudinal stability and an unstable Dutch-roll, neither of which are beyond the means of artificial control. The most immediate need for future work is a structural analysis and determination as to the structural and dynamic feasibility of the configuration.

14. SUBJECT TERMS Semi-tailless, P 208, RAM, VORVIEW, ACSYNT			**15. NUMBER OF PAGES** 108
			16. PRICE CODE
17. SECURITY CLASSIFICATION OF REPORT Unclassified	**18. SECURITY CLASSIFICATION OF THIS PAGE** Unclassified	**19. SECURITY CLASSIFICATION OF ABSTRACT** Unclassified	**20. LIMITATION OF ABSTRACT** UL

NSN 7540-01-280-5500 Standard Form 298 (Rev. 2-89)
Prescribed by ANSI Std. 239-18

THIS PAGE INTENTIONALLY LEFT BLANK

Approved for public release; distribution is unlimited

ANALYSIS OF A SEMI-TAILLESS AIRCRAFT DESIGN

Kurt W. Muller
Lieutenant, United States Navy
B.S., U.S. Naval Academy, 1993

Submitted in partial fulfillment of the
requirements for the degree of

MASTER OF SCIENCE IN AERONAUTICAL ENGINEERING

from the

NAVAL POSTGRADUATE SCHOOL
March 2002

Author: Kurt W. Muller

Approved by: Conrad F. Newberry, Thesis Advisor

Richard Howard, Second Reader

Max Platzer, Chairman
Department of Aeronautics and Astronautics

THIS PAGE INTENTIONALLY LEFT BLANK

ABSTRACT

Many unique aircraft configurations came out of Germany in World War II, one of these was the Blohm and Voss BV P 208. By using longitudinal and directional control surfaces located outboard of the wing tips they are removed from the downwash of the main wing. Additionally, the result is fewer component surfaces with less total surface area, thereby reducing both friction and interference drag and manufacturing cost.

The configuration should lend itself well to low-observability, making it a good stealth candidate.

The P 208 provided the author an opportunity to analyze an unconventional configuration with the conceptual NASA design codes RAM, VORVIEW, and ACSYNT. A lack of wind tunnel or flight data prevented the evaluation of the performance of these codes for this configuration. However, results are presented for future comparison and evaluation.

Claims of aerodynamic benefits of the P 208 configuration appear largely to be verified. The P 208 suffers from poor natural short-period longitudinal stability and an unstable Dutch-roll, neither of which are beyond the means of artificial control. The most immediate need for future work is a structural analysis and determination as to the structural and dynamic feasibility of the configuration.

THIS PAGE INTENTIONALLY LEFT BLANK

TABLE OF CONTENTS

THIS PAGE INTENTIONALLY LEFT BLANK

LIST OF FIGURES

THIS PAGE INTENTIONALLY LEFT BLANK

LIST OF TABLES

THIS PAGE INTENTIONALLY LEFT BLANK

LIST OF SYMBOLS AND ABBREVIATIONS

a, AOA	Angle of Attack
ß	Sideslip
d	Control deflection, subscript ‘e’ for elevator and ‘a’ for aileron
e	downwash angle (positive downwards)
?	Damping ratio
?	Pitch angle
?	Roots of quadratic equation (characteristic equation)
f	Roll angle
$?_n$	Natural frequency
AR	Aspect Ratio; b^2/S
AC	Aerodynamic Center
b	Wing span
c	Chord
C_D	Coefficient of drag
C_{Di}	Coefficient of induced drag
C_{Do}	Zero lift coefficient of drag
C_l	2-D wing coefficient of lift
C_L	Coefficient of lift for the aircraft
C_{LW}	3-D wing coefficient of lift
C_M	Coefficient of pitching moment
C_{Ht}	Horizontal tail volume coefficient
C_{Vt}	Vertical tail volume coefficient

D	Drag
e	Oswald span efficiency
h	Altitude
I_{XX}	Moment of inertia with respect to the X axis
I_{YY}	Moment of inertia with respect to the Y axis
I_{ZZ}	Moment of inertia with respect to the Z axis
I_{XZ}	Product of inertia with respect to the X and Z axes
L	Lift
M	Mach number
p	Roll rate
q	Pitch rate
r	Yaw rate
Re	Reynolds number
S	Wing area
u	Perturbation velocity
U,V	Freestream velocity
Y	y/(b/2); where y = displacement from mid-span

ACKNOWLEDGMENTS

Even if written by a single author every thesis is a team effort. I would like to acknowledge and thank the team that made this effort possible. First I must thank Andy Hahn of the NASA Ames Research Center, his willingness to help and patience made the use of the NASA computer codes possible. I must, of course, thank my thesis advisor, Professor Newberry for filling that critical role. I would like to thank Professor Howard for being a consistent datum. His knowledge of aircraft design and stability and control was continually helpful. My greatest appreciation goes to my wife, Amy, and my children, Katrina and Alex, whose sacrifice and support was steady and unyielding.

"The fear of the LORD is the beginning
of wisdom;
all who follow his precepts have good understanding.
To him belongs eternal praise.
Psalm 111:10

THIS PAGE INTENTIONALLY LEFT BLANK

I. INTRODUCTION

A. BACKGROUND

Tremendous innovation permeated the German aircraft industry throughout World War II. Some of these innovations actually flew, e.g. the ME 262, ME 163, V-1 and V-2; however, many more never left the drawing board. Attracted by the advantages offered by a tailless design, Dr. Vogt and George Haag of the Blohm and Voss design bureau, spent over two years researching the concept which resulted in a unique semitailless configuration. Flight tests in the summer of 1944 on a modified Skoda SL-6 went well enough for the incorporation of the concept into future designs. [Ref. 1] The design, utilizing an outboard placement of the lateral-directional controls, was the central configuration theme in a series of Blohm and Voss's proposed fighter/ interceptors,

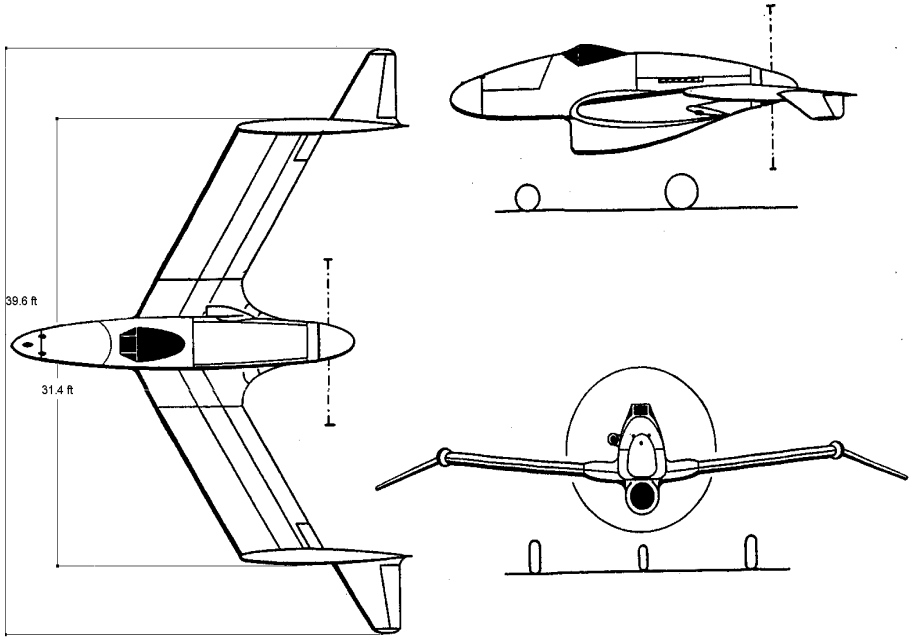

Figure 1. BV P 208.03 3-View [After: Ref. 2]

namely the P 208 (three versions), thru the P 215. [Ref. 3] In theory, the configuration has the advantage of removing the empennage from the region behind the main wing consisting of downwash and a velocity deficit due to skin friction. Rather, the empennage is in the upwash region of the wing-tip vortex with a corresponding dynamic

pressure of at least freestream magnitude. [Ref. 4] This theoretical advantage presents the option of having a smaller or a more effective stability and control surface.

B. PURPOSE OF THE STUDY

This unique semi-tailless configuration appears to have aerodynamic advantages over traditional configurations, including reduced parasite and induced drag, and simplifies production efforts and reduces cost with fewer surfaces. [Ref. 2] Additionally, though not investigated herein, the configuration appears to suit itself well to low observability, both visual and radar. These apparent advantages make the configuration suited for consideration in the burgeoning unmanned aerial vehicle (UAV) and combat UAV (UCAV) market. As such, it was considered desirable to further assess the concept's suitability.

As materials and robust controllers make many unconventional aircraft configurations more feasible than when they were first conceived, the need for quick, inexpensive and accurate analysis of such configurations at the conceptual level increases. It was the primary purpose of this study to establish a level of confidence in the ability of the NASA code, VORVIEW, to analyze an unconventional design. The original means of evaluation was to be against experimental data from wind tunnel test. In the absence of a wind tunnel model, the purpose became to develop an analytical "plant" or baseline of the P 208 aircraft. Such a baseline configuration would permit the future evaluation of VORVIEW, via wind tunnel data or higher order computer codes with which configuration changes and trade studies can be compared.

Additionally, it was desired to gain in-house experience with ACSYNT to permit its usage in NPS design classes. A discussion of the computer programs used for analysis follows.

C. NASA DESIGN CODES

Rapid Aircraft Modeler (RAM) and VORVIEW are aircraft conceptual design codes developed by the NASA Ames Research Center. These codes have been extensively used at the Naval Postgraduate School (NPS) in aircraft design classes. Both

codes are FORTRAN based and are run via graphical user interfaces (GUIs) on Silicon Graphics® machines with Unix operating systems. RAM 2.0 dated November 1998 was used herein. RAM is a geometry code that allows for quick development and manipulation of an aircraft's shape. An example of the RAM GUI is seen in Figure 2 with an "exploded" view of the P 208 model showing its components. RAM provides wetted surface area and volume data. It has an internal vortex-lattice code, which is less sophisticated than VORVIEW and therefore remains largely unused.

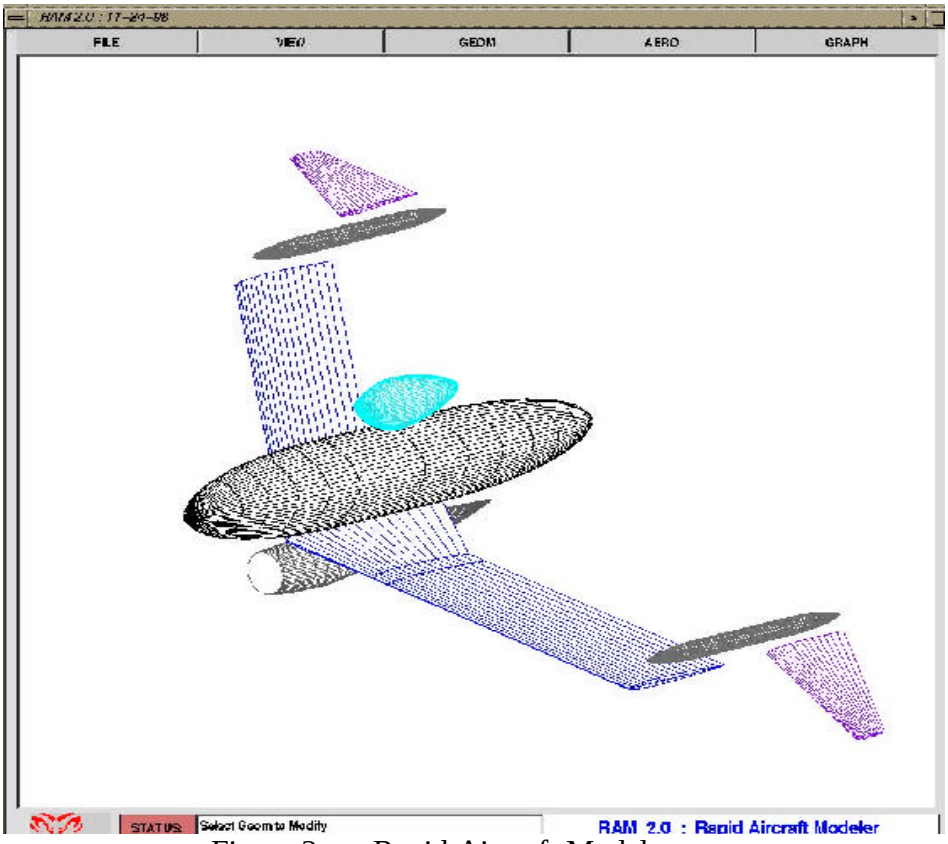

Figure 2. Rapid Aircraft Modeler

VORVIEW is an extensively modified form of Vorlax, a generalized vortex lattice (VL) program written by L.R. Miranda, R.D. Elliott and W.M. Baker of the Lockheed Corporation. [Ref. 4] Geometry inputs from RAM are modeled in VORVIEW as a series of "slices" with camber information used for boundary conditions. In VORVIEW a Trefftz-plane calculation for lift and induced drag was added as a check to the pressure integration values. Because Trefftz-plane analysis can't generate a moment

value, no comparison is possible for this value. [Ref. 5] Pressure integration values were used throughout this analysis. VORVIEW version 1.7.4, dated June 1999, was used herein. In addition to providing values for lift, induced drag and pitching moment, this version of VORVIEW will generate longitudinal and lateral/directional stability derivatives, control derivatives, and hinge moments. VORVIEW will also determine control deflection for trimmed conditions, aerodynamic center, and friction drag via the strip method. A further explanation of the strip method is found in Chapter II. Figure 3 shows the VORVIEW GUI. The box in the upper-right hand corner of the GUI shows some of the reference parameters of the particular run. This information is followed by the pressure integration calculation results, then the Trefftz-plane results, the strip method results and the number of iterations required to complete the computations. Evident in Figure 3 are the length-wise "slices" of the aircraft, created during the VORVIEW analysis.

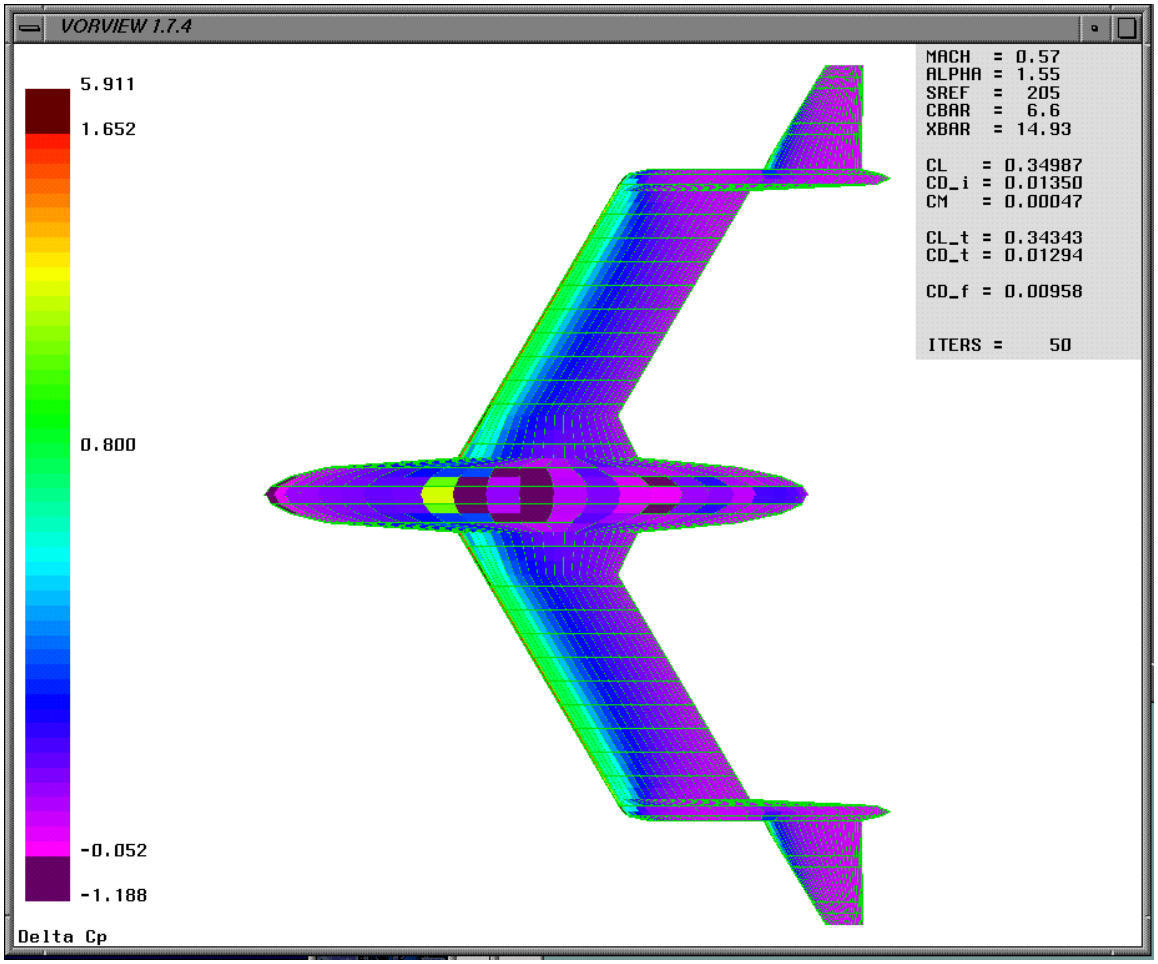

Figure 3. VORVIEW Example

Aircraft Synthesis (ACSYNT), also developed at NASA Ames, is a conceptual design code that can perform aerodynamic and performance analysis on an aircraft configuration based on semi-empirical equations. Three analysis method types are available: simple analysis, sensitivity and optimization. The simple analysis method will analyze the design and output the performance details. The sensitivity method is useful for examining the effect one variable has on another. The optimization method will minimize or maximize a variable subject to constraints placed on the configuration by the designer. [Ref. 6] A simple analysis was made on the P 208. ACSYNT enables one to perform quick trade studies and therefore has tremendous potential use in the conceptual design stage of an aircraft

.

D. CONFIGURATION THEORY

Recently (1991-2001), extensive work has been done by John Kentfield of the University of Calgary on what he calls the outboard-horizontal-stabilizer (OHS) configuration, an example of which is seen in Figure 4. The OHS configuration differs from the P 208 configuration in that the main wing is unswept and the empennage is moved aft on wingtip-mounted booms of two to four chord lengths. Kentfield's configuration also utilizes vertical stabilizers. Though results obtained for the OHS configuration cannot be directly compared with the P 208 configuration, the theories presented would appear largely to apply as the dynamics are similar. Given that no alternate existing term more adequately describes the P 208's configuration, the OHS label will be applied to it. Kentfield states that OHS configurations should employ the tail as a lifting surface, thereby providing the advantage of a canard configuration. In fact, the OHS configuration does not have the canard's disadvantage of requiring the canard to stall first, thereby reducing the maximum lift capability of the main wing. Kentfield also suggests that the induced drag of tail lift is somewhat offset by a forward inclined lift

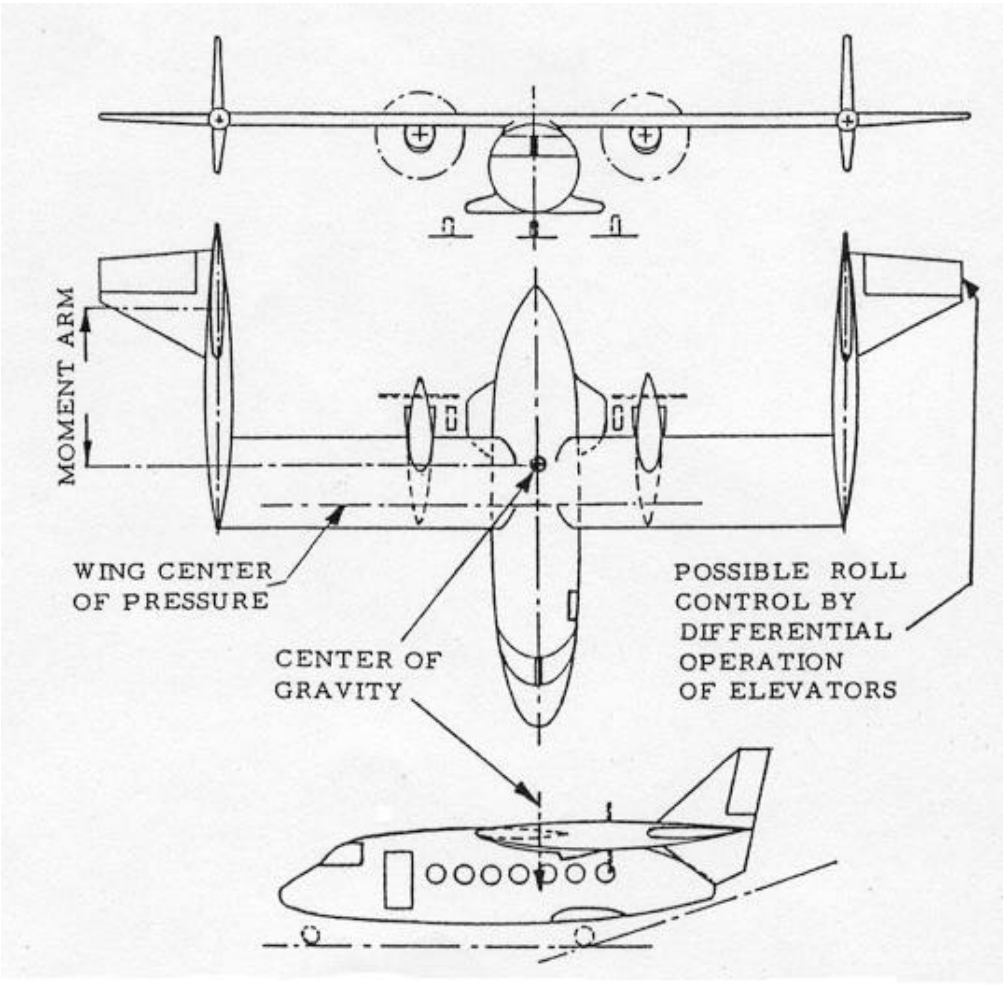

Figure 4. Outboard Horizontal Stabilizer Configuration [From: Ref. 7]

vector due to upwash at the tail. [Ref. 8] What appears to be a configuration lacking in roll performance, due to high moments of inertia, would be somewhat aided, Kentfield theorizes, by the flow field alteration caused by aileron deflection. An increase in lift on one side with a corresponding decrease on the other would create a beneficial change in the upwash flow field at the tail. [Ref. 9]

The outboard tail has the implication of greater pitch stability compared to a conventional configuration. Given a nose up perturbation, both the wing and tail see an increase in AOA. The tail's lift is further increased due to an increased effective angle-of-attack due to the increased upwash angle provided by the wing's lift increase. The preceding argument is born out in the conventional pitching moment relationship, Eq. 1 [Ref. 9]:

$$\frac{dC_m}{da} = -C_1\left(1 - \frac{de}{da}\right) \tag{1}$$

where C_1 is a positive constant. A conventional configuration will generally have a positive value for de/da, due to the immersion of the tail in downwash of the main wing. An outboard tail configuration will typically have a negative de/da value. Figure 5 shows, for varying wing lift coefficients (C_{LW}), upwash flow angles, e_U, vs. displacement

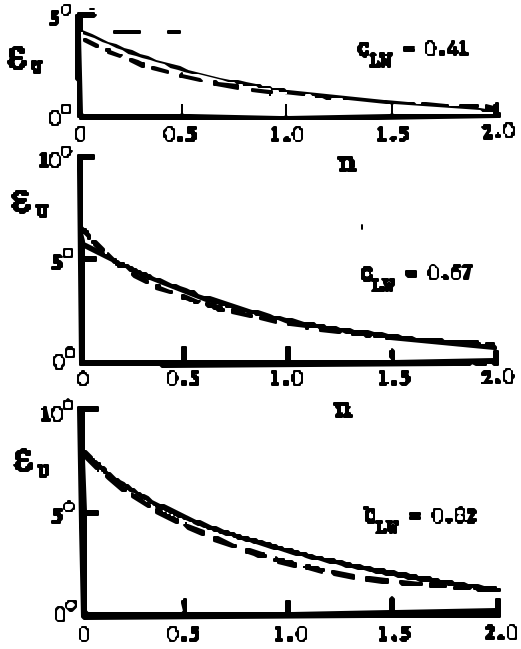

Figure 5. Upwash Flow Angle Over Horizontal Stablizer [From: Ref. 10]

outboard of the wing tip as multiples, n, of the chord of a rectangular planform wing. An analytical potential flow model of a wing tip vortex far downstream of an aircraft, specifically Eq. 2, [Ref 10]:

$$\frac{w}{U} = \frac{C_{LW}}{AR_W}\frac{4}{p^2}\left\{\frac{1}{1-\left[\left(4/p\right)Y\right]^2}\right\} \tag{2}$$

was empirically modified to arrive at Eq. 3 below. Equation 3 describes, in degrees, the upwash flow in the region from two to four chord lengths downstream of the wing tip.

[Ref. 10] This equation was used to generate the dotted line in Figure 5. For a complete discussion of assumptions incorporated the reader is directed to reference 10.

$$e_U = \left\{ \frac{3.871}{\left[\left(4/\Lambda \right) \left(1.0333 - n/3 \right) \right]^2 - 1} \right\} \left(1.7667 - \frac{n}{3} \right) \qquad (3)$$

Kentfield completed direct comparison studies between conventional and OHS configurations and arrived at the conclusion that an OHS configuration can generate the same value of C_{LW} as a conventional configuration, with a 15% smaller wing planform area, largely due to a lifting tail. Additionally, when comparing maximum L/D values, the OHS configuration's planform area is an additional 30% smaller than the conventional configuration. Kentfield also noted that the outboard tailplanes experience an effective washout due to the decreasing upwash moving outboard of the wingtip as noted in Figure 5 above.[Ref. 10] It was also determined that increased elevator effectiveness, due to upwash, resulted in elevator deflections required for level flight of approximately one-half those required for a conventional aircraft over the lift coefficient range, $0.2 \leq C_L \leq 1.2$ [Ref. 9]

Scaled Composites, Incorporated built, for NASA, an 18% scale model of a high altitude research aircraft, the Alliance 1, utilizing the OHS concept, Figure 6. A

Figure 6. Alliance I

VORVIEW analysis was performed on this aircraft by Andrew Hahn, of the NASA Ames Research Center. [Ref 5] Vortex lattice analysis will yield a known vortex position. This is an artificial characteristic, but it is sometimes useful. By moving the location of the tails, it was found that the Alliance 1 configuration was very sensitive to the placement of these surfaces with respect to the core of the wing tip vortex. The study showed that if the tails were off by 3.5 degrees (a one foot "miss" in the study cited) from the wingtip vortex core that the span efficiency dropped by 18%. Such a "miss" of the vortex core could likely result from the typical movement of the vortex, inboard and down as it moves aft.

Also stated in reference 5 was the assertion that for the Blohm and Voss design, with the leading edge of the horizontal tail at the trailing edge of the wing, "…the coring out of the tip vortex was virtually assured" meaning that no such miss of the vortex by the horizontal tail will occur.[Ref. 5]

Blohm and Voss anticipated the following benefits from their OHS configuration, [Refs. 3 and 11]:

- The simplest pusher engine arrangement without the need for a propellor extension shaft, i.e. lightweight, cheap, easy to maintain and reliable.
- Minimum total surface area, combining a short fuselage with small wings and control surfaces, to permit the highest possible maximum speed.
- Lowest overall weight, contingent upon a lighter engine installation, small wings and short fuselage.
- Simplest production, due to constant chord wing and deletion of fin and rudder; load bearing fuselage structure unbroken by integral engine compartment.
- Limited proportion of Duraluminum to overall weight by extensive use of sheet metal in easily manufactured thicknesses.

The previous list is quite interesting for a couple of reasons. First, it is interesting to note the preoccupation with ease of production and limited use of strategic materials which is a commentary on the state of Germany in 1944. Secondly, and more interesting, however, is the absence of any mention of the potential aerodynamic benefits of the design aside from minimized form drag. This apparent oversight could be explained by a couple of situations: 1) Blohm and Voss didn't recognize the aerodynamic benefits,

which seems unlikely, or (2) Blohm and Voss didn't think that the above mentioned aerodynamic benefits existed. These possibilities seem unlikely since the P 208 is quite a drastic departure from convention to obtain the benefits listed above. A third possibility might be that the original reference from which the above list of benefits was taken may have been part of a proposal to an audience that cared nothing for aerodynamics but was concerned only about production.

II. P 208 COMPUTER MODEL DEVELOPMENT

A. P 208 MODEL DEVELOPMENT

1. Basic P 208 Parameters

Computer model results are, obviously, only as good as the initial data. Gathering sufficient data to build an accurate model of a German, World War II era, non-production aircraft presented obvious challenges. A limited amount of original data was available

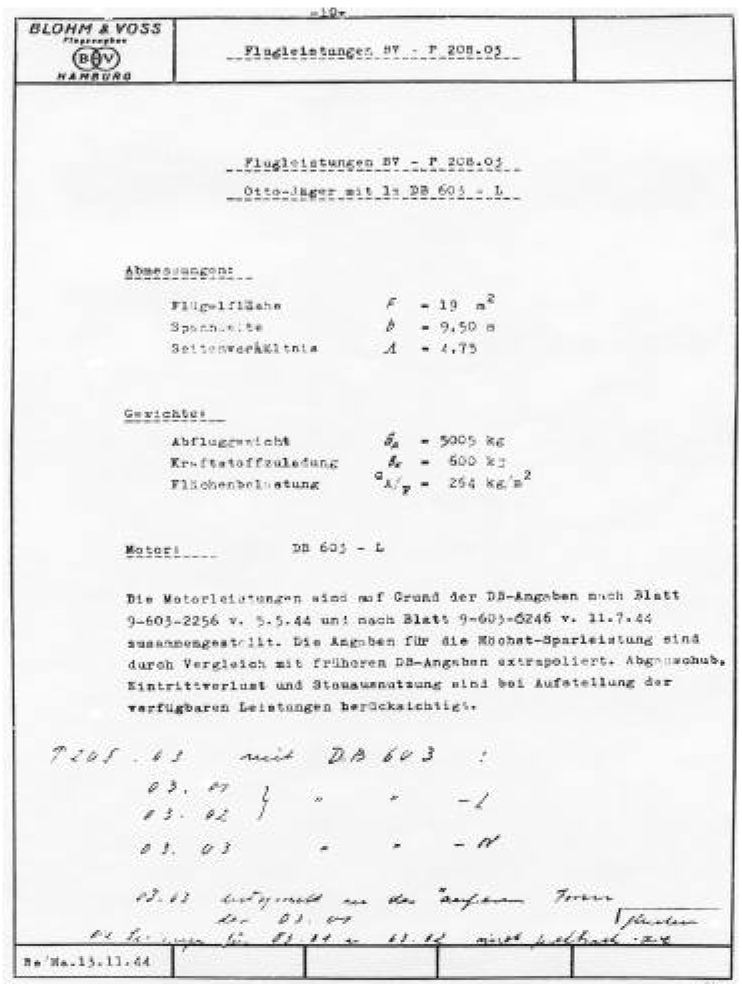

-19-

BLOHM & VOSS
HAMBURG

Flugleistungen BV - P 208.03

Flugleistungen BV - P 208.03
Otto-Jäger mit 1x DB 603 - L

Abmessungen:

Flügelfläche	F	= 19 m^2
Spannweite	b	= 9,50 m
Seitenverhältnis	Λ	= 4,75

Gewichte:

Abfluggewicht	G_a	= 5005 kg
Kraftstoffzuladung	G_K	= 600 kg
Flächenbelastung	$G_{A/F}$	= 264 kg/m^2

Motor: DB 603 - L

Die Motorleistungen sind auf Grund der DB-Angaben nach Blatt 9-603-2256 v. 5.5.44 und nach Blatt 9-603-6246 v. 11.7.44 zusammengestellt. Die Angaben für die Höchst-Sparleistung sind durch Vergleich mit früheren DB-Angaben extrapoliert. Abgasschub, Eintrittverlust und Stauausnutzung sind bei Aufstellung der verfügbaren Leistungen berücksichtigt.

P 208.03 mit DB 603 :
03.01 } " " - L
03.02 }
03.03 " " - N

Re/Ma.13.11.44

Figure 7. Example of Primary Blohm and Voss Data [From: Ref. 12]

through the Captured German and Japanese Air Technical Documents holdings of the National Air and Space Museum Archives Division, [Refs 3 and 12], and through a 1976 German periodical, "Luftfahrt International", reference 11. Three versions of the P 208 were considered by Blohm and Voss, only the third version with the Daimler-Benz DB

603-L engine, the BV P 208.03 is considered in this thesis and, for brevity, will be referred to as the P 208. One reason the third version was selected was because previous work had been completed on it at the University of Oklahoma, reference 4. Basic dimensions were available from primary documents, of which Figure 7 is an example. References 11 and 12 were used to compile a table of basic data, Table 1. All reference numbers used with respect to the wing are minus the tails. The 3-view of the P 208, shown in Figure 1, was scaled using the known data in Table 1 and used to generate data

Table 1. Technical Data

Geometry		Performance	
Wing Area	19.0 m^2	Wing Loading (GW)	264 kg/m^2
Span	9.58 m	Power Loading (GW)	2.4 kg/PS
Aspect Ratio	4.75	Takeoff Power	2100 PS
Span w/tails	12.08 m	Climb Power	1800 PS
Length	9.2 m	Max Continuous Pwr	1500 PS
Height	3.46 m	Reduction Gear	1:1.93
Prop Diameter	3.4 m	Time to Max Altitude	27 min
Wing Surface Area	34.4 m^2	Takeoff Distance	360 m
Fuselage Area	25.0 m^2	Flight Distance (h = 0 km)	1040 km
Tail Boom Area	2 x 2.5 m^2	Flight Distance (h = 9 km)	1230 km
Tail Surface Area	6.5 m^2	Flight Duration (h = 0 km)	1.79 h
Wing .25c sweep	30^o	Flight Duration (h = 9 km)	1.85 h

*note, 1 PS = 0.986 HP

for use in the NASA computer codes. This data consisted primarily of body diameters, fineness ratios, control moment arms and locations for reference points. Because no anticipated changes to the design were anticipated, all longitudinal measurements were taken from a zero station defined at the nose of the aircraft. Lateral measurements were taken from the center line of the fuselage. The degree of accuracy of Figure 1 is unknown and therefore some uncertainty is introduced in numbers derived from it. The mean aerodynamic chord (mac) was easily enough determined since the wing is a constant chord of 2 meters (6.56 ft); the mac was then located at the geometric center of the wing, i.e., b/4. The only data available on the airfoil was that it was 12½ % thick. [Ref. 11] It is highly likely that the particular airfoil used was a Blohm and Voss

proprietary airfoil. A NACA 23012 airfoil was chosen for analysis since it is representative of the technology of the times and has good performance. No wing twist was used and an angle of incidence of two degrees was taken from reference 4. For the tail surfaces a NACA 0010 at minus three and a half degrees of incidence was used in accordance with reference 4. RAM has the capability to accept an airfoil coordinate file and apply it to the geometry of the aircraft under consideration. Lacking any information on location of the center of gravity (CG) of the aircraft, an estimate was made using the tip-back angle. Raymer states that the most aft CG location should be forward of a line that is defined by a 15 degree angle forward of a vertical line at the point where the main gear touch the ground. [Ref. 13] Using this methodology the P 208's CG was placed at

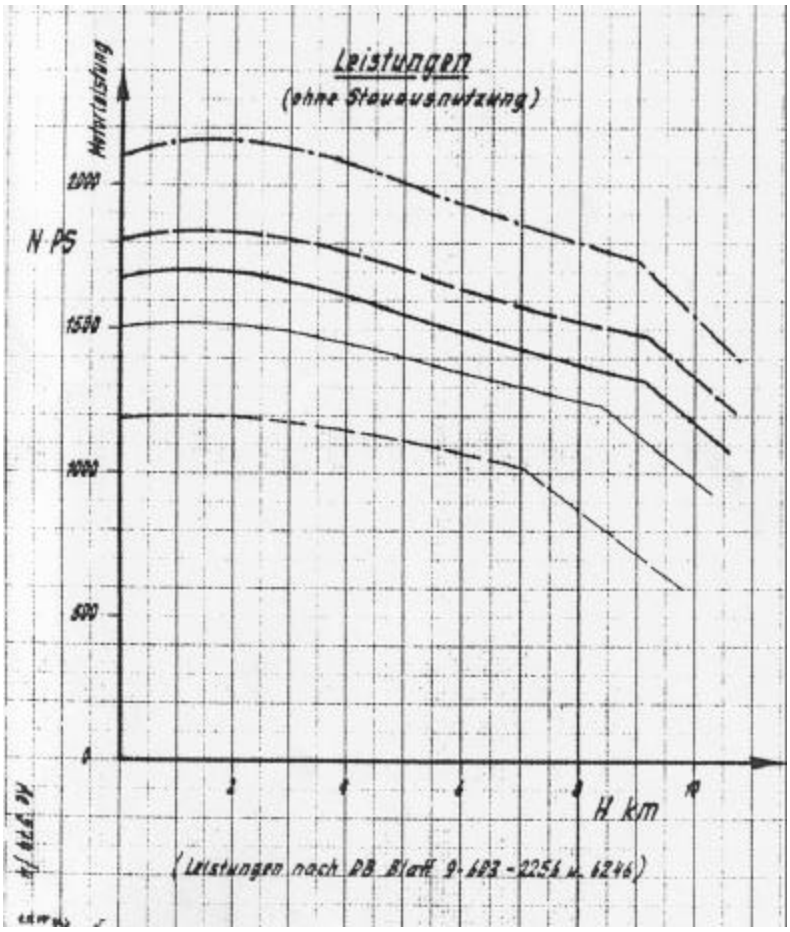

Figure 8. Engine Power vs. Altitude [From: Ref. 12]

32% mac. VORVIEW calculated the aerodynamic center (AC) of the aircraft to be at 50% mac. Sufficient engine data was available from Table 1 and Figure 8 to model the power plant in ACSYNT. Moments of inertia were estimated using the weight values

given in the table in Appendix A and approximating their point mass location. These estimates were within 10% of those given in reference 4 and so the values of reference 4 were used as shown in Table 2.

Table 2. Moments of Inertia (slug ft^2)

I_{XX} = 18,143	I_{YY} = 12,370
I_{ZZ} = 28,474	I_{XZ} = 200

Determining a configuration's zero lift drag coefficient (C_{Do}) is a significant task since it is a major factor in determining the aircraft's performance. Primary data on a C_{Do} build-up was available as shown in Figure 9, and resulted in a C_{Do} equal to 0.0201. Reference 4 also performed a component build-up for C_{Do} determination resulting in a

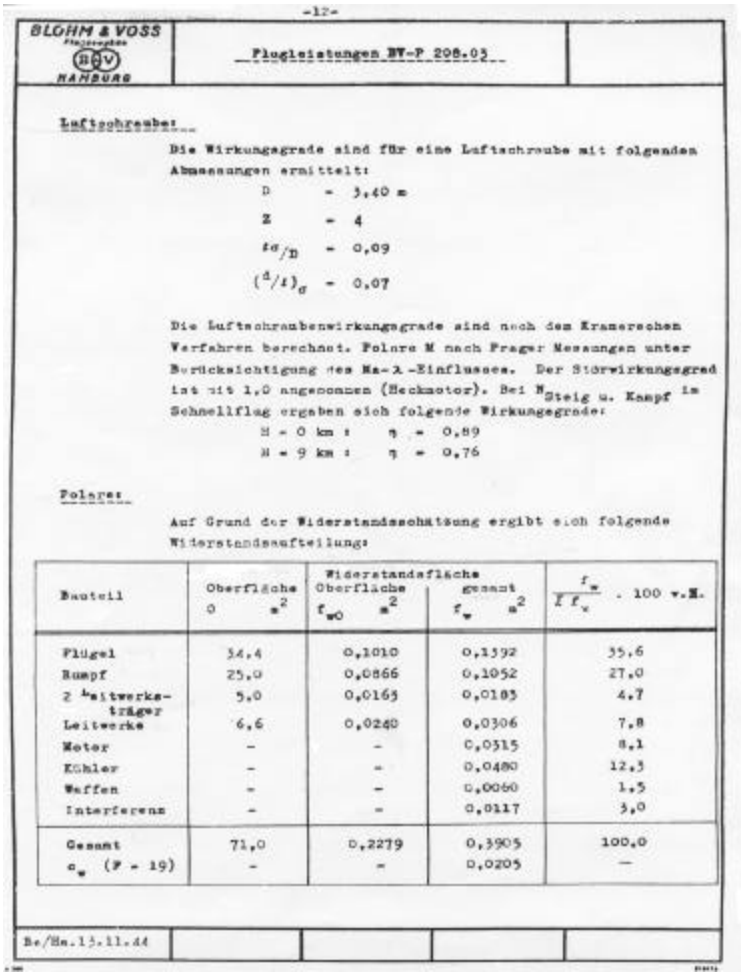

-12-

BLOHM & VOSS HAMBURG

Flugleistungen BV-P 208.03

Luftschrauben:

Die Wirkungsgrade sind für eine Luftschraube mit folgenden Abmessungen ermittelt:

D = 3,40 m

Z = 4

$f\sigma/D$ = 0,09

$(d/t)_\sigma$ = 0,07

Die Luftschraubenwirkungsgrade sind nach dem Kramerschen Verfahren berechnet. Polare M nach Prager Messungen unter Berücksichtigung des Ma-λ-Einflusses. Der Störwirkungsgrad ist mit 1,0 angenommen (Heckmotor). Bei N_{Steig} u. N_{Kampf} im Schnellflug ergaben sich folgende Wirkungsgrade:

H = 0 km : η = 0,89

H = 9 km : η = 0,76

Polare:

Auf Grund der Widerstandsschätzung ergibt sich folgende Widerstandsaufteilung:

Bauteil	Oberfläche O m^2	Widerstandsfläche Oberfläche f_{wO} m^2	Widerstandsfläche gesamt f_w m^2	$\frac{f_w}{f f_w} \cdot 100$ v.H.
Flügel	34,4	0,1010	0,1392	35,6
Rumpf	25,0	0,0866	0,1052	27,0
2 Leitwerksträger	5,0	0,0165	0,0183	4,7
Leitwerke	6,6	0,0240	0,0306	7,8
Motor	-	-	0,0315	8,1
Kühler	-	-	0,0480	12,3
Waffen	-	-	0,0060	1,5
Interferenz	-	-	0,0117	3,0
Gesamt	71,0	0,2279	0,3905	100,0
c_w (F = 19)	-	-	0,0205	—

Be/Hm.13.11.44

Figure 9. Drag Polar Build Up [From: Ref. 12]

significantly lower value of 0.0152. Unfortunately, the Reynolds number at which each of the aforementioned C_{Do} values was determined is unknown. ACSYNT also performs a component build up, based on geometry inputs, and estimated a C_{Do} at each flight condition analyzed. For the P 208, ACSYNT estimated a C_{Do} of 0.0166 in the cruise condition. Though it is an inviscid code, VORVIEW has the capability to estimate friction drag. The term 'friction drag' is used, as opposed to, C_{Do} because the VORVIEW values are not restricted to the zero lift condition. VORVIEW can accept drag polar data files for specified Reynolds numbers. As the aircraft's planform is 'sliced' chordwise the drag polar corresponding to the local characteristic length is applied to the slice. Due to the difficulty of obtaining drag polars for input, only a cursory look at this feature of VORVIEW was taken. Drag polars, provided by Andrew Hahn of NASA Ames Research Center, using MSES polar driver version 3.0, were entered for a NACA 0010 airfoil at Re = 3.8510^6 corresponding to the tail, a NACA 23012 airfoil at Re = $13.8x10^6$ corresponding to the wing and a fuselage-like shape at Re = $55.5x10^6$. These Reynolds numbers correspond to a mid-envelope flight condition of 21,000 feet and a flight Mach number of M = 0.55. The use of these three sectional drag polars resulted in an average friction drag estimate of 0.0199 that varied from a low value of 0.00958 at 2 degrees AOA to a high value of 0.048 at 15 degrees AOA.

EXCEL was used to program the USAF DATCOM equations for the P 208 component drag build up. The spreadsheet allows the computation of the P 208 C_{Do} under any given flight condition, with the local Reynolds Number for each component calculated for the given condition. For a cruise condition of 29,500 ft at M_a = 0.57, a C_{Do} = 0.0168 was calculated via this method; for the flight condition used for the VORVIEW analysis (above) C_{Do} = 0.162.

Figure 10 illustrates the dependence of the C_{Do} for the XP-41 on seemingly small factors. Because of this small factor dependence, and the fact that Blohm and Voss had more detailed information on the aircraft and likely expended more effort than anyone else, the Blohm and Voss value of C_{Do} was used in this current analysis of the P 208, despite the lack of Reynolds number information on which it was based. A non-varying C_{Do} should be accurate for a first order linear analysis.

The previous discussion of C_{Do} should cast doubt on any attempt to directly compare various aircraft C_{Do} values of unknown origin as a means of determining any relative aerodynamic benefits of a given configuration. For example it would be folly to attempt to compare the P 208's C_{Do}, using any of the methods above, to that of the P-51

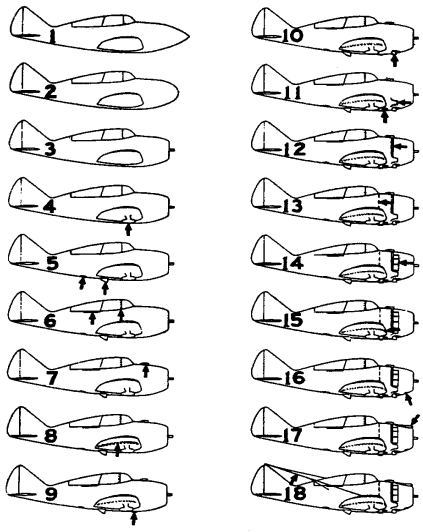

Condition number	Description	C_D (C_L = 0.15)	ΔC_D	ΔC_D, percent [a]
1	Completely faired condition, long nose fairing	0.0166		
2	Completely faired condition, blunt nose fairing	.0169		
3	Original cowling added, no airflow through cowling	.0186	0.0020	12.0
4	Landing-gear seals and fairing removed	.0188	.0002	1.2
5	Oil cooler installed	.0205	.0017	10.2
6	Canopy fairing removed	.0203	-.0002	-1.2
7	Carburetor air scoop added	.0209	.0006	3.6
8	Sanded walkway added	.0216	.0007	4.2
9	Ejector chute added	.0219	.0003	1.8
10	Exhaust stacks added	.0225	.0006	3.6
11	Intercooler added	.0236	.0011	6.6
12	Cowling exit opened	.0247	.0011	6.6
13	Accessory exit opened	.0252	.0005	3.0
14	Cowling fairing and seals removed	.0261	.0009	5.4
15	Cockpit ventilator opened	.0262	.0001	.6
16	Cowling venturi installed	.0264	.0002	1.2
17	Blast tubes added	.0267	.0003	1.8
18	Antenna installed	.0275	.0008	4.8
	Total		0.0109	

[a] Percentages based on completely faired condition with long nose fairing.

Figure 10. Drag Study on the XP-41 [From: Ref. 15]

Mustang which reference 15, using none of the above methods, has as 0.0161. Furthermore, though it may be tempting to compare a unique configuration such as the P 208s against a very conventional configuration such as the P-51, Figure 10 indicates that any proposed configuration advantage/disadvantage may be masked by other factors. For example, the boundary layer diverter, on the radiator intake, that is widely accepted as a key feature leading to the P-51's outstanding performance, is not evident on the P 208; this one feature could mask any potential drag reduction of the OHS configuration. Though it looks like the P 208 should have a form drag advantage given the shortened fuselage and small vee-tail, a proper comparison would require developing a simple OHS model and a conventional configuration, with the wing parameters and tail volume coefficients held constant, and analyzing each with the same method. Such an analysis was not performed for this thesis.

2. Flight Conditions

Four flight conditions were chosen for performance and stability and control analysis, in accordance with reference 15. These flight conditions, summarized in Table 3, should adequately cover the flight envelope shown in Figure 11. Flight condition lift coefficients are based on unaccelerated flight at a weight of 10,300 pounds, corresponding to the weight on which the flight envelope was developed. Figure 11 depicts a clean (i.e. flaps and landing gear retracted), unaccelerated flight envelope and therefore the Approach configuration is not depicted. The sea level penetration condition is maximum velocity at sea level.

Table 3. Flight Conditions

	Flight Condition	Altitude	M	C_L
1	Approach (40^o flaps)	0	0.17	1.2
2	Sea Level Penetration	0	0.52	0.125
3	Cruise	29,500 ft (9 km)	0.57	0.344
4	Maximum Velocity (Vmax)	31,000 ft (9.5 km)	0.73	0.225

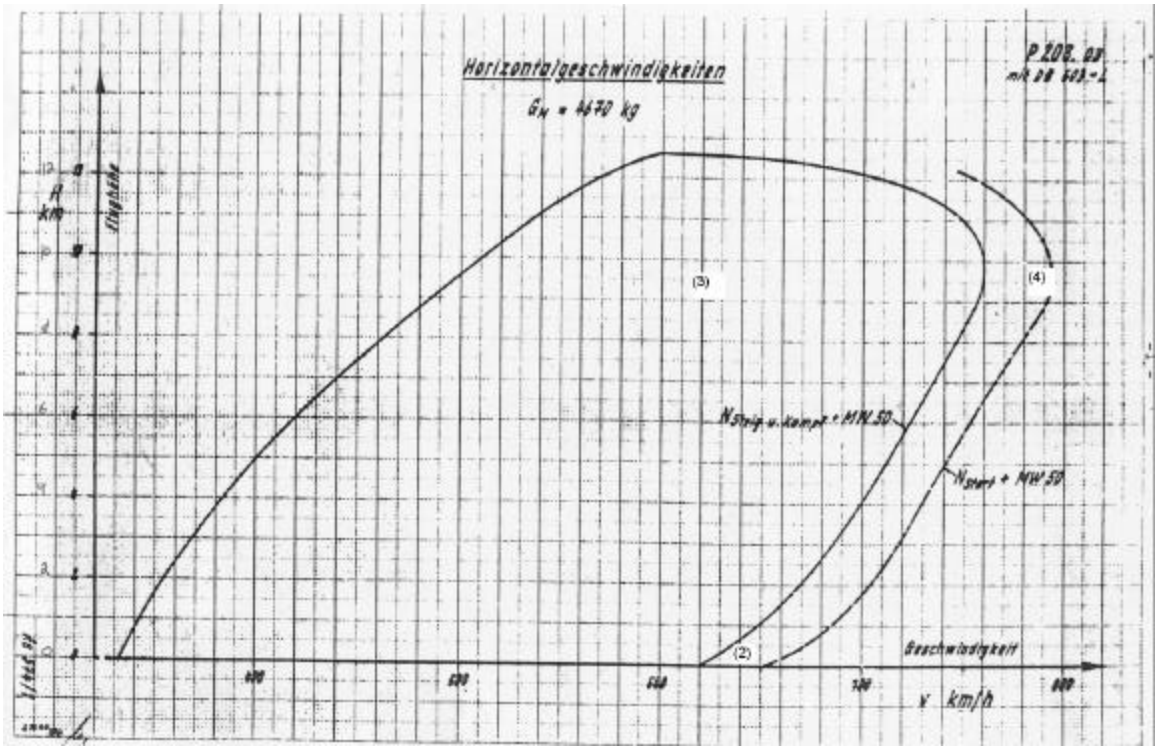

Figure 11. P 208 1 G Performance Envelope [After: Ref. 12]

THIS PAGE INTENTIONALLY LEFT BLANK

III. P208 PERFORMANCE

A significant volume of German performance estimates for the P 208 is available for numerous altitudes and power settings, reference 3. However, its interpretation was beyond the author's capability. The interpretation was not merely a matter of language but variable definition. An example of the data available is included as Appendix B.

The primary analysis tool used to examine the performance of the P 208 was VORVIEW. Example VORVIEW summary output and stability and control derivative output files are included as Appendix C. As previously mentioned, VORVIEW is an inviscid code that uses a Trefftz-plane analysis as a check to the pressure integration method. VORVIEW computes both pressure integration and Trefftz-plane values for C_{Di}/C_L^2; these values where checked for agreement. When a disagreement occurred in the C_{Di}/C_L^2 values, it was always due to a pressure integration value that was too optimistic, often resulting in span efficiency factors greater than one. To remedy this situation, the leading edge suction/vortex lift multiplier (SPC), in the VORVIEW initial conditions file, was varied by iteration until agreement was reached between the two analyses.

The SPC variable is used to account for the presence of vortex lift using the Polhamus suction analogy and was therefore typically quite low for the P 208, about 0.2 for the cruise condition. The Polhamus suction analogy states that the extra normal force that is produced by a leading edge vortex on a highly swept wing at high angles of attack is equal to the loss of leading edge suction associated with the separated flow.

VORVIEW provides a value of span efficiency for every flight condition analyzed. Span efficiency as a function of C_L is shown in Figure 12. The large variation that occurs at low values of AOA is not unexpected as span efficiency is sensitive to C_L. The large negative AOAs, thought impractical, are included to show that the curve will tend to smooth out at larger absolute values of C_L. Figure 12 shows an average span efficiency of about 61% with a peak of 71% at lift coefficients corresponding to high airspeeds. A drag polar, for an unknown flight condition, is available from primary German data: $C_D = 0.0201+0.0960C_L^2$. A value of span efficiency, e, can be backed out

by solving for e in, 0.0960 = 1/(peAR), resulting in a value of 70%. Reference 4 uses an empirical method to arrive at a value of 74% for span efficiency, again for an unknown flight condition. VORVIEW is likely the most sophisticated and accurate of these results.

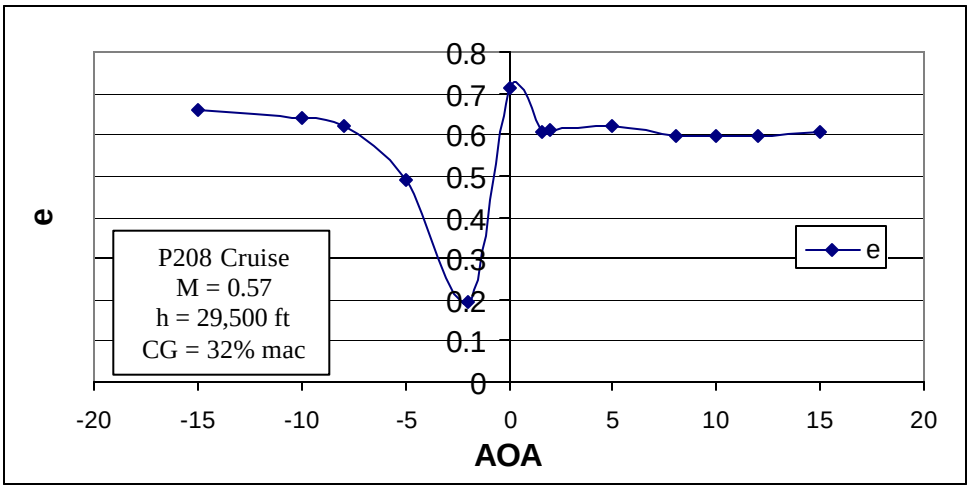

Figure 12. Span Efficiency vs. Lift Coefficient

Another, more revealing, method of analyzing span efficiency is to look at the span loading compared to an elliptic distribution as in Figure 13. A parabolic distribution is also shown as an elliptic lift distribution is not always "ideal". Prandtl was the first to note that the spanload for minimum induced drag was not the "optimum" spanload when bending moment and structural weight are taken into consideration. [Ref. 17] With a

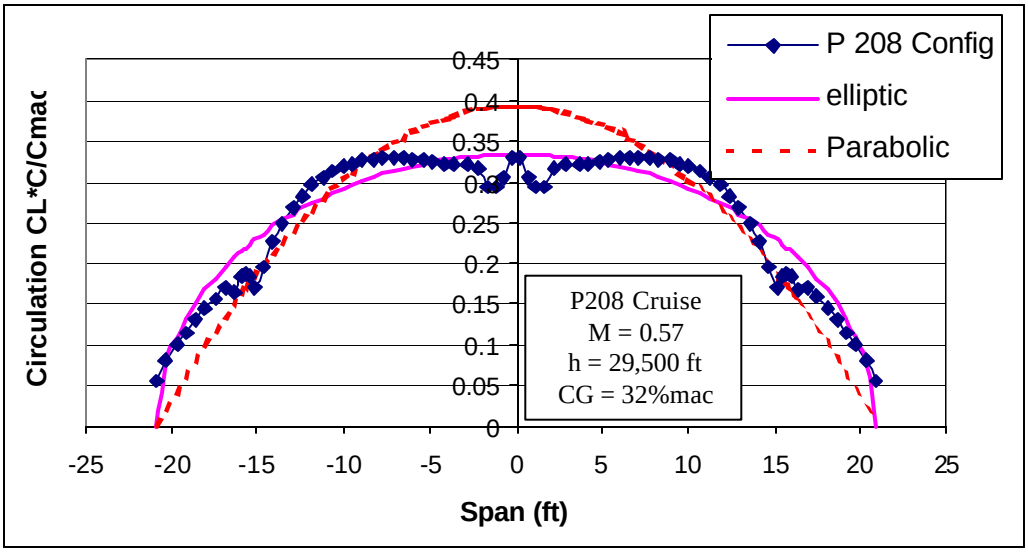

Figure 13. P 208 Spanloading

configuration like the P 208, it is likely that a more parabolic lift distribution would be desirable for structural reasons. Figure 13 shows that the P 208 lift distribution falls somewhere between the elliptic and parabolic ideals. The tail booms are at 15 ft. with the tails outboard of the booms. It should be noted that in the cruise condition, as shown in Figure 13, that the tails are in fact lifting surfaces.

Figure 14 show a comparative lift distribution with and without aileron deflection. This condition was examined to evaluate Kentfield's theory that the OHS configuration can aerodynamically offset some of the configuration's roll performance penalty due to its high moments of inertia. Figure 14 clearly shows that the increased lift due to a negative aileron deflection (down) results in increased lift on the adjacent tail, as predicted by Kentfield. The increased lift on the tail is due to the strengthened wing-tip vortex caused by the local lift increase resulting from the aileron deflection. For a positive aileron deflection (up) the opposite is true and lift is reduced. The coupling effect seen should assist the aircraft in its roll performance.

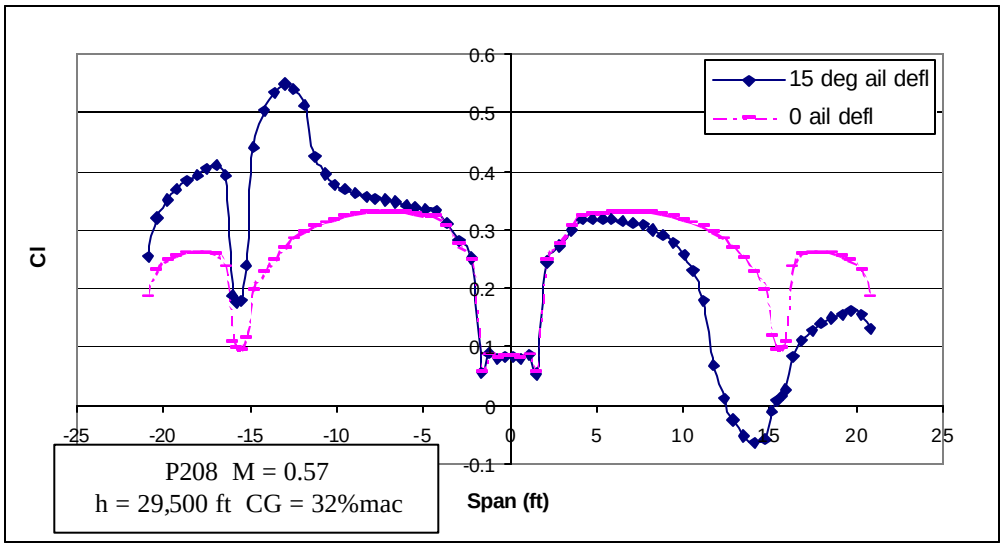

Figure 14. Spanloading with Aileron Deflection

The lift curve for the aircraft at Mach 0.57 is shown in Figure 15. Because it is an inviscid code, VORVIEW will not predict stall for the aircraft. The figure shows that the zero lift AOA for the aircraft is –2.7 degrees and that $C_{L\alpha} = 0.0824$. Additionally, the zero AOA $C_L = 0.216$ which roughly corresponds to the V_{max} flight condition. This could

mean that Blohm and Voss optimized the aircraft for top speed or that the angle of incidence of the main wing or the airfoil section chosen for this analysis was incorrect.

With the previous discussion of C_{Do}, it would seem inevitable that drag polars from various sources or methods would differ somewhat. Four drag polars are shown in Figure 16. The first polar (square symbols) is VORVIEW generated with both form drag and span efficiency varying for each data point. The second polar (diamond symbols) is

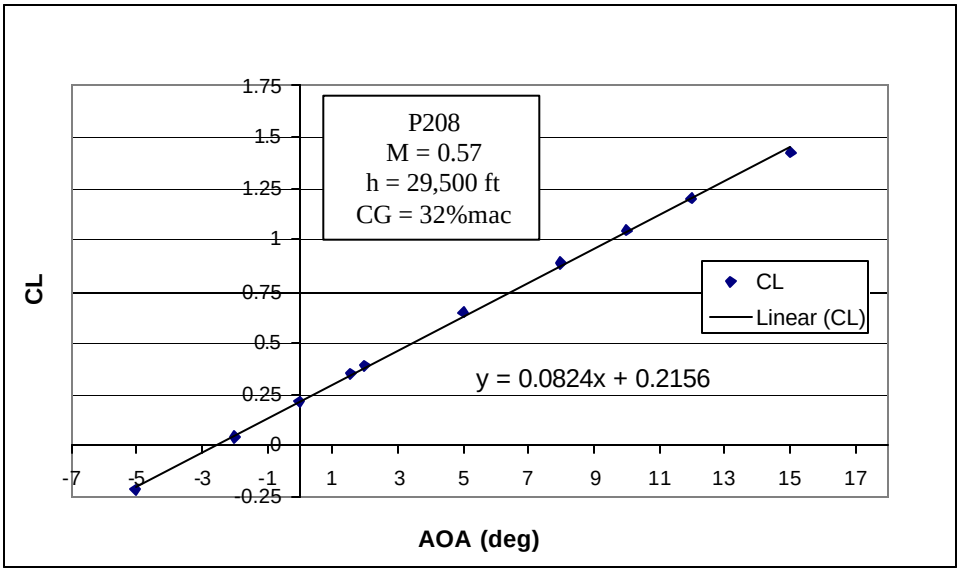

Figure 15. P 208 Lift Curve

the Blohm and Voss drag polar. The third polar (triangle symbols) was generated by Tipton: $C_D=0.0152+0.906C_L^2$. [Ref. 4] The last polar (X symbols) represents a combination of a DATCOM C_{Do} with VORVIEW C_{Di}s. The first polar shows a large variation in friction drag, explained in the previous discussion in Chapter II. While this variation is more realistic than a non-varying C_{Do}, the magnitude of the change is

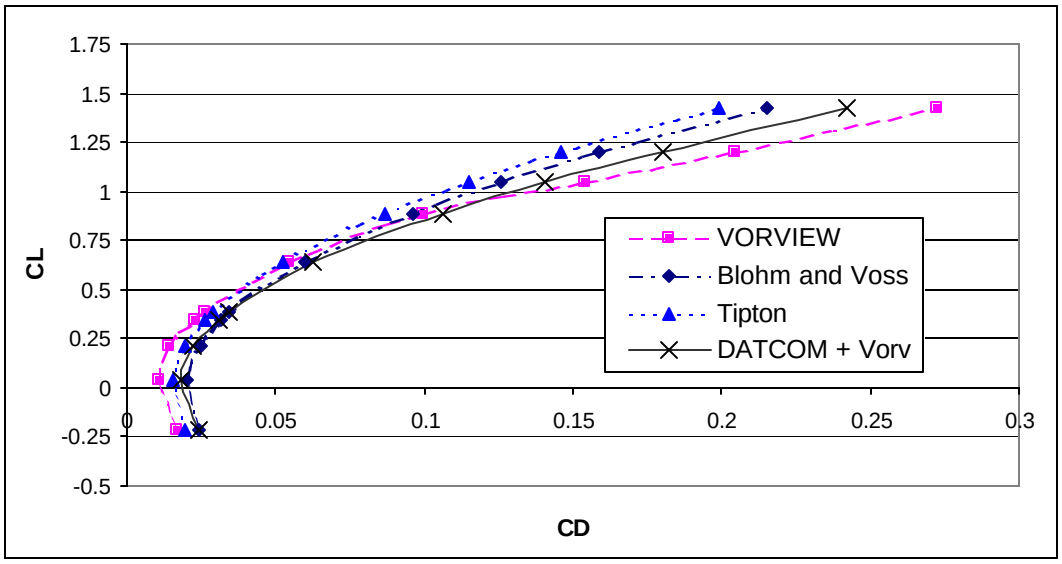

Figure 16. Drag Polar Comparison

questionable. The fourth polar provides for the greatest flexibility; a C_{Do} for any given flight condition can be used and C_{Di} variations can be captured with VORVIEW.

In all likelihood, the most accurate drag polar for the P 208 is one that incorporates the most accurate, Blohm and Voss derived, C_{Do} with the C_{Di}s from VORVIEW. This polar is plotted against the Blohm and Voss polar in Figure 17. VORVIEW C_{Di} values are probably the most accurate because they are calculated at each flight condition and do not rely on a non-varying value of C_{Di}/C_L^2.

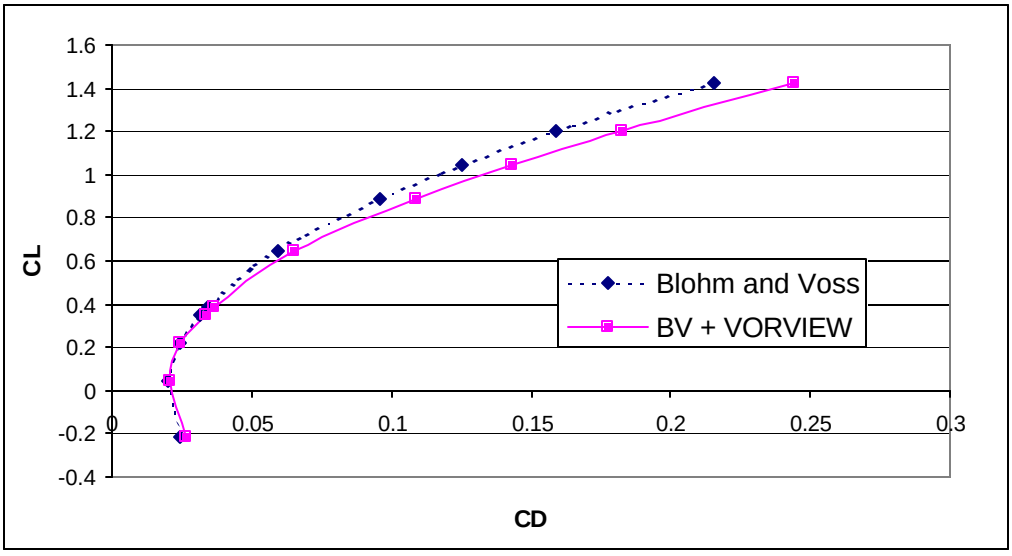

Figure 17. P 208 Drag Polar

Lift over drag ratios are given, in Table 4,for each flight condition using each of the drag polars in Figure 17. For the approach condition, a $C_{Do} = 0.18$ from reference 4 was used to account for landing gear and flaps. A comparison of the results in Table 4 generally shows agreement within 5%. The composite polar resulted in the more conservative estimate.

Table 4. P 208 L/D

	Approach	SL Penetration	Cruise	Max Velocity
Blohm and Voss	3.8	5.8	10.9	9.0
BV + VORVIEW	3.5	5.6	10.6	8.8

IV. STABILITY AND CONTROL

A. ELEVATOR TRIM

With the CG at 32% mac and the neutral point at 50% mac, the P 208 has a rather large static margin (SM) of 18%. In the approach condition, strong wing tip vortices will be present due to high lift generation. This condition makes the tail surfaces effective at generating lift, but hinders their ability to counter the nose-down pitching moment due to the flaps. The above condition results in a large elevator deflection (δ_e) required to trim the approach condition, see Table 5. Because this is such a critical phase of flight, a few scenarios were examined to address the large control deflection requirement. A full-span flap configuration was also considered. It has been suggested that due to the increased effectiveness of the ailerons, or by using the outboard surfaces for roll control, larger or even full-span flaps could be utilized by the OHS configuration. Table 5 is a summary of

Table 5. Approach Configuration Trim

Condition	Configuration	CG/SM	AOA	d_e
1	Standard (70% Span Flaps)	32%mac/18%	1.42^o	-19.8^o
2	Full-Span Flaps	32%mac/18%	-1.17^o	-47.1^o
3	All Moving Tail	32%mac/18%	1.23^o	-17.0^o
4	Reduced Static Margin	40%mac/10%	0.61^o	-9.3^o
5	Reduced Flaps (40% Span)	32%mac/18%	4.11^o	-7.7^o

Trimmed for C_L=1.2, 40^o flap deflection

five conditions examined for an approach condition of M_a = 0.17 and a flap deflection, d_F = 40^o. Control surface deflections and AOAs were determined by VORVIEW. The first condition is for the standard configuration. Condition 1 assumed a flap size of 70% span (excluding the fuselage area) and an elevator surface of 30% of the chord of the stabilizer. Condition 1 resulted in a rather large control deflection of almost 20 degrees. Condition 2 looked at a configuration using full-span flaps. For the given static margin it is obvious that full-span flaps are not an option as the control deflection shown would result in control surface stall. Condition 3 was added to examine any increase in control power of an all-moving tail. An all-moving control surface does not appear to provide

the requisite control force at an acceptable deflection. Condition 4 looked at a reduced static margin. Reducing the static margin to 10% by moving the CG back to 40% mac resulted in an acceptable control deflection. The feasibility of the CG shift or its affect on stability and control was not considered by the author. Condition 5 looked at the result of reducing the flap span. The flaps were reduce to 40% span. Because the wings are swept, reducing the span of the flaps brings their center of pressure inboard and forward. This movement of the center of pressure reduces the nose down pitching moment created by the flaps and results in the lowest required control deflection to trim the approach configuration.

Trim conditions for the four flight conditions, defined in Chapter II, are shown in Table 6. The fact that the cruise condition control deflection for trim is negligible suggests that the assumed angle of incidence for the tail of -3.5^{o} is probably correct.

Table 6. Trimmed Conditions

Flight Condition	**CG/SM**	**AOA**	d_e
Approach	0.32c/18%	1.42^{o}	-19.8^{o}
Sea Level Penetration	0.32c/18%	-0.6^{o}	3.27^{o}
Cruise	0.32c/18%	1.55^{o}	0.04^{o}
Maximum Velocity	0.32c/18%	-0.08^{o}	2.15^{o}

B. LONGITUDINAL STABILITY

The coordinate sign convention utilized for the trim and stability and control analysis is that shown in Figure 18.

A casual observation of the P208 may lead one to believe that the tails surfaces are too small. An examination of tail volume coefficients will support this observation. Dividing the P 208's vee-tail into projected vertical and horizontal areas allows an analysis of the tail volume coefficients. Using these areas as given in reference 4, the horizontal tail volume coefficient (C_{HT}) was found to be $C_{HT} = 0.326$. With a 5% reduction in required C_{HT} that Raymer suggests for a T-tail, due to the clean air seen by the horizontal, and a further arbitrary 5% reduction due to the proposed increased dynamic pressure from the wing tip vortex, a typical value of C_{HT} for this application

should be about C_{HT} = 0.45. [Ref. 14] This comparison suggests that the horizontal tail is approximately 28% too small.

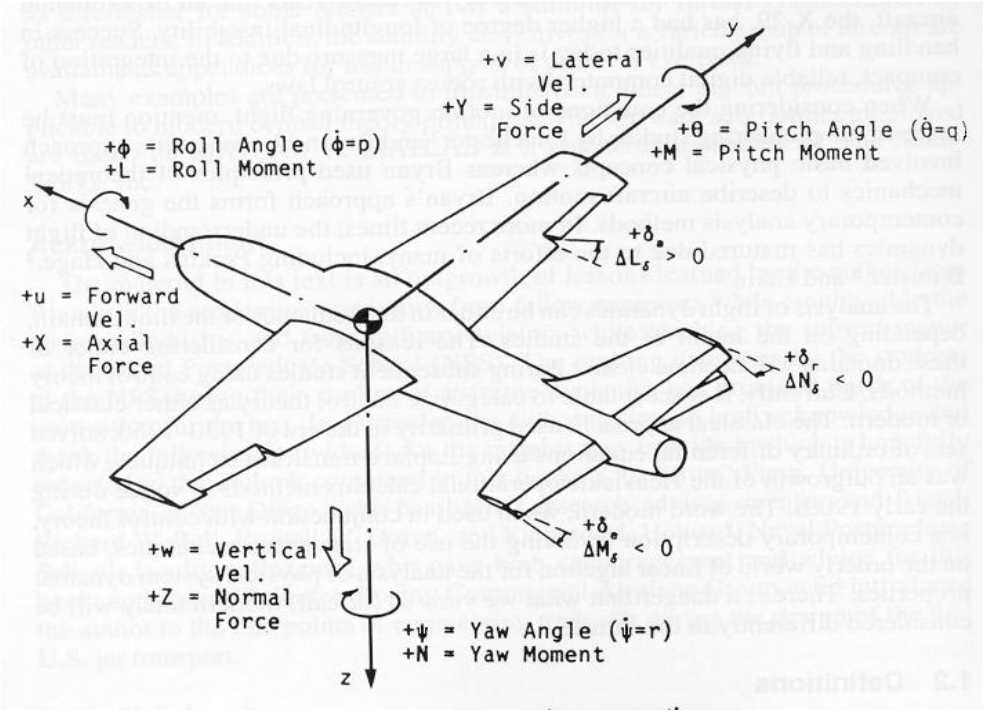

Figure 18. Coordinate Sign Convention [From: Ref. 17]

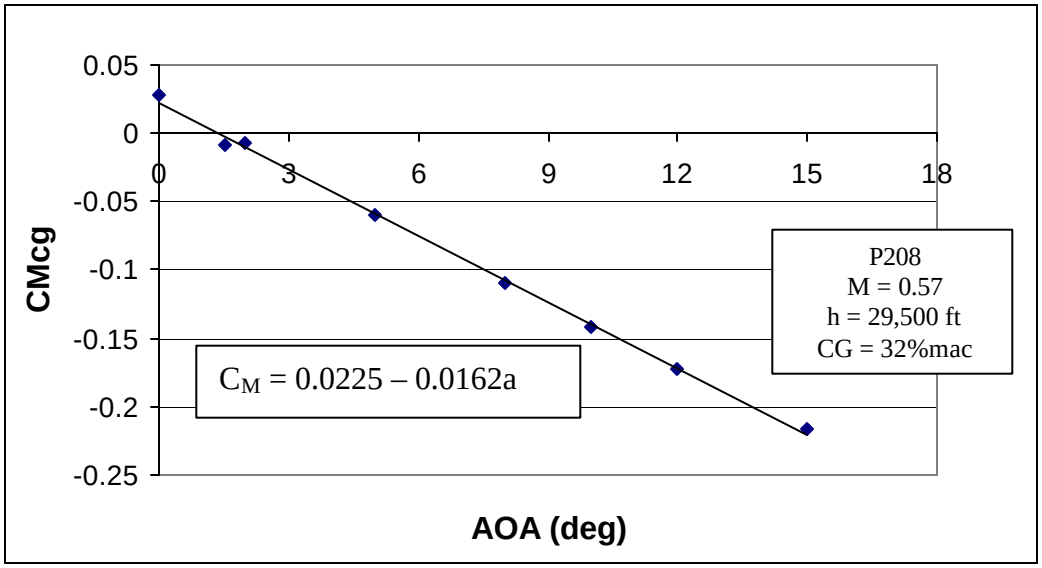

Figure 19. Static Stability

Utilizing C_M values determined by VORVIEW, an initial look at static stability shows that, for the given flight conditions, the aircraft is longitudinally statically stable, that is its initial tendency upon being disturbed will be to return to its equilibrium position. This result was not surprising given the large static margin. Figure 19 shows that both criteria necessary for longitudinal static stability exist, namely that C_{M0} is positive, $C_{M0} = 0.0225$, and the slope of the curve is negative, $C_{Ma} = -0.0162$ per degree.

VORVIEW is an excellent tool for examining an aircraft's dynamic stability. The code will perturb the aircraft's initial conditions by one degree around each axis to determine dimensionless stability derivatives. Dimensionless derivatives were determined for a trimmed aircraft in each of the following flight conditions: Approach, Sea Level Penetration, Cruise and Maximum Velocity, as defined in Chapter II. The dimensionless derivatives were dimensionalized as shown in Appendix D and are given in the Appendix. The equations of motion, which have been linearized as described by Schmidt [Ref. 18], were grouped into longitudinal and lateral-directional and considered separately in the governing state space equation, $\{\dot{x}\} = [A]\{x\} + \{B\}d$. The longitudinal plant matrix, [A], state vector, {x}, and control matrix, {B} are shown below in equations 4, 5 and 6 respectively.

$$[A] = \begin{bmatrix} X_U & X_a/U & 0 & -(g/U)\cos\Theta_0 \\ UZ_U/(U-Z_{\dot{a}}) & Z_a/(U-Z_{\dot{a}}) & (V+Z_q)/(U-Z_{\dot{a}}) & -g\sin\Theta_0/(U-Z_{\dot{a}}) \\ UM_U+M_{\dot{a}}UZ_U/(U-Z_{\dot{a}}) & M_a+M_{\dot{a}}Z_a/(U-Z_{\dot{a}}) & M_q+M_{\dot{a}}(U+Z_q)/(U-Z_{\dot{a}}) & 0 \\ 0 & 0 & 0 & 1 \end{bmatrix} \tag{4}$$

$$\{x\} = \begin{bmatrix} u/U & a & q & q \end{bmatrix}^T \tag{5}$$

$$\{B\} = \begin{Bmatrix} X_d/U & Z_d/(U-Z_{\dot{a}}) & M_d + M_{\dot{a}}Z_d/(U-Z_{\dot{a}}) & 0 \end{Bmatrix}^T \tag{6}$$

An aircraft's linearized longitudinal dynamics will normally consist of two pairs of complex conjugate roots corresponding to the short-period and long-period or phugoid modes. The real part of the root will indicate the modal damping, a negative value corresponds to positive damping. The imaginary part of the root is the mode's damped natural frequency. The state equation was coded in MATLAB; a code listing is given in Appendix E. Solving the corresponding longitudinal eigenvalue problem results in the information about the longitudinal dynamics of the system found in Table 7.

Table 7. Longitudinal Roots

		Approach	SL Penetration	Cruise	Max Velocity
Short-Period	Roots (λ)	-0.7025 ± 1.789i	-2.5182 ± 6.284i	-0.9644 ± 3.9415i	-1.2422 ± 5.1247i
	ωn (rad/sec)	1.9223	6.7694	4.0578	5.2731
	ζ	0.3654	0.372	0.2377	0.2356
Long-Period	Roots (λ)	-0.0200 ± 0.2248i	-0.0204 ± 0.0708	-0.0365 ± 0.0713i	-0.0107 ± 0.0601i
	ωn (rad/sec)	0.2257	0.0737	0.0801	0.061
	ζ	0.0884	0.2768	0.0455	0.175

The MATLAB code allows one to excite a stability mode with its eigenvector, via the *initial* command, and for exciting the system with a simulated control input, via the *step* command. Although the aircraft's plant matrix contains information on all modes, the use of an initial condition corresponding to a mode's eigenvector will assure only that mode will respond. [Ref. 18]

The short-period roots for the cruise condition show the mode is positively damped. Likewise, Figure 20 shows that, in the cruise condition, the short period is stable and damped, evident from the decay of the oscillations. The eigenvector normalized to alpha gives clarifying information to the figure, namely it shows: that the velocity perturbation (u/U) is small, about 1.7% of the trim speed, pitch angle (θ) is close to the angle-of-attack (α) in magnitude (98.4%) and phase (lags by 12.6°), pitch rate (q) leads α by 91° and that q leads the θ by 103.5° all of which are normal short-period behavior. [Ref. 18] Each flight condition examined showed normal short-period behavior with the cruise and V_{max} conditions being relatively lightly damped.

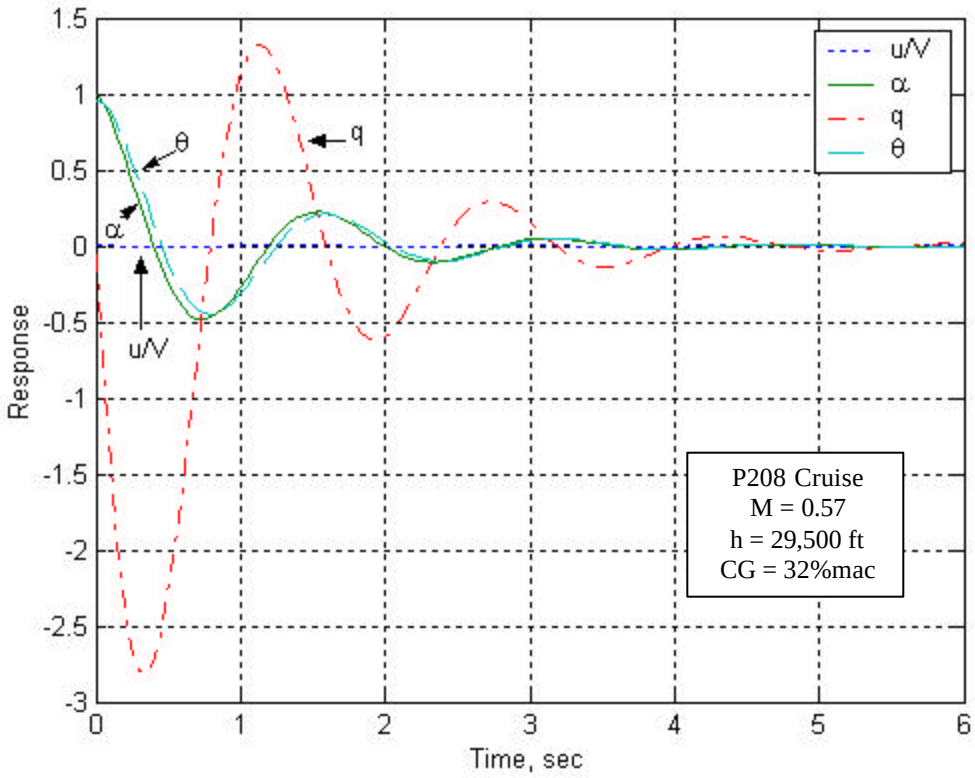

Figure 20. Short-Period Response to Initial Condition

$$\begin{Bmatrix} u/U \\ a \\ q \\ q \end{Bmatrix} = \begin{Bmatrix} 0.0170\angle\ 66.5^\circ \\ 1 \\ 3.992\angle\ 90.9^\circ \\ 0.984\angle\ -12.6^\circ \end{Bmatrix} \tag{7}$$

Figure 21 shows the long-period response to eigenvector excitation. The eigenvector, normalized to the velocity perturbation, is shown as equation 8 for amplification. In the cruise condition, the P208, demonstrates a typical long-period response. Light damping is evident with a 78 second period and a slow decay of the oscillation amplitude. Comparatively, the damping ratio, ?, for the long-period is an order of magnitude smaller than that for the short period, Table 7. Also typical of the long-period is that the α component of the eigenvector is much smaller than the u/U component, opposite of the short period. Again it is seen that the rate term, q, leads

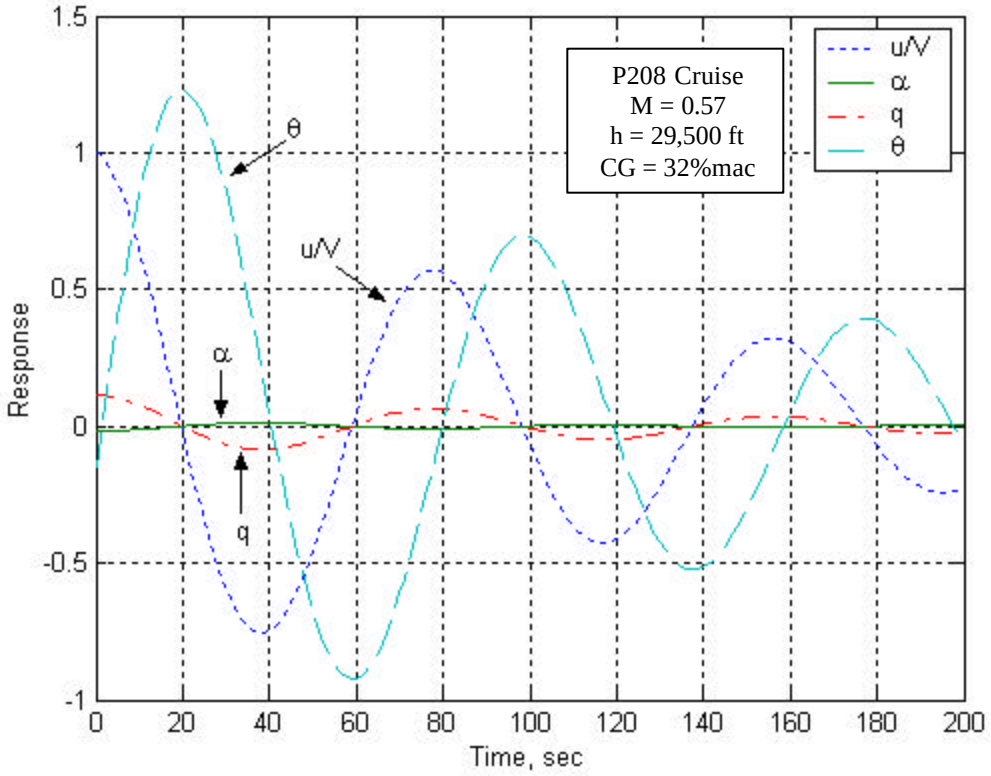

Figure 21. Long-Period Response to Initial Condition

$$\begin{Bmatrix} u/U \\ a \\ q \\ q \end{Bmatrix} = \begin{Bmatrix} 1 \\ 0.0168\angle -178.4^\circ \\ 0.1140\angle -0.9^\circ \\ 1.400\angle -96.0^\circ \end{Bmatrix}) \qquad (8)$$

displacement term, θ, by 95° in this case. The P208 exhibited normal long-period behavior for the four flight conditions examined.

The complete system response for the P208, due to an elevator control step input, can be seen in Figure 22. For the given flight condition, the P208 exhibits a typical system response to the given input. Figure 22 shows that the short-period motion, characterized by a, is mostly damped by 5 seconds while the long-period motion, characterized by u/U, will continue to oscillate for a few minutes. A positive elevator step control input will result in a nose-down pitch attitude, after the short-period damps out, the long-period exhibits normal features. The α component maintains a nearly

constant negative value. Pitch rate, q, will oscillate and finally reach a zero value. Pitch angle, θ, will oscillate and finally reach a constant slightly negative value. The u/U component will oscillate and eventually reach a positive steady value. The P 208 exhibited typical longitudinal behavior to a step input for all flight conditions examined. [Ref. 18]

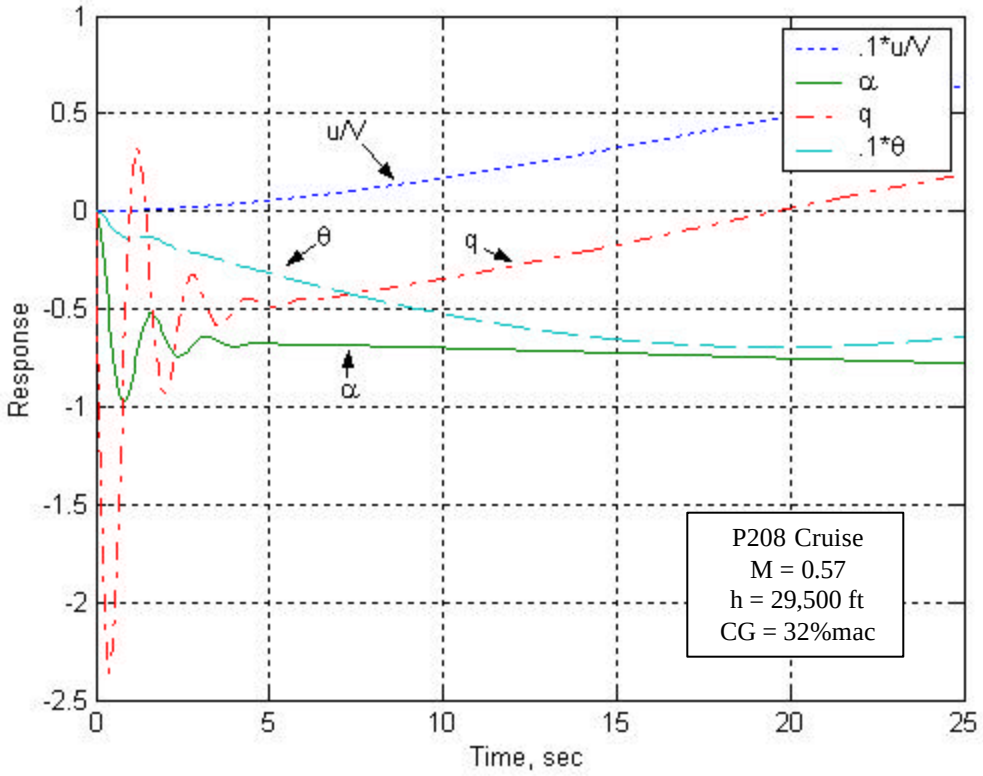

Figure 22. Longitudinal Response to Elevator Step Input

C. LATERAL-DIRECTIONAL STABILITY

Again using areas from reference 4, the vertical tail volume coefficient (C_{VT}) was found to be C_{VT} = 0.0248. Looking to Raymer [Ref. 14] once again for a representative C_{VT} and subtracting a nominal 5% for increased dynamic pressure due to the wing tip vortices results in a desired C_{VT} value of about 0.05. [Ref. 14] Thus, it appears that the vertical surface is prehaps 50% too small. This can indicate a directional stability problem with the design. Lateral stability increases with both wing sweep and dihedral.

Thus, with 30 degrees of sweep and six degrees of dihedral the design should be laterally stable.

VORVIEW and MATLAB, with the linearized equations of motion, were used to examine the P208's lateral-directional dynamic stability. Lateral-directional dimensional stability derivative values, computed from VORVIEW dimensionless derivatives, are given in Appendix D. The lateral-directional plant matrix, control vector (applied for rudder or aileron deflection as required) and state vector used in the governing state space equation are given below as equations 9, 10 and 11 respectively, with short-hand notation equations 12 – 14.

$$[A]=\begin{bmatrix} Y_b/U & Y_p/U & \left(g/U\right)\cos\Theta_0 & \left(Y_r-U\right)/U \\ L'_b & L'_p & 0 & L'_r \\ 0 & 0 & 0 & 1 \\ N'_b & N'_p & 0 & N'_r \end{bmatrix} \tag{9}$$

$$\{B\}=\left\{Y_d/U \quad L'_d \quad 0 \quad N'_d\right\}^T \tag{10}$$

$$\{x\}=\{b \quad p \quad f \quad r\}^T \tag{11}$$

where:

$$L'_n = G\left[L_n + N_n\left(I_{xz}/I_x\right)\right] \tag{12}$$

$$N'_n = G\left[N_n + L_n\left(I_{xz}/I_x\right)\right] \tag{13}$$

$$G = 1\Big/\left[1-(I_{xz})^2/(I_x I_z)\right] \tag{14}$$

Solving the eigenvalue problem for the lateral-directional (4x4) plant will normally give a complex conjugate pair of roots that describe the Dutch-roll and two real roots; the faster of the real roots describes the roll response and the slower one describes the spiral. [Ref. 18] Table 8 gives the results of solving the eigenvalue problem for the lateral-directional plant matrix. It should be noted that only the sea level penetration condition has a complex conjugate pair of roots with a negative real part, thus only this condition is

Table 8. Lateral-Directional Roots

		Approach	SL Penetration	Cruise	Max Velocity
Dutch-	Roots (λ)	0.2196 ± 1.075i	-0.1537 ± 0.4126i	0.0093 ± 1.252i	0.0190 ± 0.7750i
Roll	ωn (rad/sec)	1.0980	0.4403	1.2520	0.7752
	ζ	-0.2001	0.3491	-0.0075	-0.0245
Roll	Roots (λ)	-1.6040	-3.5549	-1.5390	-1.8732
	ωn (rad/sec)	1.6040	3.5549	1.5390	1.8732
	ζ	1.0000	1.0000	1.0000	1.0000
Spiral	Roots (λ)	-0.0412	-0.0242	-0.0110	-0.0154
	ωn (rad/sec)	0.0412	0.0242	0.0110	0.0154
	ζ	1.0000	1.0000	1.0000	1.0000

damped. Both the roll and spiral modes exhibit negative real roots, indicating that these modes are non-oscillatory and convergent.

Once again, for each of the four flight conditions, each lateral-directional mode was excited by its eigenvector. Figure 23 shows the Dutch-roll response to excitation by the eigenvector normalized to the sideslip angle, β. Although yaw angle (ψ) is not an eigenvector component, and not shown in Figure 22, it is useful when examining the Dutch-roll mode shape. For a typical Dutch-roll, the magnitudes of ψ and β will be nearly equal while their phase angles will be about 180 degrees out of phase. This relationship gives an aircraft's c.g. a nearly straight trajectory during a Dutch-roll oscillation, when viewed from overhead. [Ref. 18] The yaw angle perturbation was estimated by, $y = \frac{1}{w_n} \dot{y} e^{-i\hat{f}}; where \dot{y} \; r$, resulting in $y = 0.93 \; 93.2$. Figure 23 and the Dutch-roll eigenvalue roots show that the Dutch-roll mode is undamped and slightly

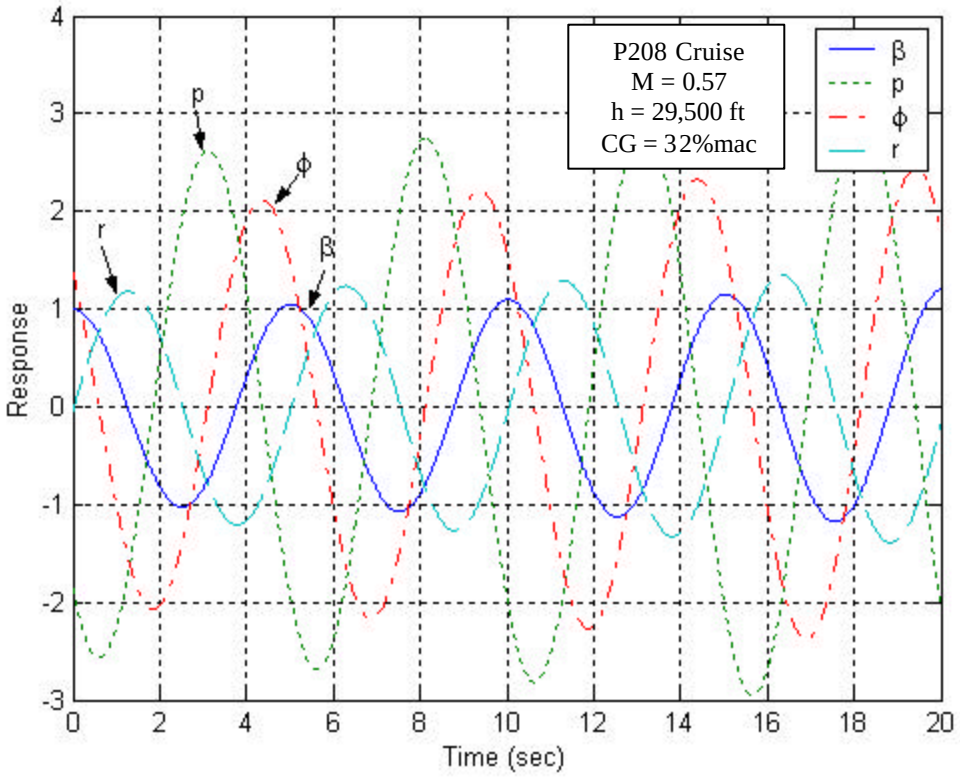

Figure 23. Dutch-Roll Response to Initial Condition

$$\begin{Bmatrix} b \\ p \\ f \\ r \end{Bmatrix} = \begin{Bmatrix} 1 \\ 2.550\angle -137.0 \\ 2.037\angle -47.5 \\ 1.664\angle -268.4 \end{Bmatrix} \tag{15}$$

unstable for the cruise condition of flight. As expected, only the sea-level penetration condition exhibited a stable Dutch-roll mode.

Figure 24 shows the roll response, as excited by the eigenvector normalized to p. The roll mode is, characteristically, dominated by roll angle, ϕ, and roll rate, p, with small β and yaw rate, r, components. All flight conditions exhibited similar roll characteristics.

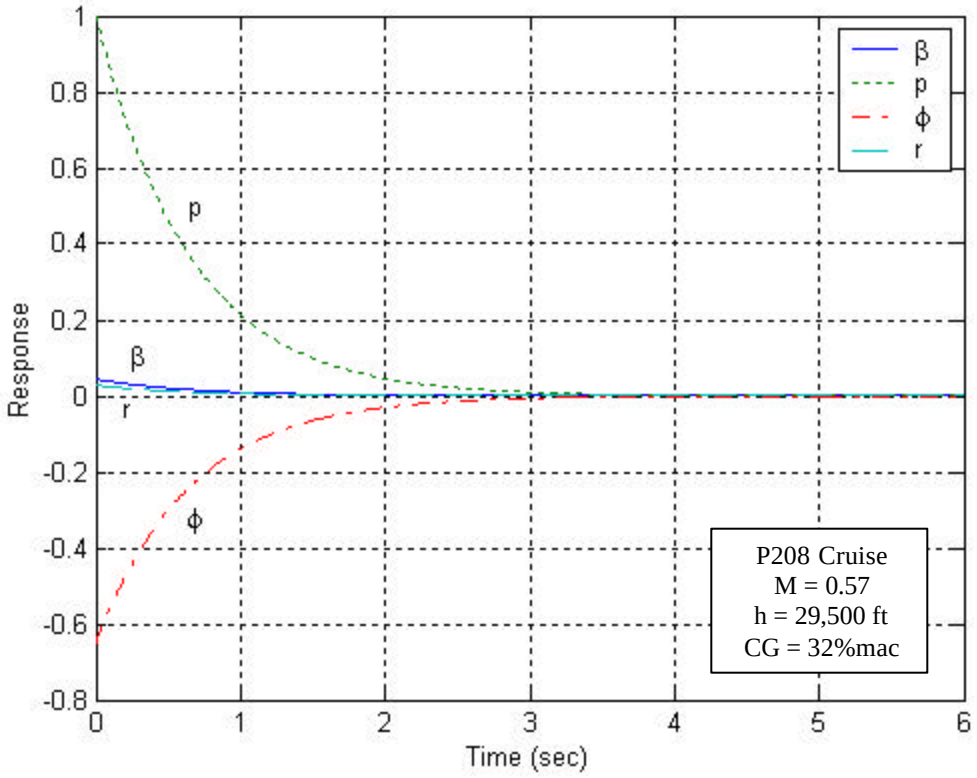

Figure 24. Roll mode Response to Initial Condition

$$\begin{Bmatrix} b \\ p \\ f \\ r \end{Bmatrix} = \begin{Bmatrix} 0.0447 \\ 1 \\ 0.6498 \\ 0.0282 \end{Bmatrix} \tag{16}$$

Figure 25 shows the spiral mode as excited by the eigenvector normalized to ϕ. The cruise condition spiral shown is stable and is typical of all flight conditions examined. The spiral mode is, characteristically, dominated by the roll angle component, ϕ. [Ref. 18]

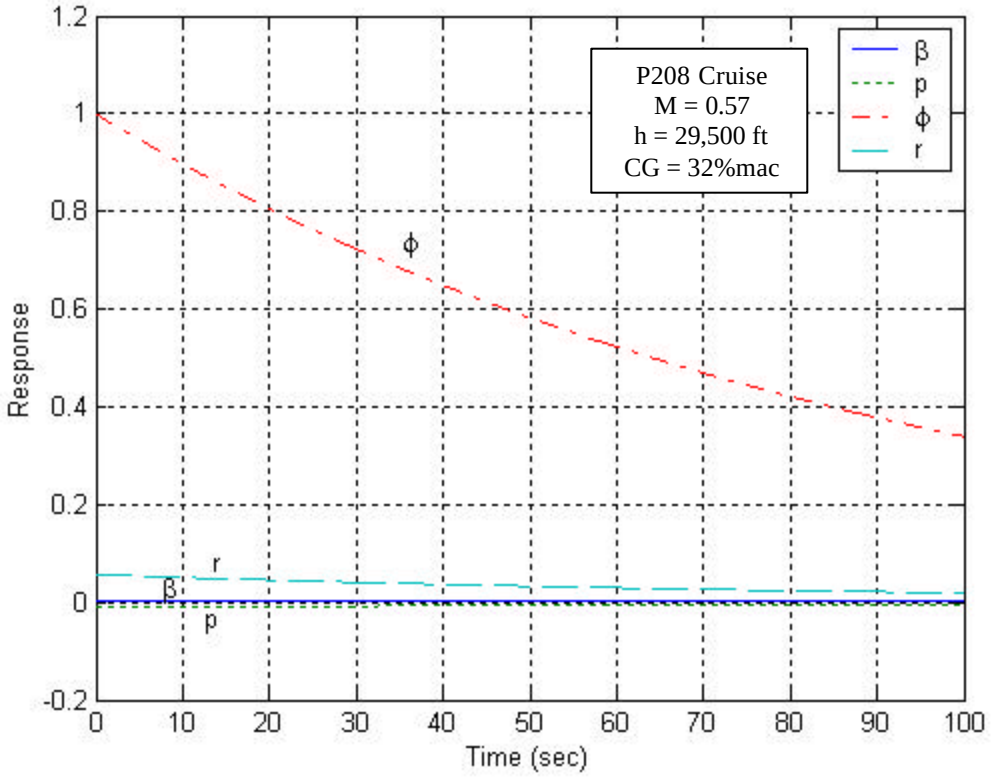

Figure 25. Spiral mode Response to Initial Condition

$$\begin{Bmatrix} b \\ p \\ f \\ r \end{Bmatrix} = \begin{Bmatrix} 0.0031 \\ 0.0108 \\ 1 \\ 0.0564 \end{Bmatrix} \tag{17}$$

D. FLYING QUALITIES

Using the previous stability and control data, the P 208's flying qualities were assessed in accordance with MIL-F-8785C, (Military Specification Flying Qualities of Piloted Airplanes). Each of the four flight conditions were assessed in the trimmed, stick-fixed mode. The P 208 was evaluated as a Class IV aircraft, that is, a high maneuverability aircraft. The three flight phase categories and three levels of flying qualities from MIL-F-8785C are discussed below. [Ref. 18]

Flight Phase Categories-

A. Non-terminal Flight Phases that require rapid maneuvering, precision tracking, or precise flight-path control, i.e., air-to-air combat, ground attack, terrain following, ect.

B. Non-terminal Flight Phases that are normally accomplished using gradual maneuvers and without precision tracking, i.e., climb, cruise, loiter, ect.

C. Terminal Flight Phases normally accomplished using gradual maneuvers and usually require accurate flight-path control, i.e., takeoff, approach, landing, ect.

Levels of Flying Qualities-

1. Flying qualities clearly adequate for the mission Flight Phase.
2. Flying qualities adequate to accomplish the mission Flight Phase, but some increase in pilot workload or degradation in mission effectiveness, or both exists.
3. Flying qualities such that the airplane can be controlled safely, but pilot workload is excessive or mission effectiveness is inadequate, or both.

For the short-period motion, the P 208 has Level 1 flying qualities for category C Flight Phases and for category A at low altitude and high airspeed. At higher altitudes the short-period drops to Level 2 for category B Flight Phases and Level 3 for category A. The P 208's long-period is Level 1 across the board. The P 208 has unacceptable flying qualities in the Dutch-roll mode, except at low altitudes and high airspeeds where it exhibits Level 1 qualities for Flight Phases A and B, except for air-to-air combat and ground attack where it is Level 2. The P 208 is Level 1, for all flight conditions examined, in roll and spiral performance.

V. CONCLUSIONS AND RECCOMENDATIONS

A. CONCLUSIONS

1. Configuration Suitability

It is, of course, the configuration and its applicability to future designs, and not the P 208 itself that is of primary interest. Some of Kentfield's conclusions on the OHS configuration have been observed in the analysis of the P 208. The tails are, in fact, lifting surfaces for most phases of flight, and therefore his claims of reduced main wing planform area versus a conventional configuration appear valid. Roll performance is adequate, as seen by the P 208's Level 1 roll performance. Again, Figure 14 appears to verify Kentfield's theory on increased roll performance as stated in Chapter I. Greater pitch stability, as theorized by Kentfield, did not materialize as the P 208 had Level 2 and 3 short period flying qualities at higher altitudes and airspeeds. This is likely due to the low lift coefficients and corresponding low circulations and weak wing tip vortices occurring at the cruise and V_{max} conditions in addition to the short coupling and small tail size of the P 208. Pitch control presented a problem in the approach configuration for the P 208 as analyzed herein. Reducing the static margin corrected the problem but no effort was made to examine how this would further affect stability and control, which may pose a problem since already small tail volume coefficients would be further reduced by an aft movement of the CG. Stability and control should present no major difficulties, even with the small tails, but require a pitch and a yaw damper at a minimum to bring the short-period and Dutch-roll up to Level 1. As far as performance is concerned, Blohm and Voss predicted a lower weight and surface area due to small wings, control surfaces and fuselage. Nothing in the analysis would appear to contradict these predictions.

2. NASA codes

RAM was an excellent tool for the analysis of the P 208. The code lends itself well to quick building and adjusting of concepts, though adding fine nuances, such as complex body shapes, requires much more skill and time. Despite its lack of documentation the code is quickly learned by sitting down and using it. For

reproducibility in future studies, a copy of the P 208 RAM input file is included as Appendix F.

VORVIEW allows for a very quick examination of a proposed configuration developed in RAM. The inputs to and execution of VORVIEW require a fraction of the time necessary to produce the same results by empirical methods. Unfortunately, a true evaluation of VORVIEW's accuracy in predicting an unconventional configuration's performance was not possible. Insufficient Blohm and Voss data was available to make such an evaluation. Also lacking any flight data or wind tunnel data it would be unwise to evaluate a modern design code against 1940s prediction methods. Some comparisons are, however, available. Span efficiency, as predicted by VORVIEW was apparently 13% lower than the German value and 18% lower than the value given in reference 4. Reference 4 also presented non-dimensional stability derivatives, derived using Roskam, reference 15, and longitudinal and lateral-directional roots for two flight conditions. Damping ratios and natural frequencies were calculated from the roots given and compared to those obtained from VORVIEW derivatives. Considering the fact that the flight conditions in reference 4 were no further defined than "Powered Approach" and "High-Speed Cruise" at a static margin of 5%, the agreement of the longitudinal characteristics was exceptional. All values of damping ratio and natural frequency for the longitudinal modes agreed within 28% except for long-period damping in the approach configuration which was 2.6 times greater in reference 4. Conversely, there was no agreement for the lateral-directional modes. VORVIEW showed an unstable Dutch-roll mode where reference 4 was stable, a stable spiral mode where reference 4 showed the mode as unstable and roll roots that were three times greater than found in reference 4. Unfortunately no useful conclusions can be drawn from these comparisons since no "correct" answer is available.

ACSYNT is a powerful tool. However, its utility was not ideally suited to the problem at hand. ACSYNT is not so much an analysis as it is a development tool. Through its sensitivity and optimization routines ACSYNT can quickly apply empirical equations drastically reducing man-hours required to perform trade studies. A working ACSYNT file for the P 208 has been created, Appendix G, and preliminary convergence to VORVIEW performance numbers completed. ACSYNT should be further used to

optimize the configuration for various defined missions. The requirements for its products occur early in the design process, before someone could learn the code and become proficient at its use.

The common weakness among the NASA codes, as far as their utilization at NPS is concerned, was the reliance on support from NASA personnel for their utilization. The minimal documentation, for RAM and VORVIEW, was the cause of much of this reliance.

B. RECCOMMENDATIONS

1. If more than an academic interest exists in the OHS configuration, the next course of action should be a detailed structural analysis to determine if any structural penalties of the configuration will outweigh its benefits.
2. With a wind-tunnel model now available, experiments should be conducted to determine the accuracy of VORVIEW in the analysis of the configuration; thus giving a confidence level to any VORVIEW analysis of similar designs.
3. The P 208 ACSYNT model should be refined, and sensitivity and optimization analysis run to improve the configuration.
4. A direct RAM/VORVIEW comparison should be completed of a conventional and OHS configuration with wing planforms and tail volume coefficients held constant.
5. A radar cross-section analysis should be performed to determine the configuration's potential benefits in this area.

THIS PAGE INTENTIONALLY LEFT BLANK

LIST OF REFERENCES

1. Cowin, Hugh W., "Blohm und Voss Projects of World War II," *Air Pictorial*, pp. 312- 316, October, 1963.

2. Schick, Walter and Ingolf Meyer, *Luftwaffe Secret Projects: Fighters 1939-1945*, World Print Limited, Hong Kong, 1997.

3. Blohm & Voss "Performance data for various Blohm und Voss fighter airplanes," National Air and Space Museum, German/Japanese Captured Air Technical Documents Microfilms Hamburg, Germany, May-December 1944.

4. Tipton, Brian, "The Preliminary Design Analysis of a Unique Semi-tailless Aircraft Configuration," Masters Thesis, University of Oklahoma, Norman, OK, 1995.

5. Hahn, Andrew, "An Independent Assessment of Scaled Composites Incorporated's Model M287-9 (Alliance 1) Inviscid Aerodynamics Using a Vortex Lattice Code," NASA Ames Research Center, November 16, 1998.

6. "User Guide to Acsynt and Create," Naval Postgraduate School, Monterey, CA, No Date.

7. Kentfield, John, "Aircraft Configurations with Outboard Horizontal Stabilizers," *Journal of Aircraft*, vol. 28, no. 10, pp. 670-672, October, 1991.

8. Kentfield, John, "Case for Aircraft with Outboard horizontal Stabilizers," *Journal of Aircraft*, vol. 32, no. 2, pp. 398-403, March-April 1995.

9. Kentfield, John, "The Aspect-Ratio Equivalence of Conventional Aircraft with Configurations Featuring Outboard Horizontal Stabilizers," Paper 975591, 1997 SAE/AIAA World Aviation Congress, October 13-16, 1997.

10. Kentfield, John, "Influence of Aspect Ratio on the Performance of Outboard Horizontal-Stabilizer Aircraft," *Journal of Aircraft*, vol. 37, no. 1, pp. 62-67, January-February 2000.

11. "Blohm & Voss P 208," Luftfahrt International, vol. 15, pp. 2325-2339, May-June 1976.

12. Blohm & Voss "Blohm und Voss Jet Airplanes." National Air and Space Museum, German/Japanese Captured Air Technical Documents Microfilms Hamburg, Germany, 1944-45.

13. Hoak, D.E., *USAF Stability and Control DATCOM*, McDonnell Douglas Corporation Douglas Aircraft Division, April 1978.

14. Raymer, Daniel P., *Aircraft Design: A Conceptual Approach*, American Institute of Aeronautics and Astronautics, Washington, D.C., 1989.

15. Loftin, Laurence K., *Subsonic Aircraft: evolution and the matching of size to performance*, NASA RP 1060, August 1960.

16. Roskam, Jan, *Airplane Design*, Roskam Aviation & Engineering Corporation, Ottawa, KS, 1986.

17. Iglesias, S. and W.H. Mason, "Optimum Spanloads Incorporating Wing Structural Weight," AIAA-2001-5234, First AIAA Aircraft Technology, Integration, and Operations Forum, Los Angeles, CA, October, 2001.

18. Schmidt, Louis V., *Introduction to Aircraft Flight Dynamics*, American Institute of Aeronautics and Astronautics, Washington, D.C., 1998.

19. MIL-F-8785C, Military Specification: Flying Qualities of Piloted Airplanes, November 1980.

APPENDIX A: WEIGHTS

A Weight statement for the P 208, from the Blohm and Voss data is given in Figure 26. An English units weight statement is also available in reference 4.

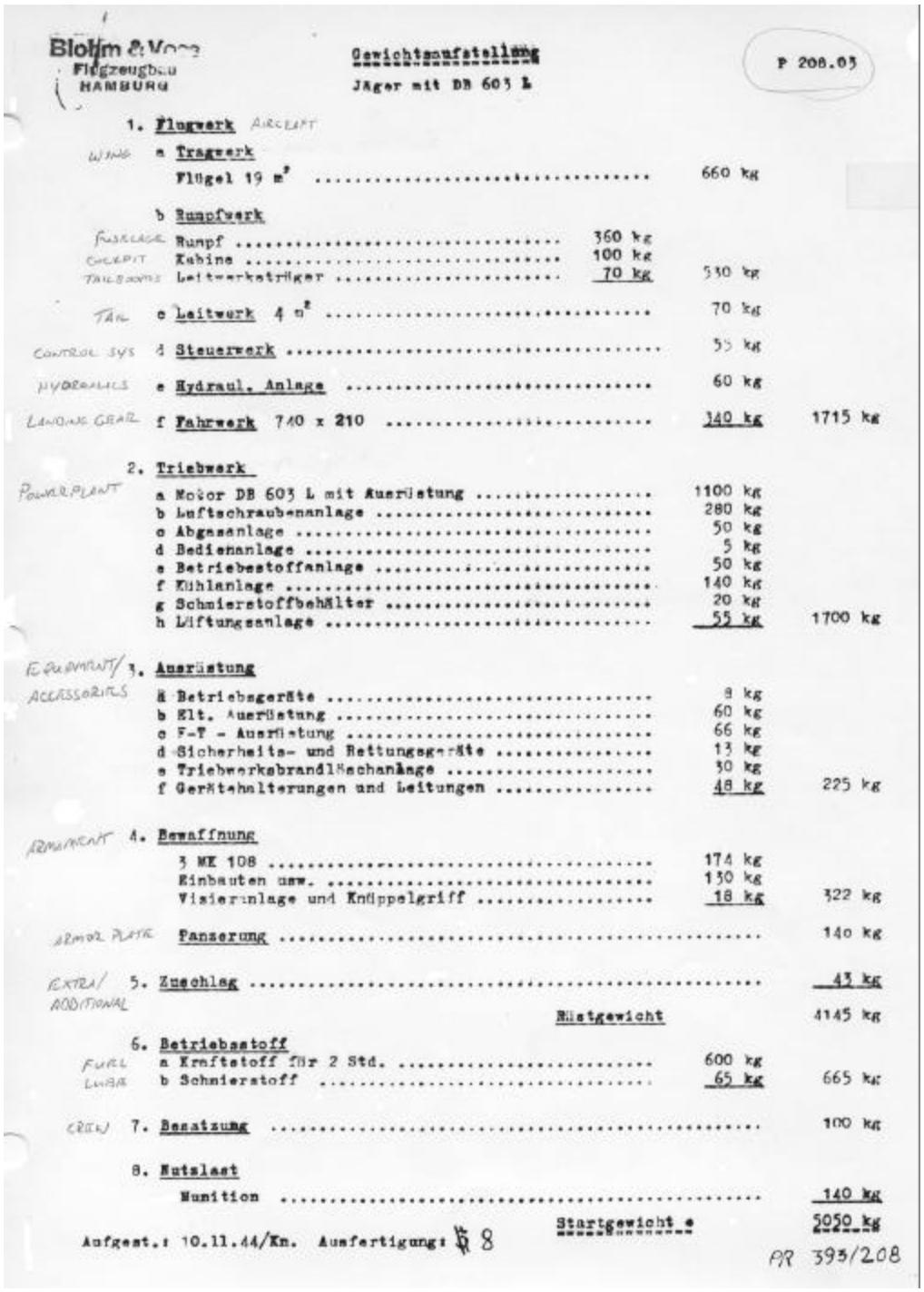

Blohm & Voss
Flugzeugbau
HAMBURG

Gewichtsaufstellung
Jäger mit DB 603 L

P 208.03

1. Flugwerk AIRCRAFT			
WING a **Tragwerk**			
Flügel 19 m²		660 kg	
b **Rumpfwerk**			
FUSELAGE Rumpf	360 kg		
COCKPIT Kabine	100 kg		
TAILBOOMS Leitwerksträger	70 kg	530 kg	
TAIL c **Leitwerk** 4 m²		70 kg	
CONTROL SYS d **Steuerwerk**		55 kg	
HYDRAULICS e **Hydraul. Anlage**		60 kg	
LANDING GEAR f **Fahrwerk** 740 x 210		140 kg	1715 kg
2. Triebwerk			
POWERPLANT a Motor DB 603 L mit Ausrüstung		1100 kg	
b Luftschraubenanlage		280 kg	
c Abgasanlage		50 kg	
d Bedienanlage		5 kg	
e Betriebsstoffanlage		50 kg	
f Kühlanlage		140 kg	
g Schmierstoffbehälter		20 kg	
h Lüftungsanlage		55 kg	1700 kg
EQUIPMENT/ ACCESSORIES **3. Ausrüstung**			
a Betriebsgeräte		8 kg	
b Elt. Ausrüstung		60 kg	
c F-T - Ausrüstung		66 kg	
d Sicherheits- und Rettungsgeräte		13 kg	
e Triebwerksbrandlöschanlage		30 kg	
f Gerätehalterungen und Leitungen		48 kg	225 kg
ARMAMENT **4. Bewaffnung**			
3 MK 108		174 kg	
Einbauten usw.		130 kg	
Visieranlage und Knüppelgriff		18 kg	322 kg
ARMOR PLATE **Panzerung**			140 kg
EXTRA/ ADDITIONAL **5. Zuschlag**			43 kg
Mustgewicht			4145 kg
6. Betriebsstoff			
FUEL a Kraftstoff für 2 Std.		600 kg	
LUBE b Schmierstoff		65 kg	665 kg
CREW **7. Besatzung**			100 kg
8. Nutzlast			
Munition			140 kg
Startgewicht			5050 kg

Aufgest.: 10.11.44/Kn. Ausfertigung: 8

PR 393/208

Figure 26. Original Weights Data [From: Ref. 12]

THIS PAGE INTENTIONALLY LEFT BLANK

APPENDIX B: EXAMPLE BV PERFORMANCE DATA

An example of the available Blohm and Voss data for the P 208 is shown in Tables 9 thru 12. Data sheets for various power settings at altitudes from sea level to 12 km are available. Low and high power settings for sea level and 9 km are presented.

Table 9. Sea-level Performance Data [From: Ref. 12]

BLOHM & VOSS Flugzeugbau HAMBURG — **Luftschraubenwirkungsgrade**

Baumuster : Projekt P 208; 03	mit Motor : DB 603 L mit MW 50; Leistungen nach Blatt 9-603-2256 vom 5.5.44
Luftschraube	Flughöhe H = 0 km
Durchmesser D = 3,40 m	Leistung $N_{Steigen}$ = 1800 PS
Blattzahl z = 4	Untersetzung i = 1: 1,93
Tiefenverhältnis $\tau_\sigma = b/D$ = 0,09	Motordrehzahl n_M = 2500 1/min
Dickenverhältnis $\delta_\sigma = (d/l)_\sigma$ = 0,07	Luftschr.-Drehzahl n_p = 1295 1/min = 21,6 1/sek
$l_\sigma = \tau_\sigma \cdot D$ = 0,306 m	ϱ = 0,125 — Polare: „M" (mit Zölungen)
$F_p = \frac{\pi \cdot D^2}{4}$ = 9,075 m²	$\frac{150}{\varrho}$ = 1200 — + λ, Ma Einfluß; δ = 0,07 Mittelwert
D^3 = 39,35 m³	$\varrho \cdot z \cdot D^3 \cdot \left(\frac{n_p}{100}\right)^2_{(1/min)}$ = 3300
F_W = — (Halbschwinge) m²	$c_l = \frac{150}{\varrho} \cdot \frac{N}{F_p \cdot v^3}$
$\xi_e = 1-\left(0,4-\frac{\lambda}{5}\right) \cdot \frac{F_W}{F_p}$	$c_a \cdot l = N_{(PS)} / \varrho \cdot z \cdot D^3 \cdot \left(\frac{v}{100}\right)_{km/h} \cdot \left(\frac{n_p}{100}\right)^2_{1/min} \cdot B$

No.		Unit						
1	v	km/h	300	350	400	500	600	700
2	v	m/s	83,3	97,2	111,1	139	167	194,5
3	v^3	(m/s)³·10⁻⁶	0,580	0,920	1,37	2,68	4,63	7,35
4	u	m/s	231	"	"	"	"	"
5	λ	—	0,361	0,421	0,482	0,604	0,725	0,844
6	Ma	—	0,725	0,735	0,75	0,78	0,83	0,88
7	c_l	—	0,412	0,2595	0,174	0,089	0,0516	0,0325
8	$\eta_{geschätzt}$	—	0,80	0,84	0,86	0,85	0,89	0,85
9	B	—	0,933	0,925	0,943	1,01	1,065	1,17
10	$c_a \cdot l$	—	0,195	0,1685	0,1448	0,108	0,0855	0,0667
11	c_a	—	0,638	0,552	0,473	0,353	0,2795	0,218
12	$\varepsilon_{x)}^{x)}$	—	0,018	0,0189	0,020	0,0245	0,033	0,054 (0,008)
13	c_l/c_{li}	—	1,035	1,03	1,03	1,03	1,032	1,045
14	c_{li}	—	0,399	0,2519	0,169	0,0865	0,050	0,0311
15	η_i	—	0,852	0,88	0,908	0,932	0,951	0,963
16	α_i	°	4,00	3,32	2,65	1,950	1,40	1,00
17	γ	°	1,031	1,081	1,145	1,405	1,89	3,095
18	$\alpha_i+\gamma$	°	5,031	4,401	3,795	3,355	3,29	4,095
19	η_{frei}	—	0,818	0,846	0,87	0,89	0,89	0,862
20	ξ_e	—						
21	η_{ges}	—						
22	x) $\Delta\varepsilon_p$ = λ, Ma Einfluß							
23	xx) ε + Δ ε_p							
24								
25								

[illegible] 1944 [illegible]

Table 10. High Power Sea-level Performance [From: Ref. 12]

BLOHM & VOSS Flugzeugbau BV HAMBURG

Luftschraubenwirkungsgrade

Baumuster Projekt P 208; 03-02 | mit Motor: DB 603 L | Leistungen nach Blatt 4-603-2256 vom 5.5.44

Luftschraube		Flughöhe	$H = 0$ km
Durchmesser	$D = 3{,}40$ m	Leistung	$N_{Start+MW50} = 2100$ PS
Blattzahl	$z = 4$	Untersetzung	$i = 1:1{,}93$
Tiefenverhältnis	$\tau_\sigma = b/D = 0{,}09$	Motordrehzahl	$n_M = 2700$ 1/min
Dickenverhältnis	$\delta_\sigma = (d/l)_\sigma = 0{,}07$	Luftschr.-Drehzahl	$n_p = 1400$ 1/min $= 23{,}4$ 1/sek
$l_\sigma = \tau_\sigma \cdot D = 0{,}306$ m		$\rho = 0{,}125$	Polare: „M"
$F_p = \frac{\pi \cdot D^2}{4} = 9{,}075$ m²		$\frac{150}{\rho} = 1200$	+ λ, Ma Einfluß; δ 0,07 ermittelt
$D^3 = 39{,}35$ m³		$\rho \cdot z \cdot D^3 \cdot \left(\frac{n_p}{100}\right)^2_{(1/min)} = 3855$	
$F_W =$ — (Hubschraube) m²		$c_l = \frac{150}{\rho} \cdot \frac{N}{F_p \cdot v^3}$	$\lambda = \frac{v}{u}$
$\xi_e = 1 - \left(0{,}4 - \frac{\lambda}{5}\right) \cdot \frac{F_W}{F_p}$		$c_a \cdot l = N_{(PS)} / \rho \cdot z \cdot D^3 \cdot \left(\frac{v}{100}\right)_{km/h} \cdot \left(\frac{n_p}{100}\right)^2_{1/min} \cdot B$	

No.		Unit						
1	V	km/h	200	300	400	500	600	700
2	v	m/s	55,6	83,3	111,1	139	167	194,5
3	v^3	$(m/s)^3 \cdot 10^{-6}$	0,172	0,580	1,37	2,68	4,63	7,35
4	u	m/s	250	"	"	—	—	"
5	λ	—	0,2225	0,333	0,445	0,556	0,669	0,779
6	Ma	—	0,75	0,77	0,80	0,835	0,88	0,93
7	c_l	—	1,615	0,481	0,2025	0,1035	0,0600	0,0378
8	$\eta_{geschätzt}$	—	0,70	0,84	0,84	0,88	0,89	0,83
9	B	—	1,005	0,89	0,93	0,96	1,03	1,13
10	$c_a \cdot l$	—	0,271	0,204	0,1469	0,1136	0,0822	0,0689
11	c_a	—	0,886	0,668	0,480	0,341	0,288	0,255
12	ε x) xx)	—	0,023	0,019	0,020	0,0255	0,007 0,039	0,018 0,062
13	c_l/c_{li}	—	1,068	1,04	1,03	1,032	1,035	1,055
14	c_{li}	—	1,516	0,463	0,1965	0,1001	0,058	0,0358
15	η_i	—	0,76	0,848	0,90	0,932	0,95	0,962
16	α_i	°	5,05	3,90	2,80	2,00	1,45	1,00
17	γ	°	1,318	1,089	1,145	1,46	2,24	3,56
18	$\alpha_i + \gamma$	°	6,368	4,989	3,945	3,46	3,69	4,56
19	η_{frei}	—	0,71	0,81	0,862	0,883	0,88	0,85
20	ξ_e	—					x	
21	η_{ges}	—						
22	x) $\Delta\varepsilon_p$ = λ, Ma Einfluß							
23	xx) $\varepsilon + \Delta\varepsilon_p$							
24								
25								

…1944 Mal.

Table 11. High Altitude Performance [From: Ref. 12]

BLOHM & VOSS
Flugzeugbau
HAMBURG

Luftschraubenwirkungsgrade

Baumuster : Projekt P 208 ; 03

mit Motor : DB 603L mit MW50
Leistungen nach Blatt 9-613-2256 vom 5.5.44

Luftschraube	Flughöhe H = 9 km
Durchmesser D = 3,40 m	Leistung N [illegible] = 1490 PS
Blattzahl z = 4	Untersetzung i = 1: 1,93
Tiefenverhältnis $\tau_\sigma = b/D$ = 0,09	Motordrehzahl n_M = 2500 1/min
Dickenverhältnis $\delta_\sigma = (d/l)_\sigma$ = 0,07	Luftschr.-Drehzahl n_p = 1295 1/min = 21,6 1/sek
$l_\sigma = \tau_\sigma \cdot D$ = 0,306 m	ϱ = 0,0476 Polare „M"
$F_p = \frac{\pi \cdot D^2}{4}$ = 9,075 m²	$\frac{150}{\varrho}$ = 3151 + λ, Ma Einfluß; δ = 0,07 Mittelwert
D^3 = 39,35 m³	$\varrho \cdot z \cdot D^3 \cdot \left(\frac{n_p}{100}\right)^2_{(1/min)}$ = 1256
F_W = —— (Rechenwerte) — m².	$c_l = \frac{150}{\varrho} \cdot \frac{N}{F_p \cdot v^3}$
$\xi_e = 1 - \left(0{,}4 - \frac{\lambda}{5}\right) \cdot \frac{F_W}{F_p}$	$c_a \cdot l = N_{(PS)} / \varrho \cdot z \cdot D^3 \cdot \left(\frac{v}{100}\right)_{km/h} \cdot \left(\frac{n_p}{100}\right)^2_{1/min} \cdot B$

No.		Unit						
1	V	km/h	400	500	550	600	700	800
2	v	m/s	111,1	139	152,9	167	194,5	222
3	v^3	$(m/s)^3 \cdot 10^{-6}$	1,37	2,68	3,56	4,65	7,35	10,99
4	U	m/s	231	"	"	"	"	"
5	λ	—	0,482	0,604	0,663	0,725	0,844	0,964
6	Ma	—	0,84	0,88	0,91	0,935	0,99	1,07
7	c_l	—	0,378	0,193	0,1452	0,1118	0,0704	0,0472
8	η geschätzt	—	0,74	0,82	0,83	0,84	0,79	0,64
9	B	—	1,005	1,028	1,056	1,09	1,195	1,337
10	$c_a \cdot l_\sigma$	—	0,295	0,231	0,205	0,1815	0,1419	0,111
11	c_a	—	0,965	0,754	0,67	0,594	0,464	0,363
12	ε x) / xx)	—	— / 0,0865	0,003 / 0,082	0,008 / 0,0395	0,018 / 0,040	0,030 / 0,074	0,088 / 0,166
13	c_l/c_{li}	—	1,048	1,038	1,035	1,035	1,06	1,115
14	c_{li}	—	0,361	0,1862	0,1405	0,108	0,0664	0,0423
15	η_i	—	0,83	0,877	0,89	0,90	0,921	0,935
16	α_i	°	5,10	3,80	3,35	3,00	2,30	1,85
17	γ	°	2,09	1,835	1,92	2,29	4,24	9,42
18	$\alpha_i + \gamma$	°	7,19	5,635	5,27	5,29	6,54	11,27
19	η_{frei}	—	0,442	0,82	0,83	0,82	0,788	0,634
20	ξ_e	—						
21	η ges	—						
22	x) $\Delta\varepsilon_p$: λ, Ma Einfluß							
23	xx) $\varepsilon + \Delta\varepsilon_p$							
24								
25								

24.5. 1944 Mwd.

Table 12. High Altitude High Power Performance [From: Ref.12]

BLOHM & VOSS Flugzeugbau (B V) HAMBURG

Luftschraubenwirkungsgrade

Baumuster : Projekt P 208 ; 03	mit Motor : DB 608 L mit MW 50; Leistungen nach Blatt 9-603-2256 vom 5.5.44
Luftschraube	Flughöhe H = 9 km
Durchmesser D = 3,40 m	Leistung $N_{Start+Not}$ = 1750 PS
Blattzahl z = 4	Untersetzung i = 1: 1,93
Tiefenverhältnis $\tau_\sigma = b/D$ = 0,09	Motordrehzahl n_M = 2700 1/min
Dickenverhältnis $\delta_\sigma = (d/l)_\sigma$ = 0,07	Luftschr.-Drehzahl n_p = 1400 1/min = 23,4 1/sek
$l_\sigma = \tau_\sigma \cdot D$ = 0,306 m	ϱ = 0,0476; Polare: „17'
$F_p = \frac{\pi \cdot D^2}{4}$ = 9,075 m²	$\frac{150}{\varrho}$ = 3151; + λ, Ma Einfluß, δ: 0,07 Mittelwert
D^3 = 39,35 m³	$\varrho \cdot z \cdot D^3 \cdot \left(\frac{n_p}{100}\right)^2_{(1/min)}$ = 1469
F_W = — ([illegible]) m²	$c_l = \frac{150}{\varrho} \cdot \frac{N}{F_p \cdot v^3}$
$\xi_e = 1 - \left(0{,}4 - \frac{\lambda}{5}\right) : \frac{F_W}{F_p}$	$c_a \cdot l = N_{(PS)} / \varrho \cdot z \cdot D^3 \cdot \left(\frac{v}{100}\right)_{km/h} \cdot \left(\frac{n_p}{100}\right)^2_{1/min} \cdot B$

No.		Unit						
1	V	km/h	400	500	550	600	700	800
2	v	m/s	111,1	139	152,9	167	194,5	222
3	v^3	(m/s)³·10⁻⁶	1,37	2,68	3,56	4,63	7,35	10,99
4	U	m/s	250	"	"	"	"	"
5	λ	—	0,445	0,556	0,611	0,669	0,779	0,888
6	Ma	—	0,895	0,94	0,96	0,98	1,0[illegible]	1,09
7	c_l	—	0,444	0,226	0,1705	0,1310	0,0726	0,0554
8	$\eta_{geschätzt}$	—	0,75	0,79	0,80	0,85	0,75	0,65
9	B	—	1,003	1,02	1,04	1,05	1,17	1,28
10	$c_a \cdot l$	—	0,2945	0,234	0,2085	0,1895	0,1455	0,1165
11	c_a	—	0,972	0,766	0,682	0,619	0,476	0,381
12	ε x) xx)	—	0,002 / 0,059	0,005 / 0,0425	0,008 / 0,0475	0,019 / 0,052	0,038 / 0,0935	0,076 / 0,156
13	c_l/c_{li}	—	1,075	1,055	1,05	1,055	1,08	1,115
14	c_{li}	—	0,413	0,214	0,1625	0,1241	0,0765	0,0496
15	η_i	—	0,825	0,866	0,88	0,899	0,912	0,935
16	α_i	°	5,15	4,10	3,65	3,35	2,40	1,90
17	γ	°	2,86	2,44	2,55	2,98	5,34	8,86
18	$\alpha_i + \gamma$	°	8,01	6,54	6,20	6,33	7,74	10,76
19	η_{frei}	—	0,745	0,793	0,802	0,80	0,758	0,66
20	ξ_e	—						
21	η_{ges}	—						
22	x) $\Delta\varepsilon_p$ = λ, Ma Einfluß							
23	xx) $\varepsilon + \Delta\varepsilon_p$							
24								
25								

9? X 1944 [illegible]

APPENDIX C: VORVIEW PRODUCTS

Examples of VORVIEW output file, “P208_C.out”, and stability derivatives output, “P208_C.lon” are shown.

```
***********************************************
*****        VORLAX/VORVIEW                *****
***** -       SUMMARY OUTPUT FILE           *****
*****                                       ****
***********************************************

 FILE NAME: P208_C

*** SOLUTION INPUT PARAMETERS ***
 LAX    =       0    EQUAL CHORDWISE VORTICE SPACING
 HAG    =    0.000    HEIGHT ABOVE GROUND
 ITRMAX =      200    MAX NUMBER OF ITERATIONS
 NPAN   =       78    NUMBER OF MAJOR PANELS
 NAP    =       20    NUMBER OF CAMBER POINTS
 TOTPAN =     1950    NUMBER OF SUB-PANELS
 SPC    =    0.100    LEADING EDGE SUCTION MULT (SPC < 0.0 - POLHAMUS ANALOGY)

*** GEOMETRY PARAMETERS ***
 SREF   =  204.540    REF WING AREA
 AR     =    4.750    REF WING ASPECT RATIO
 TAPER  =    1.000    REF WING TAPER RATIO
 WSPAN  =   31.170    REF WING SPAN
 CBAR   =    6.560    PITCHING MOMENT REF LENGTH
 XBAR   =   14.930    X VALUE OF MOMENT REF POINT
 ZBAR   =    0.000    Z VALUE OF MOMENT REF POINT

*** FLIGHT CONDITION PARAMETERS ***
 LATRAL =       0    SYMETRIC FLIGHT/CONFIG
 PSI    =    0.000    SIDESLIP ANGLE (DEGREES)
 PITCHQ =    0.000    PITCH RATE (DEGS/SEC)
 ROLLQ  =    0.000    ROLL RATE (DEGS/SEC)
 YAWQ   =    0.000    YAW RATE (DEGS/SEC)
 NMACH  =    1        NUMBER OF MACH NOS
 MACH NO =    0.730
 NALPHA =       1    NUMBER OF ATTACK ANGLES
 ALPHA  =   -0.083

*** RESULTS ***
 CLTOT  - TOTAL LIFT COEFFICIENT
 CDTOT  - TOTAL PRESSURE DRAG COEFFICIENT
 CYTOT  - TOTAL LATERAL FORCE COEFFICIENT
 CMTOT  - TOTAL PITCHING MOMENT COEFFICIENT
 CRMTOT - TOTAL ROLLING MOMENT COEFFICIENT
 CYMTOT - TOTAL YAWING MOMENT COEFFICIENT
 E      - OSWALDS EFFICIENCY FACTOR
 ITER   - NUMBER OF ITERATIONS TO CONVERGENCE
```

MACH NO = 0.730

ALPHA	CLTOT	CDTOT	CLTRF	CDTRF	CYTOT
CMTOT	CRMTOT	CYMTOT	CD/CL^2	E	(CD/CL^2)_TRF
E_TRF	ITER				
-0.08	0.22499	0.00468	0.22035	0.00533	0.00000
0.00000	0.00003	0.00000	0.09248	0.72459	0.10978
0.61044	53				

CONVERGED ON TRIM CONDITION!
CL AT TRIM POINT IS: 0.2249999
CM AT TRIM POINT IS: -5.4944127E-07
TRIM ALPHA IS: -8.2743317E-02
TRIM DELTA IS: 2.150649

***** LONGITUDINAL DERIVATIVES OUTPUT, .lon FILE ****

########################

MACH_o: 0.7300000
ALPHA_o: -8.3000004E-02
U_o: 1.000000

CLo: 0.22499
CDo: 0.01447
CYo: 0.00000
Clo: -0.00003
Cmo: 0.00000
Cno: 0.00000

CL_alpha: 5.96435
CL_beta: -0.00017
CL_mach: 0.17873
CL_p: 0.00970
CL_q: 7.44119
CL_r: 0.02858
CL_u: 0.13047
CL_alpha_2: -1.62546
CL_alpha_dot: 5.93396
CD_alpha: 0.19646
CD_beta: -0.58471
CD_mach: 0.10037
CD_p: -0.01154
CD_q: 0.21466
CD_r: -0.04337
CD_u: 0.07327
CD_alpha_2: 75.25758
CD_alpha_dot: 0.00000
CY_alpha: 0.00007
CY_beta: -0.11861
CY_mach: 0.00000
CY_p: 0.17894
CY_q: 0.00025
CY_r: 0.07042
CY_u: 0.00000
CY_alpha_2: 0.00595
CY_alpha_dot: 0.00000
Cl_alpha: -0.00062
Cl_beta: -0.03616
Cl_mach: 0.00000
Cl_p: -0.96391
Cl_q: -0.00199
Cl_r: -0.01365
Cl_u: 0.00000
Cl_alpha_2: 0.04811
Cl_alpha_dot: 0.00000
Cm_alpha: -1.12150
Cm_beta: 0.00007
Cm_mach: -0.03812

Cm_p: -0.00640
Cm_q: -6.60028
Cm_r: -0.07526
Cm_u: -0.02783
Cm_alpha_2: 0.20415
Cm_alpha_dot: -5.26338
Cn_alpha: -0.00003
Cn_beta: 0.01719
Cn_mach: 0.00000
Cn_p: -0.12378
Cn_q: -0.00023
Cn_r: -0.02608
Cn_u: 0.00000
Cn_alpha_2: 0.00365
Cn_alpha_dot: 0.00000

########################
name: elevator

MACH: 0.73000
ALPHA: -0.08300

CL_delta: 0.41949
CD_delta: -0.01177
CY_delta: 0.00000
Cl_delta: 0.00001
Cm_delta: -0.75488
Cn_delta: 0.00000

########################
name: flap

MACH: 0.73000
ALPHA: -0.08300

CL_delta: 1.51916
CD_delta: 0.60356
CY_delta: -0.00002
Cl_delta: 0.00017
Cm_delta: -0.16041
Cn_delta: 0.00002

########################
name: aileron

MACH: 0.73000
ALPHA: -0.08300

CL_delta: 0.50592
CD_delta: 0.56625
CY_delta: 0.00001
Cl_delta: -0.00008
Cm_delta: -0.43908
Cn_delta: -0.00001

APPENDIX D: DIMENSIONAL STABILITY DERIVATIVES

Table 13, from reference 17, shows the dimensionalization equations and units for the dimensional derivatives in Table 14. Table 14 list the values for the stability derivatives calculated for the P 208 by VOREVIEW in dimensionalized form.

Table 13. Dimensional Derivative Description [Ref. 17]

Term	Description	Units
X_u	$-\frac{QS}{mV}\left(2C_D + M\frac{\partial C_D}{\partial M}\right)$	s^{-1}
X_α	$\frac{QS}{m}\left(C_L - \frac{\partial C_D}{\partial \alpha}\right)$	$ft \cdot s^{-2}$
$X_{\dot{\alpha}}$	$-\frac{QS}{m}\left(\frac{c}{2V}\right)\frac{\partial C_D}{\partial(\dot{\alpha}c/2V)}$	$ft \cdot s^{-1}$
X_q	$-\frac{QS}{m}\left(\frac{c}{2V}\right)\frac{\partial C_D}{\partial qc/2V}$	$ft \cdot s^{-1}$
X_δ	$-\frac{QS}{m}\frac{\partial C_D}{\partial \delta}$	$ft \cdot s^{-2}$
Z_u	$-\frac{QS}{mV}\left(2C_L + M\frac{\partial C_L}{\partial M}\right)$	s^{-1}
Z_α	$-\frac{QS}{m}\left(C_D + \frac{\partial C_L}{\partial \alpha}\right)$	$ft \cdot s^{-2}$
$Z_{\dot{\alpha}}$	$-\frac{QS}{m}\left(\frac{c}{2V}\right)\frac{\partial C_L}{\partial(\dot{\alpha}c/2V)}$	$ft \cdot s^{-1}$
Z_q	$-\frac{QS}{m}\left(\frac{c}{2V}\right)\frac{\partial C_L}{\partial(qc/2V)}$	$ft \cdot s^{-1}$
Z_δ	$-\frac{QS}{m}\frac{\partial C_L}{\partial \delta}$	$ft \cdot s^{-2}$
M_u	$\frac{QSc}{I_y V}M\frac{\partial C_m}{\partial M}$	$ft^{-1} \cdot s^{-1}$
M_α	$\frac{QSc}{I_y}\frac{\partial C_m}{\partial \alpha}$	s^{-2}
$M_{\dot{\alpha}}$	$\frac{QSc}{I_y}\left(\frac{c}{2V}\right)\frac{\partial C_m}{\partial(\dot{\alpha}c/2V)}$	s^{-1}
M_q	$\frac{QSc}{I_y}\left(\frac{c}{2V}\right)\frac{\partial C_m}{\partial(qc/2V)}$	s^{-1}
M_δ	$\frac{QSc}{I_y}\frac{\partial C_m}{\partial \delta}$	s^{-2}

Term	Description	Units
Y_β	$\frac{QS}{m}\frac{\partial C_Y}{\partial \beta}$	$ft \cdot s^{-2}$
Y_p	$\frac{QS}{m}\left(\frac{b}{2V}\right)\frac{\partial C_Y}{\partial(pb/2V)}$	$ft \cdot s^{-1}$
Y_r	$\frac{QS}{m}\left(\frac{b}{2V}\right)\frac{\partial C_Y}{\partial(rb/2V)}$	$ft \cdot s^{-1}$
Y_δ	$\frac{QS}{m}\frac{\partial C_Y}{\partial \delta}$	$ft \cdot s^{-2}$
L_β	$\frac{QSb}{I_x}\frac{\partial C_l}{\partial \beta}$	s^{-2}
L_p	$\frac{QSb}{I_x}\left(\frac{b}{2V}\right)\frac{\partial C_l}{\partial(pb/2V)}$	s^{-1}
L_r	$\frac{QSb}{I_x}\left(\frac{b}{2V}\right)\frac{\partial C_l}{\partial(rb/2V)}$	s^{-1}
L_δ	$\frac{QSb}{I_x}\frac{\partial C_l}{\partial \delta}$	s^{-2}
N_β	$\frac{QSb}{I_z}\frac{\partial C_n}{\partial \beta}$	s^{-2}
N_p	$\frac{QSb}{I_z}\left(\frac{b}{2V}\right)\frac{\partial C_n}{\partial(pb/2V)}$	s^{-1}
N_r	$\frac{QSb}{I_z}\left(\frac{b}{2V}\right)\frac{\partial C_n}{\partial(rb/2V)}$	s^{-1}
N_δ	$\frac{QSb}{I_z}\frac{\partial C_n}{\partial \delta}$	s^{-2}

Table 14. P 208 Dimensional Derivatives

	Appr	SL pen	Cruise	Vmax
Xu, s-1	-0.0567	-0.0412	-0.0159	-0.0225
Xa, ft/s2	-1.9336	22.8578	-7.6871	4.0856
Mu, ft-1?s-1	-2.96E-04	-5.37E-04	-3.64E-04	-9.36E-04
Ma, s-2	-3.5536	-43.5811	-16.1411	-27.2726
Madot, s-1	-0.3549	-1.1944	-0.4514	-0.5809
Mq, s-1	-0.4451	-1.4977	-0.5661	-0.7285
Zu, s-1	-0.3194	-0.1218	-0.128	-0.1151
Za, ft/s2	-112.4707	-1.40E+03	-506.0536	-857.8977
Zadot, ft/s	-2.1722	-7.9257	-2.9555	-3.8608
Zq, ft/s	-2.724	-9.9389	-3.7062	-4.8414
Xde, ft/s2	-0.2415	2.694	-0.7908	1.6873
Mde, s-2	-2.8815	-30.1954	-11.0846	-18.3576
Zde, ft/s2	-9.047	-100.64	-36.2656	-60.1372
$Y_{ß}$, ft/s^2	-14.6865	-95.0953	-57.1661	-55.8333
Y_p, ft/s	0.3286	1.0185	0.4246	0.4958
Y_r, ft/s	2.20E-05	5.88E-05	2.65E-05	2.78E-05
$L_{ß}$, s^{-2}	-5.8041	-1.3831	-4.6904	-3.7639
L_p, s^{-1}	-1.0294	-3.503	-1.3291	-1.6686
L_r, s^{-1}	0.3129	-0.0488	0.008	-0.0084
$N_{ß}$, s^{-2}	0.3576	0.0353	1.3073	0.2741
N_r, s^{-1}	-0.0987	-0.216	-0.1003	-0.1031
N_p, s^{-1}	-0.0983	-0.2875	-0.0881	-0.1317
Y_{dr}, ft/s^2	2.156	23.4442	8.4733	13.7298
Y_{da}, ft/s^2	-0.0794	-1.1416	-0.4754	-0.7418
L_{dr}, s^{-2}	0.0902	1.0647	0.3179	0.582
L_{da}, s^{-2}	2.5926	26.355	9.8276	15.0431
N_{dr}, s^{-2}	-0.2838	-2.8604	-1.0657	-1.6956
N_{da}, s^{-2}	-0.029	-0.4701	-0.0351	-0.0537
$L'_{ß}$, s^{-2}	-5.8006	-1.3829	-4.6764	-3.7612
L'_p, s^{-1}	-1.0306	-3.5064	-1.3302	-1.6702
L'_r, s^{-1}	0.3118	-0.0512	0.0069	-0.0095
$N'_{ß}$, s^{-2}	0.3169	0.0256	1.2745	0.2477

N'_p, s^{-1}	-0.1055	-0.3122	-0.0975	-0.1434
N'_r, s^{-1}	-0.0965	-0.2163	-0.1003	-0.1032
L'_{dr}, s^{-2}	0.0871	1.0333	0.3062	0.5634
N'_{dr}, s^{-2}	-0.2832	-2.8531	-1.0636	-1.6917
L'_{da}, s^{-2}	2.5925	26.3519	9.828	15.0436
N'_{da}, s^{-2}	-0.0108	-0.285	0.0339	0.052

THIS PAGE INTENTIONALLY LEFT BLANK

APPENDIX E: MATLAB CODE

The following is a listing of the MATLAB, Version 6.0, code used to determine the P 208's longitudinal and lateral-directional eigenvalues, roots, natural frequencies, damping ratios and mode response.

```
% Longitudinal Dimentional derivatives
% P208 Cruise Profile (M=.57, H=29500)
% Vorview generated dimensionless derivatives

Ix=18143;
Iy=12370;
Iz=28474;
Ixz=200;
G=1/(1-Ixz^2/(Ix*Iz));
Q=146.6;
U=568.28;
S=204.53;
b=31.43;
c=6.56;
m=10300/32.2;
M=.57;

Cl=0.35;
Cd=0.0201;
Clalpha=5.4834;
ClM=0.1598;
Clq=6.9833;
Clalphadot=5.5688;
Cdalpha=0.4336;
CdM=0.10195;
Cmalpha= -1.0151;
CmM=-0.0228;
Cmq=-6.1682;
Cmalphadot=-4.9188;

Clde=0.3944;
Cdde=0.0086;
Cmde=-0.6971;

Xu=-Q*S/(m*U)*(2*Cd+M*CdM)
Xalpha=Q*S*(Cl-Cdalpha)/m
Mu=Q*S*c*M*CmM/(Iy*U)
Malpha=Q*S*c*Cmalpha/Iy
Malphadot=Q*S*c^2*Cmalphadot/(2*U*Iy)
Mq=Q*S*c^2*Cmq/(2*U*Iy)
Zu=-Q*S/(m*U)*(2*Cl+M*ClM)
Zalpha=-Q*S*(Cd+Clalpha)/m
Zalphadot=-Q*S*c*Clalphadot/(2*U*m)
Zq=-Q*S*c*Clq/(2*U*m)
```

```
Xde=-Q*S*Cdde/m
Mde=Q*S*c*Cmde/Iy
Zde=-Q*S*Clde/m

A=[Xu Xalpha/U 0 -32.174/U;
   U*Zu/(U-Zalphadot) Zalpha/(U-Zalphadot) (U+Zq)/(U-Zalphadot) 0;
   U*Mu+Malphadot*U*Zu/(U-Zalphadot) Malpha+Malphadot*Zalpha/(U-Zalphadot)
Mq+Malphadot*(U+Zq)/(U-Zalphadot) 0;
   0 0 1 0];

B=[Xde/U;Zde/(U-Zalphadot); Mde+Malphadot*Zde/(U-Zalphadot);0];
b=zeros(4,1);
d=zeros(4,1);
C=eye(4);
p=poly(A)
r=roots(p)
[Wn,Z]=damp(r)
[V,D]=eig(A)

%Short period magnitude and phasing

MAGshort=abs(V(:,1));PHshort=angle(V(:,1));
magnormalph=MAGshort'/MAGshort(2)    %Magnitude relative to alpha
phasenormalph=PHshort'-PHshort(2)     %Phase relative to alpha in radians
Wnshort=Wn(1);

%Long period magnatude and phasing

MAGlong=abs(V(:,3));PHlong=angle(V(:,3));
magnormu=MAGlong'/MAGlong(1)   %Magnitude relative to u/V
phasenormu=PHlong'-PHlong(1)   %Phase relative to u/V
Wnlong=Wn(3);

% INITIAL CONDITIONS
%    Normalized to alpha for short period
%    Normalized to u/V for long period

x0short=[magnormalph.*cos(phasenormalph)+i.*magnormalph.*sin(phasenormalph)]';
x0long=[magnormu.*cos(phasenormu)+i.*magnormu.*sin(phasenormu)]';

sysini=ss(A,B,C,d);

x0shortreal=real(x0short);
[yshort,tshort,xshort]=initial(sysini,x0shortreal,6);

figure
plot(tshort(:,1),xshort(:,1),':',tshort(:,1),xshort(:,2),'-',tshort(:,1),xshort(:,3),'-
',tshort(:,1),xshort(:,4),'--')
legend('u/V','\alpha','q','\theta')
xlabel('Time, sec')
ylabel('Response')
grid on

figure
x0longreal=real(x0long);
```

```
[ylong,tlong,xlong]=initial(sysini,x0longreal,[0:1:200]);
plot(tlong,xlong)
plot(tlong(:,1),xlong(:,1),':',tlong(:,1),xlong(:,2),'-',tlong(:,1),xlong(:,3),'-.',tlong(:,1),xlong(:,4),'--')
legend('u/V','\alpha','q','\theta')
xlabel('Time, sec')
ylabel('Response')
grid on

sysstep=ss(A,B,C,d);
[ystep,tstep,xstep]=step(sysstep,10);
figure
plot(tstep,ystep(:,2),tstep,ystep(:,3))
legend('\alpha','q')
xlabel('Time, sec')
ylabel('Response')
grid on

[ystep2,tstep2,xstep2]=step(sysstep,25);
figure
plot(tstep2,.1*ystep2(:,1),':',tstep2,ystep2(:,2),'-',tstep2,ystep2(:,3),'-.',tstep2,.1*ystep2(:,4),'--')
legend('.1*u/V','\alpha','q','.1*\theta')
xlabel('Time, sec')
ylabel('Response')
grid on
```

LATERAL – DIRECTIONAL CODE

```
% Lateral-Directional
% P208  Cruise Profile (M=.57, H=29500')
% Vorview generated dimensionless derivatives


clear
Ix=18143;
Iy=12370;
Iz=28474;
Ixz=200;
G=1/(1-Ixz^2/(Ix*Iz));
Q=146.6;
U=568.28;
S=204.53;
b=31.43;
c=6.56;
m=10500/32.2;
M=.57;

Cyb=-0.6217;
Cyp=0.1670;
Cyr=0.2967;
Clb=-0.0903;
Clp=-0.9253;
Clr=0.00556;
Cnb=0.03950;
Cnp=-0.09631;
```

```
Cnr=-0.1096;


Cydr=0.09215;
Cldr=0.00612;
Cndr=-0.0322;
Cyda=-0.00517;
Clda=0.1892;
Cnda=-0.00106;

Yb=Q*S*Cyb/m;
Yp=Q*S*b*Cyp/(2*U*m);
Yr=Q*S*b*Cyr/(2*U*m*Iz);
Lb=Q*S*b*Clb/(Ix);
Lp=Q*S*b^2*Clp/(2*U*Ix);
Lr=Q*S*b^2/(2*U*Ix)*Clr;
Nb=Q*S*b*Cnb/Iz;
Nr=Q*S*b^2*Cnr/(2*U*Iz);
Np=Q* S*b^2*Cnp/(2*U*Iz);

Ydr=Q*S*Cydr/m;
Yda=Q*S*Cyda/m;
Ldr=Q*S*b*Cldr/Ix;
Lda=Q*S*b*Clda/Ix;
Ndr=Q*S*b*Cndr/Iz;
Nda=Q*S*b*Cnda/Iz;


Lbpr=(Lb+Nb*(Ixz/Ix))*G;
Lppr=(Lp+Np*Ixz/Ix)*G;
Lrpr=(Lr+Nr*Ixz/Ix)*G;
Nbpr=(Nb+Lb*Ixz/Iz)*G;
Nppr=(Np+Lp*Ixz/Iz)*G;
Nrpr=(Nr+Lr*Ixz/Iz)*G;

Ldrpr=(Ldr+Ndr*Ixz/Ix)*G;
Ndrpr=(Ndr+Ldr*Ixz/Iz)*G;
Ldapr=(Lda+Nda*Ixz/Ix)*G;
Ndapr=(Nda+Lda*Ixz/Iz)*G;

A=[Yb/U Yp/U 32.2/U (Yr-U)/U;
   Lbpr Lppr 0 Lrpr;
   0 1 0 0;
   Nbpr Nppr 0 Nrpr];

Bdr=[Ydr/U;Ldrpr;0;Ndrpr];
Bda=[Yda/U;Ldapr;0;Ndapr];
b=zeros(4,1);
d=zeros(4,1);
C=eye(4);
[V,D]=eig(A)
p=poly(A)
r=roots(p)
[Wn,Z]=damp(r)

%Dutch roll values
```

```
MAGdr=abs(V(:,3));PHdr=angle(V(:,3));
magnormbeta=MAGdr'/MAGdr(1)    %Magnitude relative to beta
phasenormbeta=PHdr'-PHdr(1)     %Phase relative to beta in radians
Wndr=Wn(3);

%Roll values

MAGroll=abs(V(:,1));PHroll=angle(V(:,1));
magnormp=MAGroll'/MAGroll(2)    %Magnitude relative to roll rate
phasenormp=PHroll'-PHroll(2)     %Phase relative to roll rate in radians
Wnroll=Wn(1);

%Spira1 mode

MAGspiral=abs(V(:,4));PHspiral=angle(V(:,4));
magnormphi=MAGspiral'/MAGspiral(3)    %Magnitude relative to roll angle
phasenormphi=PHspiral'-PHspiral(3)     %Phase relative to roll angle in radians
Wnroll=Wn(4);

% Initial Conditions

x0dr=[magnormbeta.*cos(phasenormbeta)+i.*magnormbeta.*sin(phasenormbeta)]';
x0roll=[magnormp.*cos(phasenormp)+i.*magnormp.*sin(phasenormp)]';
x0spiral=[magnormphi.*cos(phasenormphi)+i.*magnormphi.*sin(phasenormphi)]';

x0drreal=real(x0dr);
x0rollreal=real(x0roll);
x0spiralreal=real(x0spiral);

sysini=ss(A,b,C,d);
syssteprudd=ss(A,Bdr,C,d);

figure
[ydr,tdr,xdr]=initial(sysini,x0drreal,[0:.01:20]);
plot(tdr,xdr(:,1),'-',tdr,xdr(:,2),':',tdr,xdr(:,3),'-.',tdr,xdr(:,4),'--')
legend('\beta','p','\phi','r')
grid on
xlabel('Time (sec)');
ylabel('Response')

figure
[yroll,troll,xroll]=initial(sysini,x0rollreal,[0:.01:6]);
plot(troll,xroll(:,1),'-',troll,xroll(:,2),':',troll,xroll(:,3),'-.',troll,xroll(:,4),'--')
legend('\beta','p','\phi','r')
grid on
xlabel('Time (sec)');
ylabel('Response')

figure
[yspiral,tspiral,xspiral]=initial(sysini,x0spiralreal,[0:.1:100]);
plot(tspiral,xspiral(:,1),'-',tspiral,xspiral(:,2),':',tspiral,xspiral(:,3),'-.',tspiral,xspiral(:,4),'--')
legend('\beta','p','\phi','r')
grid on
xlabel('Time (sec)');
ylabel('Response')
```

```
[time1,out1]=sim('rudderimp',[0:.1:20]);

figure
plot(time1,out1(:,1),'-',time1,out1(:,2),':',time1,out1(:,3),'-.',time1,out1(:,4),'--',time1,rudinput);
legend('\beta','p','\phi','r','input pulse')
grid on
xlabel('Time (sec)');
ylabel('Response')

[time2,out2]=sim('rudderimp',20);


figure
plot(time2,out2(:,1),time2,out2(:,3));
hold on
legend('\beta','\phi')
grid on
xlabel('Time (sec)');
ylabel('Response')

[time3,out3]=sim('ailimp',[0:.1:20]);

figure
plot(time3,out3(:,1),time3,out3(:,3),time3,input);
legend('\beta','\phi','Input pulse')
grid on
xlabel('Time (sec)');
```

APPENDIX F: RAM FILE

The following is a listing of the P 208 RAM file. This file should be of use in future studies.

```
RAM GEOMETRY FILE 1.05
7                                   Number 0f Components

//****************** WING COMPONENT ******************//
//==== General Parms ====//
0                                   Type
          Wing            Name
0                                   ID Number
       414943041                    ID String
4                                   Color
2                                   Symmetry Code
  4.075    0.000   -0.594 Translation
  0.000    2.000    0.000 Rotation
//==== Wing Parms ====//
7                                   Wing Driver Group
9.500000                            Span
4.750000                            Aspect Ratio
1.000000                            Taper Ratio
19.000000                           Area
2.000000                            Root Chord
2.000000                            Tip Chord
0.577350                            Tan Sweep
0.250000                            Sweep Loc
0.105104                            Tan Dihedral
0.000000                            Twist Loc
0.000000                            Twist
0                                   Flap Type
0.000000                            Flap Inboard Span
1.000000                            Flap Outboard Span
0.200000                            Flap Chord
0                                   Slat Type
0.000000                            Slat Inboard Span
1.000000                            Slat Outboard Span
0.200000                            Slat Chord
0                                   All Move CS
//==== Root Airfoil ====//
33                                  Num of Airfoil Pnts
0.020000                            Airfoil Camber
0.400000                            Camber Loc
0.120000                            Thickness
//==== Tip Airfoil ====//
```

```
33                              Num of Airfoil Pnts
0.020000                        Airfoil Camber
0.400000                        Camber Loc
0.120000                        Thickness

//****************** FUSE COMPONENT ******************//
//==== General Parms ====//
1                               Type
          prop            Name
1                               ID Number
        467012626               ID String
0                               Color
0                               Symmetry Code
  8.500    0.000    0.000 Translation
  0.000    0.000    0.000 Rotation
//==== Fuse Parms ====//
0.200000                        Fuse Length
0.000000                        Camber
0.500000                        Camber Location
0.000000                        Aft Offset
0.000000                        Nose Angle
0.300000                        Nose Strength
0.790297                        Nose Rho
1.686500                        Aft Rho
3                               Number of Xsecs
//==== Cross Section Number 0 ====//
0                               Fuse Xsec Type
0.000000                        Z_Offset
0.000000                        Location On Spine
33                              Number of Pnts Per Xsec
//==== Cross Section Number 1 ====//
1                               Fuse Xsec Type
0.000000                        Z_Offset
0.500000                        Location On Spine
33                              Number of Pnts Per Xsec
3.750000                        Height
//==== Cross Section Number 2 ====//
0                               Fuse Xsec Type
0.000000                        Z_Offset
1.000000                        Location On Spine
33                              Number of Pnts Per Xsec

//****************** FUSE COMPONENT ******************//
//==== General Parms ====//
1                               Type
          cooler            Name
2                               ID Number
        466757500               ID String
29                              Color
0                               Symmetry Code
  4.123    0.000   -0.892 Translation
```

```
  0.000    0.000    0.000 Rotation
//==== Fuse Parms ====//
4.419918                        Fuse Length
0.000000                        Camber
0.500000                        Camber Location
0.000000                        Aft Offset
0.000000                        Nose Angle
0.300000                        Nose Strength
0.640000                        Nose Rho
0.809312                        Aft Rho
3                               Number of Xsecs
//==== Cross Section Number 0 ====//
1                               Fuse Xsec Type
0.000000                        Z_Offset
0.000000                        Location On Spine
33                              Number of Pnts Per Xsec
0.700000                        Height
//==== Cross Section Number 1 ====//
1                               Fuse Xsec Type
0.000000                        Z_Offset
0.250000                        Location On Spine
33                              Number of Pnts Per Xsec
0.850000                        Height
//==== Cross Section Number 2 ====//
0                               Fuse Xsec Type
0.530000                        Z_Offset
1.000000                        Location On Spine
33                              Number of Pnts Per Xsec

//****************** FUSE COMPONENT *****************//
//==== General Parms ====//
1                               Type
        Fuselage                Name
3                               ID Number
       415051778                ID String
62                              Color
0                               Symmetry Code
  1.250    0.000    0.000 Translation
  0.000    0.000    0.000 Rotation
//==== Fuse Parms ====//
8.319942                        Fuse Length
0.015000                        Camber
0.500000                        Camber Location
0.000000                        Aft Offset
0.088224                        Nose Angle
0.300000                        Nose Strength
0.530000                        Nose Rho
0.542341                        Aft Rho
5                               Number of Xsecs
//==== Cross Section Number 0 ====//
0                               Fuse Xsec Type
```

0.000000 Z_Offset
0.000000 Location On Spine
33 Number of Pnts Per Xsec
//==== Cross Section Number 1 ====//
4 Fuse Xsec Type
0.000000 Z_Offset
0.336314 Location On Spine
33 Number of Pnts Per Xsec
1.400000 Height
1.250000 Width
1.200000 Top Tan Strength
1.200000 Upper Tan Strength
1.200000 Lower Tan Strength
1.200000 Bottom Tan Strength
-0.646998 Max Width Location
0.500000 Corner Radius
1.570796 Top Tan Angle
1.570796 Bot Tan Angle
//==== Cross Section Number 2 ====//
4 Fuse Xsec Type
0.000000 Z_Offset
0.500000 Location On Spine
33 Number of Pnts Per Xsec
1.400000 Height
1.250000 Width
1.200000 Top Tan Strength
1.200000 Upper Tan Strength
1.200000 Lower Tan Strength
1.200000 Bottom Tan Strength
-0.646998 Max Width Location
0.500000 Corner Radius
1.570796 Top Tan Angle
1.570796 Bot Tan Angle
//==== Cross Section Number 3 ====//
4 Fuse Xsec Type
0.000000 Z_Offset
0.607037 Location On Spine
33 Number of Pnts Per Xsec
1.400000 Height
1.250000 Width
1.200000 Top Tan Strength
1.200000 Upper Tan Strength
1.200000 Lower Tan Strength
1.200000 Bottom Tan Strength
-0.646998 Max Width Location
0.500000 Corner Radius
1.570796 Top Tan Angle
1.570796 Bot Tan Angle
//==== Cross Section Number 4 ====//
0 Fuse Xsec Type
0.000000 Z_Offset

```
1.000000                        Location On Spine
33                              Number of Pnts Per Xsec

//****************** FUSE COMPONENT ******************//
//==== General Parms ====//
1                               Type
          Canopy                Name
4                               ID Number
        415115782               ID String
22                              Color
0                               Symmetry Code
  3.750    0.000    0.530 Translation
  0.000   -3.523    0.000 Rotation
//==== Fuse Parms ====//
1.967343                        Fuse Length
0.003814                        Camber
0.225400                        Camber Location
0.005210                        Aft Offset
-0.128401                       Nose Angle
0.191410                        Nose Strength
0.752160                        Nose Rho
0.694896                        Aft Rho
3                               Number of Xsecs
//==== Cross Section Number 0 ====//
0                               Fuse Xsec Type
0.000000                        Z_Offset
0.000000                        Location On Spine
33                              Number of Pnts Per Xsec
//==== Cross Section Number 1 ====//
2                               Fuse Xsec Type
0.000000                        Z_Offset
0.342369                        Location On Spine
33                              Number of Pnts Per Xsec
0.962029                        Height
0.808479                        Width
//==== Cross Section Number 2 ====//
0                               Fuse Xsec Type
0.000000                        Z_Offset
1.000000                        Location On Spine
33                              Number of Pnts Per Xsec

//****************** FUSE COMPONENT ******************//
//==== General Parms ====//
1                               Type
             pod                Name
5                               ID Number
        415328102               ID String
11                              Color
2                               Symmetry Code
  6.800    4.750   -0.170 Translation
  0.000    0.000    0.000 Rotation
```

```
//==== Fuse Parms ====//
4.000000                        Fuse Length
0.000000                        Camber
0.500000                        Camber Location
0.000000                        Aft Offset
0.000000                        Nose Angle
0.300000                        Nose Strength
0.640000                        Nose Rho
0.640000                        Aft Rho
5                               Number of Xsecs
//==== Cross Section Number 0 ====//
0                               Fuse Xsec Type
0.000000                        Z_Offset
0.000000                        Location On Spine
33                              Number of Pnts Per Xsec
//==== Cross Section Number 1 ====//
1                               Fuse Xsec Type
0.000000                        Z_Offset
0.250000                        Location On Spine
33                              Number of Pnts Per Xsec
0.300000                        Height
//==== Cross Section Number 2 ====//
1                               Fuse Xsec Type
0.000000                        Z_Offset
0.500000                        Location On Spine
33                              Number of Pnts Per Xsec
0.300000                        Height
//==== Cross Section Number 3 ====//
1                               Fuse Xsec Type
0.000000                        Z_Offset
0.750000                        Location On Spine
33                              Number of Pnts Per Xsec
0.300000                        Height
//==== Cross Section Number 4 ====//
0                               Fuse Xsec Type
0.000000                        Z_Offset
1.000000                        Location On Spine
33                              Number of Pnts Per Xsec

//****************** WING COMPONENT ******************//
//==== General Parms ====//
0                               Type
        empennage               Name
6                               ID Number
        415366934               ID String
4                               Color
2                               Symmetry Code
  8.942    4.750   -0.180 Translation
  0.000   -3.500    0.000 Rotation
//==== Wing Parms ====//
5                               Wing Driver Group
```

```
3.400000                    Span
3.238095                    Aspect Ratio
0.354839                    Taper Ratio
3.570000                    Area
1.550000                    Root Chord
0.550000                    Tip Chord
0.431289                    Tan Sweep
0.250000                    Sweep Loc
-0.363970                   Tan Dihedral
0.000000                    Twist Loc
0.000000                    Twist
0                           Flap Type
0.000000                    Flap Inboard Span
1.000000                    Flap Outboard Span
0.200000                    Flap Chord
0                           Slat Type
0.000000                    Slat Inboard Span
1.000000                    Slat Outboard Span
0.200000                    Slat Chord
0                           All Move CS
//==== Root Airfoil ====//
33                          Num of Airfoil Pnts
0.000000                    Airfoil Camber
0.000000                    Camber Loc
0.100000                    Thickness
//==== Tip Airfoil ====//
33                          Num of Airfoil Pnts
0.000000                    Airfoil Camber
0.000000                    Camber Loc
0.100000                    Thickness

//************** AERO PARMS **************//
0             Wing          Reference Component (ID #/Name)
1.000000                    Reference Area
1.000000                    Reference Span
1.000000                    Reference Chord
  5.947    0.000    0.000 C.G. Location
-1             None         Trimming Component (ID #/Name)
```

THIS PAGE INTENTIONALLY LEFT BLANK

APPENDIX G: ACSYNT

The P 208 ACSYNT file is given below with initial simple analysis results.

```
Started at:  Fri Mar  8 15:35:47 P ST 2002

 Engine Files:
/u/wk/ahahn/projects/erast/perseus/acsynt/matched/prop/Convert_to_new_acsynt/P208C copied to fort.3 (Lewis File)
/u/wk/ahahn/projects/erast/perseus/acsynt/matched/prop/Convert_to_new_acsynt/P208C copied to fort.9 (Ames File)

Note: The above link(s) do not necessarily indicated the engine file was used.
The type of engine used depends on the engine settings in the Trajectory
portion of the ACSYNT input file (MMPROP, IP).

################################################################################
#                                                                              #
#                              JOB TITLE                                       #
#                                                                              #
################################################################################

 $JOB
  TITLE = 'p208A'
 $END

################################################################################
#                                                                              #
#                            ACSYNT CONTROL                                    #
#                                                                              #
################################################################################

 A NEGATIVE NUMBER FOR AN MEXEC INPUT INDICATES THAT MODULE WILL ONLY BE
 EXECUTED AFTER WEIGHT CONVERGENCE. CONVERGE SET TO .TRUE. INDICATES A
 WEIGHT CONVERGENCE RUN, SET TO .FALSE. INDICATES A SINGLE PASS RUN.

 $ACSYNT
  CONVERGE = .FALSE.

    MREAD  = 5, NREAD  = 1,    2,    3,    4,    6,   14,    7,    9,
    MEXEC  = 3, NEXEC  = 1,    2,    6,    7,  -14,  -9,
    MWRITE = 5, NWRITE = 1,    2,    3,    6,    4,    7,   14,   9,

    TOL    = 0.00010,
     SLOPE = 0.75,
    WGMAX = 25000.0,

    IPSUM    = 1,     KGLOBP = 0,      INIT   = 0,     IPDBG     = 0,
    IGPLT    = 1,     IRDDTR = 7,      IPDTR  = 0,     MAXTHRUST = 0.,
    G4FIXWOS = 0.     EXTMAX = 0.2,    NUMCON = 0,
  $END

################################################################################
#                                                                              #
#                          GEOMETRY NAMELISTS                                  #
#                                                                              #
################################################################################

 $FUS   BDMAX  = 4.25,      BODL   = 26.4,   FRAB   = 2.5,
        FRN    = 3.7,    FRATIO = 6.5,    SFFACT = 1.18,
        ITAIL  = 1,         OUTCOD = 3,
 $END
 $WING  AR     = 4.75,      AREA   = 204.53,    DIHED  = 6.0,
        FDENWG = 43.0,      LFLAPC = 0.00,      SWEEP  = 30.0,
        SWFACT = 1.05,      TAPER  = 0.99,      TCROOT = 0.18,
        TCTIP  = 0.12,      TFLAPC = 0.25,      WFFRAC = 0.9,
        XWING  = 0.346,   ZROOT  =  -0.594,   KSWEEP = 1,
```

```
$END
$HTAIL  AR     = 3.24,      AREA   = 38.39,   SWEEP  = 23.33,
        SWFACT = 1.68,      TAPER  = 0.35,    TCROOT = 0.10,
        TCTIP  = 0.10,      XHTAIL = 1.103,   ZROOT  = -0.5,
        KSWEEP = 1,         SIZIT  = .FALSE.,         HTFRAC = -0.30,
        CVHT   = 1.0,
$END
$CREW  NCREW  = 1,    $END
$FUEL   DEN    = 43.0,     FRAC   = 0.9,    $END
$ENGINE N      = 1,       $END

#############################################################################
#                                                           #
#                    TRAJECTORY INPUTS                              #
#                                                           #
#############################################################################

$TRDATA   CRMACH = 0.47,   QMAX   = 425.0,   DESLF  = 6.0,    ULTLF  = 9.0,
        WFUEL  = 1323.0,  WFEXT  = 0.0,    WFTRAP = 50.0,   FRFURE = 0.05,

        IPSTO1 = 5,      TIMTO1 = 5.0,    IPSTO2 = 2,      TIMTO2 = 1.0,
        IPSLND = 5,      MODLND = 7,      VMRGLD = 1.2,    WKLAND = 0.75,
        RCTOC  = 500.,    XDESC  = 100.0,   DECEL=0.25,

        IBREG  = 0,      IENDUR = 0,      WCOMBP = 0.6,    MMPROP = 7,

        NCODE  = 0,      NCRUSE = 2,      RANGE  = 820.0,  LEGRES = 0,
        NMISS  = 1,      JDPMIS =.FALSE., LENVEL =.FALSE.,
        NLEGCL = 0,      NLEGLO = 0,              NLEGCR = 0,

        IPSIZE = 0,     IPRINT = 1,      KERROR = 2,      $END
       1
      MACH NO.   ALTITUDE     HORIZONTAL     NO.  VIND
PHASE   START END  START  END    DIST  TIME   TURN  "G"S  WKFUEL M IP IX W B A P
------- ---- ----  ----- -----  ------ -----  ---- -----  ------- - -- -- - - - -
 CLIMB   0.18 0.20      0 29000     45.0  0.0   0.0 160.0  1.0000 1  3 -1 0 0 0 0
 ACCEL     -1 0.55     -1   -1     0.0   5.0   0.0   0.0  1.0000 1  3 -1 0 0 0 0
 CRUISE  0.55 0.55     -1   -1     -1.0   0.0   0.0   0.0  1.0000 1  4 -1 0 0 0 0
 COMBAT  0.65 0.65     -1 15000     0.0  20.0   0.0   0.0  0.0300 1  2  0 0 0 0 0
 CLIMB   0.20 0.18      0 29000     20.0  0.0   0.0 160.0  1.0000 1  3 -1 0 0 0 0
 CRUISE  0.55 0.55     -1 29000    -1.0   0.0   0.0   0.0  1.0000 1  4 -1 0 0 0 0
 DESCENT   -1 0.30     -1     0     0.0   0.0   0.0   0.0  1.0000 1  5  0 0 0 0 0

#############################################################################
#                                                           #
#                    AERODYNAMIC INPUTS                             #
#                                                           #
#############################################################################


$ACHAR ABOSB=0.0,  ALMAX=15.0, AMC=40.0, BDNOSE= 4.25, ISMNDR=0,
        CLO=0.00053,0.00053,0.00052,0.00052,0.0005,0.00047,0.00045,0.00043,0.00039,
                0.00027,
        CLOW=0.0812,0.0819,0.0831,0.0848,0.0872,0.0906,0.0954,0.1024,0.1141,0.1545,
        CMO=0.0493,0.0496,0.0502,0.0507,0.0515,0.0525,0.0539,0.0558,0.0582,0.0604,
        SMNSWP= 0.12, 0.17, 0.30, 0.47, 0.50, 0.57, 0.70, 0.80, 0.90, 1.00,
        SFWF=.90,
        ALELJ=2,$END
$AMULT   ESSF=1.00, FCDF=1.00, FCDL=1.00,
        FCDRA=10*1.00,
        FCDO=1.00, FCDW=1.00, FCDWB=1.00, FENG=1.00, FINTF=1.00,
        FLBCOR=1.00, FLD=1.00, FLECOR=1.00, FMDR=1.00,$END
$ATRIM  FVCAM  = 10*0.89,
       FLDM   = 10*1.072
       FLAPI =    0.0,   0.0,   0.0,   0.0,   0.0,   0.0,   0.0,   0.0,   0.0,   0.0,
       ITRIM =      1,     1,     1,     1,     1,     1,     1,     1,     1,     1,
       IT = -3.5, CGM=0.32, CFLAP=0.25, SPANF=0.64, IVCAM=1, ALFVC=5.0, $END
$ADET    ALIN=-5.,-2.,0.,2.,4.,6.,8.,10.,12.,15.,
        ALTV= 0.0,5000.0,10000.0,20000.0,25000.0,29500.0,29500.0,40000.0,
        CLINPT=0.0,0.0,0.0,0.0,0.0,0.0,0.0,0.0,0.0,0.0,
```

```
      SMN=0.47,0.3,0.4,0.4,0.4,0.47,0.57,0.45,0.17,0.17,
      ICOD=1, IPLOT=1,
      ISTRS=0,0,0,0,0,0,0,0,0,0,
      ITB=0,0,0,0,0,0,0,0,0,0,
      ITS=0,0,0,0,0,0,0,0,0,0,
      NALF=10, NMDTL=10,    $END
 $ADRAG  CDBMB=10*0.0,
      CDEXTR=10*0.0,
      CDTNK=10*0.00,
      $END
 $ATAKE  CLLAND =1.20,    CLTO   =1.20,     DELFLD = 45.0,
        DELFTO = 30.0,     DELLED = 00.0,     DELLTO = 00.0,
        LDLAND =-1.0,     LDTO   = -1.0,     ALFROT = 18.0, IFLAP=1,    $END
 $APRINT KERROR=2,   $END


################################################################################
#                                                #
#                 PROPULSION INPUTS                          #
#                                                #
################################################################################

 $PCONTR  HNOUT = 0.,0.,29500.,29500.,40000.,
                SMNOUT= 0.17, 0.47, 0.47, 0.57, 0.5,
                NOUTPT= 5,  $END
 $PENGIN  ENGNUM = 1,         NTPENG = 3, ESZMCH = 0.00,
                ESZALT = 0.,XNMAX = 2700  , HPENG = 2071  ,
                SWTENG = 1.1 , HCRIT = 42000 , FSFC = 1.0,   $END
 $PROP    AF     = 124.5,     BL     = 4,         CLI    = 0.366,
      DPROP  = 11.15,     FPRW   = 1.0,     FTHR   = 1.0,
      NTPPRP = 12,        PSZMCH = 0.00,      PSZALT = 0.,
      $END
 $PGEAR  GR     = 1.93,       ETR    = 0.90,      FGRW   = 1.0,    $END
 $PENGNC XLENG  = 8.42,       RLENG  = 1.08,       DIA1   = 3.2,
      FT     = 0.0,       FRPN   = 2.25,       FRBT   = 6,
      NBDFT  = 3.82,      ANACHP = 0.,        DQ     = 1.0,
      $END

################################################################################
#                                                #
#                   WEIGHTS INPUTS                           #
#                                                #
################################################################################

 WTYPE = TRANsport--> TRANSPORT
     = FIGHter   --> FIGHTER
     = BOMBer   --> BOMBER
     = GEAV      --> GENERAL AVIATION

 $OPTS    WTYPE  = 'FIGH',
   WTITLE = 'P208 WEIGHTS',

   WGTO     = 11133.5, KERROR = 2,
   IPRINT   = 0,        ITAIL  = 0,

  $END

 $FIXW WTSUM = 11133.5,
            WBODY = 1168.45,  WHT = 154.32,   WLG = 749.57,    WWING = 1455.05,
            WFEQ = 1153.02,   WPS = 3891.16,  WCREW = 220.46,  WAMMUN = 308.65,
            WARM = 709.89, $END

################################################################################
################################################################################
################################################################################
################################################################################
#                                                #
#   THE FOLLOWING NAMELISTS ARE FOR ADS. UNLESS YOU ARE DOING SENSITIVITY     #
#   ANALYSES OR OPTIMIZATIONS, YOU MAY LEAVE THESE VARIABLES UNTOUCHED.       #
#                                                #
```

##
##
##
##

**** Sensitivity and Optimization variables not included, Output follows:

Output for Module # 1 –> GEOMETRY
****

FUSELAGE CROSS SECTION SIZING TO ACCOMODATE PAYLOAD
PAYLOAD WIDTH..... 0.0000E+00
PAYLOAD HEIGHT..... 0.0000E+00
THICKNESS OF WING ROOT..... 1.187
MAX THICKNESS OF WING FOR FREE FIT..... 0.0000E+00
DIAMETER REQUIRED FOR WIDTH OF EMBEDDED ENGINES.. 0.0000E+00
DIAMETER REQUIRED FOR HEIGHT OF EMBEDDED ENGINES. 0.0000E+00
DIAMETER REQUIRED TO ENCLOSE BOX..... 1.187
REQUIRED DIAMETER..(MAX OF 3 ABOVE)..... 1.187

RADIUS OF ENGINE POD..... 0.0000E+00
ANGLE OF ENGINE PLACEMENT (ABOVE HORIZONTAL)..... 0.0000E+00
STAND-OFF DISTANCE (NON-DIMENSIONAL)..... 0.0000E+00
STAND-OFF DISTANCE (FT.) ..... 0.0000E+00
LOC. OF CENTER OF ENGINE..... 0.5935

AIRCRAFT INTERNAL ARRANGEMENT

ITEM	LENGTH	INITIAL STATION	FINAL STATION	ACTUAL DIAM	REQD DIAM
RADAR	0.000	0.000	0.000	0.000	0.000
CREW	3.500	8.227	11.727	3.500	3.500
FUEL	2.158	11.727	13.885	4.042	

NOSE LENGTH..... 15.73
AFTERBODY BEGINS AT..... 15.77
OVERALL LENGTH..... 26.40
MAX. AFT FUEL LOCATION..... 21.09
DELTAX DUE TO PAYLOAD AFTERBODY MISMATCH.... 1000.
DELTAX DUE TO PAYLOAD-FUEL OVERLAP..... 1000.
DELTAX DUE TO FINENESS RATIO REQ..... 0.5000E-01
ACTUAL-REQUIRED CREW DIAMETER..... 0.7500
ACTUAL-REQUIRED PAYLOAD DIAMETER..... 3.063
ACTUAL-REQUIRED POWER PLANT DIAMETER..... 3.250
WING ROOT THICKNESS IN BODY..... 1.187
FUSELAGE WALL THICKNESS..... 0.0000E+00
VOLUME OF FORWARD FUEL..... 27.69
VOLUME OF REAR FUEL..... 0.0000E+00
ACTUAL-REQUIRED FUEL VOLUME..... 31.66

Fuselage Definition (Type 2)
Nose Length..... 15.725
Nose Fineness Ratio..... 3.700
Constant Section Length..... 0.050
Afterbody Length..... 10.625
Afterbody Fineness Ratio..... 2.500
Overall Length..... 26.400
Maximum Diameter..... 4.250
Body Planform Area..... 68.526

Fuselage Definition

X	R	Area
3.15	0.99	3.06
3.93	1.14	4.11
4.72	1.28	5.17
5.50	1.41	6.23
6.29	1.52	7.26
7.08	1.62	8.26
7.86	1.71	9.21
8.65	1.79	10.10

9.44	1.86	10.92
10.22	1.93	11.66
11.01	1.98	12.31
11.79	2.02	12.88
12.58	2.06	13.34
13.37	2.09	13.71
14.15	2.11	13.97
14.94	2.12	14.13
10.46	1.71	9.21
10.99	1.79	10.10
11.52	1.86	10.92
12.06	1.93	11.66
12.59	1.98	12.31
13.12	2.02	12.88
13.65	2.06	13.34
14.18	2.09	13.71
14.71	2.11	13.97
15.24	2.12	14.13
15.77	2.12	14.19
16.31	2.12	14.13
16.84	2.11	13.97
17.37	2.09	13.71
17.90	2.06	13.34
18.43	2.02	12.88
18.96	1.98	12.31
19.49	1.93	11.66
20.02	1.86	10.92
20.56	1.79	10.10
21.09	1.71	9.21
0.00	0.00	0.00
0.00	0.00	0.00
0.00	0.00	0.00
0.00	0.00	0.00
0.00	0.00	0.00
0.00	0.00	0.00
0.00	0.00	0.00
0.00	0.00	0.00
0.00	0.00	0.00
0.00	0.00	0.00

Fuselage

Max. Diameter..... 4.250
Fineness Ratio..... 6.212
Surface Area..... 387.844
Volume..... 200.543

Dimensions of Planar Surfaces (each)

	Wing	H.Tail	V.Tail	Canard	Units
NUMBER OF SURFACES.	1.0	1.0	1.0	1.0	
PLAN AREA.....	204.5	38.4	0.0	0.0	(SQ.FT.)
SURFACE AREA.....	386.5	73.1	0.0	0.0	(SQ.FT.)
VOLUME.....	137.8	6.9	0.0	0.0	(CU.FT.)
SPAN.....	31.169	11.153	0.000	0.000	(FT.)
L.E. SWEEP.....	30.045	30.109	0.000	0.000	(DEG.)
C/4 SWEEP.....	30.000	23.330	0.000	0.000	(DEG.)
T.E. SWEEP.....	29.863	-0.832	0.000	0.000	(DEG.)
ASPECT RATIO	4.750	3.240	0.000	0.000	
ROOT CHORD.....	6.595	5.100	0.000	0.000	(FT.)
ROOT THICKNESS.....	14.245	6.119	0.000	0.000	(IN.)
ROOT T/C	0.180	0.100	0.000	0.000	
TIP CHORD.....	6.529	1.785	0.000	0.000	(FT.)
TIP THICKNESS.....	9.402	2.142	0.000	0.000	(IN.)
TIP T/C	0.120	0.100	0.000	0.000	
TAPER RATIO	0.990	0.350	0.000	0.000	
MEAN AERO CHORD....	6.562	3.708	0.000	0.000	(FT.)
LE ROOT AT.....	7.486	24.020	0.000	0.000	(FT.)
C/4 ROOT AT.....	9.134	25.295	0.000	0.000	(FT.)

TE ROOT AT..... 14.081 29.119 0.000 0.000 (FT.)
LE M.A.C. AT..... 11.985 25.377 0.000 0.000 (FT.)
C/4 M.A.C. AT..... 13.626 26.304 0.000 0.000 (FT.)
TE M.A.C. AT..... 18.547 29.085 0.000 0.000 (FT.)
Y M.A.C. AT..... 7.779 2.341 0.000 0.000
LE TIP AT..... 16.500 27.253 0.000 0.000 (FT.)
C/4 TIP AT..... 18.132 27.700 0.000 0.000 (FT.)
TE TIP AT..... 23.029 29.038 0.000 0.000 (FT.)
ELEVATION..... -1.262 -1.062 0.000 0.000 (FT.)

GEOMETRIC TOTAL VOLUME COEFF 0.410 0.000 0.000
REQUESTED TOTAL VOLUME COEFF 0.410 0.000 0.000
ACTUAL TOTAL VOLUME COEFF 0.410 0.000 0.000

E X T E N S I O N S

	Strake	Rear Extension
Centroid location at.....	0.00	0.00
Area.....	0.00	0.00
Sweep Angle.....	0.00	0.00
Wetted Area.....	0.00	0.00
Volume.....	0.00	0.00

Total Wing Area..... 204.53
Total Wetted Area..... 847.36

F U E L T A N K S

Tank	Volume	Weight	Density
Wing	62.	2685.	43.00
Fus#1	0.	0.	43.00
Fus#2	0.	0.	50.00
Total		2685.	

Mission Fuel Required = 1323. lbs.
Extra Fuel Carrying Capability = 1362. lbs.
Available Fuel Volume in Wing = 62. cu.ft.

Aircraft Weight = 11133.500 lbs.
Aircraft Volume = 345.190 cu.ft.
Aircraft Density = 32.253 lbs./cu.ft.
Actual - Required Fuel Volume = 31.665 cu.ft.

ICASE = 8 (Fineness Ratio Method)

Output for Module # 2 –> TRAJECTORY
****

Trajectory Output

Mission 1 (PAYLOAD = 1019. LB)

PHASE	M	H	CL	ALPHA	WFUEL	TIME	VEL
	SFC(I)	THRUST(I)	CD	GAMMA	W	WA	Q
	SFC(U)	THRUST(U)	CDINST	L/D	THR/THA	PR	X
WARM-UP		0.			15.6	5.00	
	0.13	1443.					
TAKEOFF	0.14	0.	2.0812	21.76	13.6	1.00	153.
	-0.02	-53631.	0.4949	90.00	11117.9	0.00	28.
	-0.02	-53631.	0.0000	4.21	0.45	1.00	1350.
2ND SEG	0.14	400.	2.0812	21.76			153.
	-0.02	0.	0.4949	14.76	11117.9	0.00	28.
	-0.02	-53631.	0.0000	4.21	0.45	1.00	
CLIMB	0.00	0.	0.0000	0.00	0.0	0.00	0.

0.00 0. 0.0000 0.00 0.0 0.00 0.
Cycle 0.00 0. 0.0000 0.00nan 0.00 0.

LANDING 0.00 0. 0.0000 0.00 0.
0.00 0. 0.0000 0.00 0.0 0.00 0.
0.00 0. 0.0000 0.00 0.00 1.00 0.

Fuel Summary

Total Fuel = 1323. Takeoff Fuel: Fuel Load:
Mission Fuel = 0. Warmup = 16. External = 0.
Reserve Fuel = 0. Takeoff = 14. Internal = 1323.
Trapped Fuel = 50.

Block Time = 0.100 hrs
Block Range = 0.0 n.m.
Block Fuel = 0.0 lb.

FAR Takeoff Field Length = 1350. ft Factor = 1.00
Landing Field Length (total run) = 0. ft Decel @ .250 Gs
Landing Field Length (ground run) = 0. ft Field Length Factor = 0.600
Weight for Landing calculation = 0. lbs
Landing Thrust to Weight ratio = 0.000
Takeoff Weight = 11134. lbs
Landing Weight = 11104. lbs

Output for Module # 3 –> AERODYNAMICS
****

Mach = 0.17 C.G. Location = 14.1 ft, 0.32 cbar Q = 42.8 Cj = 0.00 per engine
Altitude = 0. Takeoff Configuration: Flaps and Slats Thrust = 0. per engine

Parasite Drag Induced Drag

Friction	.0142	Alpha	Cl	Cd	L/D	PF	e	Zone	Cm	Cdtrim	Deltrim	StMrg
Body	.0055	-6.0	0.324	0.0187	17.4	9.9	2.22	2	0.000	-.0067	8.1	0.055
Wing	.0072	-2.9	0.570	0.0390	14.6	11.0	0.93	2	0.000	-.0084	7.3	0.048
Strakes	.0000	-0.8	0.745	0.0687	10.8	9.4	0.70	2	0.000	-.0093	6.7	0.049
H. Tail	.0015	1.2	0.887	0.0986	9.0	8.5	0.63	2	0.000	-.0095	6.0	0.058
V. Tail	.0000	3.3	1.025	0.1301	7.9	8.0	0.61	2	0.000	-.0093	5.3	0.069
Canard	.0000	5.4	1.158	0.1651	7.0	7.6	0.60	2	0.000	-.0086	4.4	0.081
Interference	.0020	7.5	1.288	0.2011	6.4	7.3	0.60	2	0.000	-.0076	3.6	0.093
Base	.0000	9.6	1.414	0.2379	5.9	7.1	0.60	2	0.000	-.0063	2.8	0.107
Wing-Body	.0009	11.7	1.537	0.2753	5.6	6.9	0.61	2	0.000	-.0049	2.0	0.121
Wing-Nacelle	.0000	14.9	1.718	0.3355	5.1	6.7	0.62	2	0.000	-.0022	0.9	0.141
Excressence	.0011											
Wave	.0000											
External	.0000											
Tanks	.0000											
Bombs	.0000											
Stores	.0000											
Extra	.0000											
Camber	.0007											
_____												
Cdmin	.0170											

Slope Factors
Cl/Alpha (per radian) 3.8327
Cdl/Cl^2 0.1083
Alpha Transition Zone 2-3 46.935
Flap Setting 30.
Slat Setting 0.
Flap Type Single 26. sq. ft

Mach = 0.17 C.G. Location = 14.1 ft, 0.32 cbar Q = 42.8 Cj = 0.00 per engine
Altitude = 0. Landing Configuration: Flaps and Slats Thrust = 0. per engine

Parasite Drag Induced Drag

Friction	.0142	Alpha	Cl	Cd	L/D	PF	e	Zone	Cm	Cdtrim	Deltrim	StMrg
Body	.0055	-5.8	0.589	0.0234	25.1	19.3	2.92	2	0.000	-.0078	6.9	0.050
Wing	.0072	-2.7	0.833	0.0777	10.7	9.8	0.75	2	0.000	-.0089	6.1	0.045
Strakes	.0000	-0.7	1.004	0.1239	8.1	8.1	0.62	2	0.000	-.0097	5.7	0.042
H. Tail	.0015	1.3	1.130	0.1679	6.7	7.2	0.56	2	0.000	-.0100	5.4	0.047
V. Tail	.0000	3.4	1.254	0.2135	5.9	6.6	0.53	2	0.000	-.0096	4.7	0.059
Canard	.0000	5.5	1.375	0.2620	5.2	6.2	0.51	2	0.000	-.0084	3.8	0.071
Interference	.0020	7.6	1.492	0.3109	4.8	5.9	0.50	2	0.000	-.0069	2.9	0.085
Base	.0000	9.7	1.606	0.3600	4.5	5.7	0.50	2	0.000	-.0052	2.0	0.099
Wing-Body	.0009	11.8	1.719	0.4091	4.2	5.5	0.50	2	0.000	-.0033	1.2	0.115
Wing-Nacelle	.0000	15.0	1.885	0.4823	3.9	5.4	0.51	2	0.000	-.0005	0.2	0.137
Excressence	.0011											
Wave	.0000											
External	.0000											
Tanks	.0000											
Bombs	.0000											
Stores	.0000											
Extra	.0000											
Camber	.0007											
_____												
Cdmin	.0170											

Slope Factors
Cl/Alpha (per radian) 3.5792
Cdl/Cl^2 0.1314
Alpha Transition Zone 2-3 46.935
Flap Setting 45.
Slat Setting 0.
Flap Type Single 26. sq. ft

Detailed Aerodynamics Output

Mach = 0.47 C.G. Location = 14.1 ft, 0.32 cbar
Altitude = 0. Reynolds Number per foot = 3.336x10^6

Parasite Drag		Induced Drag									
Friction	.0139	Alpha	Cl	Cd	L/D	PF	e	Zone	Cm	Cdtrim	Deltrim StMrg
Body	.0054	-6.2	-.361	0.0378	-9.6	5.7	0.39	2	0.000	0.0024	9.0 0.090
Wing	.0070	-3.1	-.114	0.0227	-5.0	nan	0.11	2	0.000	-.0003	8.0 0.091
Strakes	.0000	-1.0	0.061	0.0186	3.3	0.8	0.07	2	0.000	-.0019	7.3 0.093
H. Tail	.0015	1.1	0.238	0.0198	12.0	5.9	0.81	2	0.000	-.0031	6.5 0.101
V. Tail	.0000	3.2	0.407	0.0266	15.3	9.8	0.97	2	0.000	-.0039	5.6 0.110
Canard	.0000	5.3	0.571	0.0381	15.0	11.3	0.95	2	0.000	-.0043	4.8 0.119
Interference	.0020	7.4	0.729	0.0530	13.8	11.8	0.94	2	0.000	-.0042	3.9 0.129
Base	.0000	9.6	0.883	0.0729	12.1	11.4	0.90	2	0.000	-.0038	3.0 0.139
Wing-Body	.0009	11.7	1.032	0.0971	10.6	10.8	0.87	2	0.000	-.0029	2.1 0.149
Wing-Nacelle	.0000	14.9	1.250	0.1409	8.9	9.9	0.83	2	0.000	-.0008	0.5 0.163
Excressence	.0011										
Wave	.0000										
External	.0000										
Tanks	.0000										
Bombs	.0000										
Stores	.0000										
Extra	.0000										
Camber	.0008										
Cdmin	.0167										

Slope Factors
Cl/Alpha (per radian) 4.3697
Cdl/Cl^2 0.0806
Alpha Transition Zone 2-3 16.064
Programmed Flap Setting 0.
Flap Type Single 26. sq. ft

Mach = 0.30 C.G. Location = 14.1 ft, 0.32 cbar
Altitude = 5000. Reynolds Number per foot = 1.853x10^6

Parasite Drag		Induced Drag									
Friction	.0141	Alpha	Cl	Cd	L/D	PF	e	Zone	Cm	Cdtrim	Deltrim StMrg
Body	.0055	-6.2	-.347	0.0369	-9.4	5.5	0.37	2	0.000	0.0021	8.5 0.079
Wing	.0071	-3.1	-.109	0.0227	-4.8	nan	0.11	2	0.000	-.0003	7.7 0.080
Strakes	.0000	-1.0	0.059	0.0187	3.2	0.8	0.07	2	0.000	-.0018	7.2 0.082
H. Tail	.0015	1.1	0.229	0.0197	11.6	5.6	0.81	2	0.000	-.0030	6.5 0.090
V. Tail	.0000	3.2	0.392	0.0259	15.2	9.5	0.98	2	0.000	-.0039	5.8 0.099
Canard	.0000	5.3	0.549	0.0364	15.1	11.2	0.96	2	0.000	-.0044	5.1 0.109
Interference	.0020	7.4	0.702	0.0500	14.0	11.8	0.95	2	0.000	-.0045	4.4 0.119
Base	.0000	9.5	0.850	0.0685	12.4	11.4	0.91	2	0.000	-.0043	3.6 0.129
Wing-Body	.0009	11.6	0.994	0.0909	10.9	10.9	0.88	2	0.000	-.0037	2.7 0.140
Wing-Nacelle	.0000	14.8	1.204	0.1318	9.1	10.0	0.83	2	0.000	-.0021	1.4 0.154
Excressence	.0011										
Wave	.0000										
External	.0000										
Tanks	.0000										
Bombs	.0000										
Stores	.0000										
Extra	.0000										
Camber	.0008										
Cdmin	.0169										

Slope Factors
Cl/Alpha (per radian) 4.2381
Cdl/Cl^2 0.0803
Alpha Transition Zone 2-3 26.129
Programmed Flap Setting 0.
Flap Type Single 26. sq. ft

Detailed Aerodynamics Output

Mach = 0.40 C.G. Location = 14.1 ft, 0.32 cbar
Altitude = 10000. Reynolds Number per foot = 2.140x10^6

Parasite Drag		Induced Drag										
Friction	.0140	Alpha	Cl	Cd	L/D	PF	e	Zone	Cm	Cdtrim	Deltrim	StMrg
Body	.0055	-6.2	-.353	0.0373	-9.5	5.6	0.38	2	0.000	0.0023	8.7	0.086
Wing	.0071	-3.1	-.111	0.0227	-4.9	nan	0.11	2	0.000	-.0003	7.9	0.087
Strakes	.0000	-1.0	0.061	0.0187	3.3	0.8	0.07	2	0.000	-.0019	7.3	0.089
H. Tail	.0015	1.1	0.234	0.0198	11.9	5.7	0.81	2	0.000	-.0031	6.5	0.097
V. Tail	.0000	3.2	0.401	0.0263	15.2	9.6	0.97	2	0.000	-.0039	5.7	0.106
Canard	.0000	5.3	0.561	0.0374	15.0	11.3	0.95	2	0.000	-.0043	4.9	0.115
Interference	.0020	7.4	0.717	0.0516	13.9	11.8	0.95	2	0.000	-.0044	4.1	0.125
Base	.0000	9.5	0.868	0.0709	12.2	11.4	0.91	2	0.000	-.0040	3.3	0.135
Wing-Body	.0009	11.7	1.014	0.0942	10.8	10.8	0.87	2	0.000	-.0032	2.3	0.145
Wing-Nacelle	.0000	14.9	1.228	0.1366	9.0	10.0	0.83	2	0.000	-.0013	0.9	0.160
Excressence	.0011											
Wave	.0000											
External	.0000											
Tanks	.0000											
Bombs	.0000											
Stores	.0000											
Extra	.0000											
Camber	.0008											
Cdmin	.0168											

Slope Factors
Cl/Alpha (per radian) 4.3021
Cdl/Cl^2 0.0805
Alpha Transition Zone 2-3 19.206
Programmed Flap Setting 0.
Flap Type Single 26. sq. ft

Mach = 0.40 C.G. Location = 14.1 ft, 0.32 cbar
Altitude = 20000. Reynolds Number per foot = 1.581x10^6

Parasite Drag		Induced Drag										
Friction	.0140	Alpha	Cl	Cd	L/D	PF	e	Zone	Cm	Cdtrim	Deltrim	StMrg
Body	.0055	-6.2	-.355	0.0374	-9.5	5.7	0.38	2	0.000	0.0023	8.7	0.086
Wing	.0071	-3.1	-.112	0.0227	-4.9	nan	0.11	2	0.000	-.0003	7.9	0.087
Strakes	.0000	-1.0	0.060	0.0186	3.2	0.8	0.07	2	0.000	-.0019	7.3	0.089
H. Tail	.0015	1.1	0.233	0.0197	11.8	5.7	0.81	2	0.000	-.0031	6.5	0.097
V. Tail	.0000	3.2	0.400	0.0262	15.2	9.6	0.97	2	0.000	-.0039	5.7	0.106
Canard	.0000	5.3	0.560	0.0373	15.0	11.3	0.95	2	0.000	-.0043	4.9	0.115
Interference	.0020	7.4	0.716	0.0515	13.9	11.8	0.95	2	0.000	-.0044	4.1	0.125
Base	.0000	9.5	0.866	0.0707	12.3	11.4	0.91	2	0.000	-.0040	3.3	0.135
Wing-Body	.0009	11.7	1.013	0.0940	10.8	10.9	0.87	2	0.000	-.0032	2.3	0.145
Wing-Nacelle	.0000	14.9	1.226	0.1362	9.0	10.0	0.83	2	0.000	-.0014	0.9	0.160
Excressence	.0011											
Wave	.0000											
External	.0000											
Tanks	.0000											
Bombs	.0000											
Stores	.0000											
Extra	.0000											
Camber	.0008											
Cdmin	.0168											

Slope Factors
Cl/Alpha (per radian) 4.3021
Cdl/Cl^2 0.0804
Alpha Transition Zone 2-3 19.213
Programmed Flap Setting 0.
Flap Type Single 26. sq. ft

Detailed Aerodynamics Output

Mach = 0.40 C.G. Location = 14.1 ft, 0.32 cbar
Altitude = 25000. Reynolds Number per foot = 1.347x10^6

Parasite Drag Induced Drag

Friction	.0140	Alpha	Cl	Cd	L/D	PF	e	Zone	Cm	Cdtrim	Deltrim	StMrg
Body	.0055	-6.2	-.354	0.0374	-9.5	5.6	0.38	2	0.000	0.0023	8.7	0.086
Wing	.0071	-3.1	-.112	0.0227	-4.9	nan	0.11	2	0.000	-.0003	7.9	0.087
Strakes	.0000	-1.0	0.061	0.0187	3.2	0.8	0.07	2	0.000	-.0019	7.3	0.089
H. Tail	.0015	1.1	0.234	0.0197	11.8	5.7	0.81	2	0.000	-.0031	6.5	0.097
V. Tail	.0000	3.2	0.400	0.0263	15.2	9.6	0.97	2	0.000	-.0039	5.7	0.106
Canard	.0000	5.3	0.561	0.0373	15.0	11.3	0.95	2	0.000	-.0043	4.9	0.115
Interference	.0020	7.4	0.716	0.0515	13.9	11.8	0.95	2	0.000	-.0044	4.1	0.125
Base	.0000	9.5	0.867	0.0708	12.2	11.4	0.91	2	0.000	-.0040	3.3	0.135
Wing-Body	.0009	11.6	1.014	0.0940	10.8	10.9	0.87	2	0.000	-.0032	2.4	0.145
Wing-Nacelle	.0000	14.9	1.227	0.1363	9.0	10.0	0.83	2	0.000	-.0014	0.9	0.160
Excressence	.0011											
Wave	.0000											
External	.0000											
Tanks	.0000											
Bombs	.0000											
Stores	.0000											
Extra	.0000											
Camber	.0008											
Cdmin	.0168											

Slope Factors
Cl/Alpha (per radian) 4.3026
Cdl/Cl^2 0.0804
Alpha Transition Zone 2-3 19.210
Programmed Flap Setting 0.
Flap Type Single 26. sq. ft

Mach = 0.47 C.G. Location = 14.1 ft, 0.32 cbar
Altitude = 29500. Reynolds Number per foot = 1.363x10^6

Parasite Drag Induced Drag

Friction	.0139	Alpha	Cl	Cd	L/D	PF	e	Zone	Cm	Cdtrim	Deltrim	StMrg
Body	.0054	-6.2	-.361	0.0378	-9.6	5.8	0.39	2	0.000	0.0024	8.9	0.090
Wing	.0070	-3.1	-.114	0.0227	-5.0	nan	0.11	2	0.000	-.0003	8.0	0.091
Strakes	.0000	-1.0	0.061	0.0186	3.3	0.8	0.07	2	0.000	-.0019	7.3	0.093
H. Tail	.0015	1.1	0.238	0.0198	12.0	5.9	0.81	2	0.000	-.0031	6.5	0.101
V. Tail	.0000	3.2	0.408	0.0266	15.3	9.8	0.97	2	0.000	-.0039	5.7	0.110
Canard	.0000	5.3	0.571	0.0381	15.0	11.3	0.95	2	0.000	-.0043	4.8	0.119
Interference	.0020	7.4	0.729	0.0529	13.8	11.8	0.94	2	0.000	-.0043	3.9	0.129
Base	.0000	9.6	0.882	0.0728	12.1	11.4	0.90	2	0.000	-.0038	3.0	0.139
Wing-Body	.0009	11.7	1.031	0.0969	10.6	10.8	0.87	2	0.000	-.0029	2.1	0.149
Wing-Nacelle	.0000	14.9	1.248	0.1404	8.9	9.9	0.83	2	0.000	-.0008	0.5	0.163
Excressence	.0011											
Wave	.0000											
External	.0000											
Tanks	.0000											
Bombs	.0000											
Stores	.0000											
Extra	.0000											
Camber	.0008											
Cdmin	.0167											

Slope Factors
Cl/Alpha (per radian) 4.3657
Cdl/Cl^2 0.0805
Alpha Transition Zone 2-3 16.064
Programmed Flap Setting 0.
Flap Type Single 26. sq. ft

Detailed Aerodynamics Output

Mach = 0.57 C.G. Location = 14.1 ft, 0.32 cbar
Altitude = 29500. Reynolds Number per foot = 1.653x10^6

Parasite Drag		Induced Drag									
Friction	.0138	Alpha	Cl	Cd	L/D	PF	e	Zone	Cm	Cdtrim	Deltrim StMrg
Body	.0054	-6.2	-.369	0.0383	-9.6	5.8	0.39	2	0.000	0.0026	9.4 0.096
Wing	.0069	-3.1	-.113	0.0226	-5.0	nan	0.11	2	0.000	-.0003	8.3 0.097
Strakes	.0000	-0.9	0.069	0.0185	3.7	1.0	0.09	2	0.000	-.0021	7.5 0.098
H. Tail	.0015	1.1	0.252	0.0201	12.5	6.3	0.81	2	0.000	-.0033	6.6 0.106
V. Tail	.0000	3.2	0.427	0.0276	15.5	10.1	0.96	2	0.000	-.0041	5.7 0.114
Canard	.0000	5.4	0.596	0.0401	14.9	11.5	0.94	2	0.000	-.0044	4.7 0.124
Interference	.0020	7.5	0.759	0.0560	13.5	11.8	0.94	2	0.000	-.0042	3.8 0.133
Base	.0000	9.6	0.917	0.0773	11.9	11.4	0.90	2	0.000	-.0036	2.8 0.143
Wing-Body	.0009	11.8	1.070	0.1029	10.4	10.8	0.87	2	0.000	-.0025	1.7 0.153
Wing-Nacelle	.0000	15.1	1.202	0.2273	5.3	5.8	0.46	3	0.000	-.0001	-0.4 0.256
Excressence	.0011										
Wave	.0000										
External	.0000										
Tanks	.0000										
Bombs	.0000										
Stores	.0000										
Extra	.0000										
Camber	.0009										
Cdmin	.0166										

Slope Factors
Cl/Alpha (per radian) 4.2278
Cdl/Cl^2 0.1471
Alpha Transition Zone 2-3 12.804
Programmed Flap Setting 0.
Flap Type Single 26. sq. ft

Mach = 0.45 C.G. Location = 14.1 ft, 0.32 cbar
Altitude = 40000. Reynolds Number per foot = 0.861x10^6

Parasite Drag		Induced Drag									
Friction	.0139	Alpha	Cl	Cd	L/D	PF	e	Zone	Cm	Cdtrim	Deltrim StMrg
Body	.0054	-6.2	-.360	0.0377	-9.5	5.7	0.38	2	0.000	0.0024	8.9 0.089
Wing	.0070	-3.1	-.113	0.0227	-5.0	nan	0.11	2	0.000	-.0003	8.0 0.090
Strakes	.0000	-1.0	0.061	0.0186	3.3	0.8	0.07	2	0.000	-.0019	7.3 0.092
H. Tail	.0015	1.1	0.237	0.0198	12.0	5.8	0.81	2	0.000	-.0031	6.5 0.100
V. Tail	.0000	3.2	0.406	0.0265	15.3	9.7	0.97	2	0.000	-.0039	5.7 0.108
Canard	.0000	5.3	0.569	0.0380	15.0	11.3	0.95	2	0.000	-.0043	4.9 0.118
Interference	.0020	7.4	0.726	0.0526	13.8	11.8	0.94	2	0.000	-.0043	4.0 0.128
Base	.0000	9.5	0.878	0.0722	12.2	11.4	0.91	2	0.000	-.0039	3.1 0.138
Wing-Body	.0009	11.7	1.026	0.0960	10.7	10.8	0.87	2	0.000	-.0030	2.2 0.148
Wing-Nacelle	.0000	14.9	1.241	0.1390	8.9	9.9	0.83	2	0.000	-.0010	0.6 0.162
Excressence	.0011										
Wave	.0000										
External	.0000										
Tanks	.0000										
Bombs	.0000										
Stores	.0000										
Extra	.0000										
Camber	.0008										
Cdmin	.0167										

Slope Factors
Cl/Alpha (per radian) 4.3476
Cdl/Cl^2 0.0804
Alpha Transition Zone 2-3 16.868
Programmed Flap Setting 0.
Flap Type Single 26. sq. ft

Output for Module # 6 –> WEIGHTS
****

Weight Statement - Fighter
P208 WEIGHTS

Qmax: 425.
Design Load Factor: 6.00
Ultimate Load Factor: 9.00
Structure and Material: Alumin um Skin, Stringer
Wing Equation: Fixed or Structural Method
Body Equation: Fixed or Structural Method

Component	Pounds	Kilograms	Percent	Slope	Tech	Fixed
Airframe Structure	3340.1	1515.0	30.00			No
Wing	1455.1	660.0	13.07	1.00	1.00	Yes
Fuselage	1168.4	530.0	10.49	1.00	1.00	Yes
Horizontal Tail (Low)	154.3	70.0	1.39	1.00	1.00	Yes
Vertical Tail	111.3	50.5	1.00	1.00	1.00	No
Nacelles	111.3	50.5	1.00	1.00	1.00	No
Landing Gear	749.6	340.0	6.73	1.00	1.00	Yes
Propulsion	3891.2	1765.0	34.95			Yes
Engines (1)	1224.7	555.5	11.00	1.00	1.00	No
Fuel System	311.7	141.4	2.80	1.00	1.00	No
Fixed Equipment	1153.0	523.0	10.36		1.00	Yes
Hyd & Pneumatic	133.6	60.6	1.20	1.00		No
Electrical	278.3	126.3	2.50	1.00		No
Avionics	445.3	202.0	4.00	1.00		No
Instrumentation	122.5	55.6	1.10	1.00		No
De-ice & Air Cond	111.3	50.5	1.00	1.00		No
Auxiliary Gear	33.4	15.2	0.30			No
Furnish & Eqpt	311.7	141.4	2.80	1.00		No
Flight Controls	334.0	151.5	3.00	1.00		No
Empty Weight	0.0	0.0	0.00			
Operating Items	0.0	0.0	0.00			No
Flight Crew (1)	220.5	100.0	1.98			Yes
Crew Baggage and Provisions	0.0	0.0	0.00			No
Unusable Fuel and Oil	50.0	22.7	0.45			No
Operating Weight Empty	0.0	0.0	0.00			
Fuel	1273.0	577.4	11.43			
Payload	1018.5	462.0	9.15			No
Armament	709.9	322.0	6.38			Yes
Ammunition	308.6	140.0	2.77			Yes
Missiles	0.0	0.0	0.00			No
Bombs	0.0	0.0	0.00			No
External Tanks	0.0	0.0	0.00			No
Adv Weapons 1	0.0	0.0	0.00			No
Adv Weapons 2	0.0	0.0	0.00			No
Calculated Weight	11133.5	5050.2	86.39			Yes
Estimated Weight	11133.5	5050.2				
Percent Error	0.00					

Calculated Weight does not equal 100% because a group weight is being fixed.

Output for Module # 4 –> PROPULSION

****

Propulsion Output: Engine and Propeller

Engine Type:Recipricating Turbocharged to: 42000.0
Sea Level Static HP (each) 2071.0
Max. Shaft Speed (RPM) 2700.00
Multiplier for sfc 1.0000
Spcific D/Q (sq-ft/HP) 1.0000
Weight (lbs) 2278.1

Propeller Type HS Constant Speed
Number of Blades 4.
Diameter (ft) 11.15
Chord (ft) 0.89
Activity Factor 124.50
Integ. Lift Coef. 0.3660
Solidity 0.2030
Tip Speed (ft/sec) 816.72
Power Loading (HP/ft**2) 19.09
Disk Loading (lb/ft**2) 50.79
Torque (ft lbs) 6997.82
Velocity Slipstream (ft/sec) 206.73
Multiplier for thrust 1.0000
Weight Scale Factor 1.0000
Weight (lbs) 284.2

Gear Reduction
Engine/Propeller RPM Ratio 1.9300
Transmission Efficiency 0.9000
Auto. Trans. Shift Alt. 0.
Weight Scale Factor 1.0000
Weight (lbs) 440.1

Propeller Extrap. Errors
2 Advance Ratio 5 Cl integ.
3 Cp 6 Blade Angle

Propulsion System Weight/Engine 3002.4
Engine and Propeller Noise (PNdb) 98.704

Mach Number = 0.17 Altitude = 0. Maximum RPM = 2700.

Percent Power	HP/Eng Loss	Gear	ThrustU	ThrustI	Bsfc	TsfcI Mach	FFLOW Ratio	Tip effU	Advance	Prop	Cp	Ct	Blade Angle	E X
100.0%	2071.0-207.1		3859.	-84803.	0.486	-0.012	1007.5	0.73	0.7322	0.716	0.1975	0.1932	27.50	0
95.0%	1967.4-196.7		3723.	-84939.	0.498	-0.012	979.6	0.73	0.7322	0.727	0.1876	0.1864	26.99	0
90.0%	1863.9-186.4		3576.	-85086.	0.508	-0.011	947.1	0.73	0.7322	0.737	0.1777	0.1790	26.47	0
80.0%	1656.8-165.7		3273.	-85389.	0.528	-0.010	874.2	0.73	0.7322	0.759	0.1580	0.1639	25.38	0
70.0%	1449.7-145.0		2950.	-85712.	0.551	-0.009	798.6	0.73	0.7322	0.782	0.1382	0.1477	24.24	0
60.0%	1242.6-124.3		2598.	-86064.	0.583	-0.008	725.0	0.73	0.7322	0.804	0.1185	0.1301	23.00	0
50.0%	1035.5-103.6		2216.	-86446.	0.631	-0.008	653.5	0.73	0.7322	0.822	0.0987	0.1110	21.73	0

Mach Number = 0.47 Altitude = 0. Maximum RPM = 2700.

Percent Power	HP/Eng Loss	Gear	ThrustU	ThrustI	Bsfc	TsfcI Mach	FFLOW Ratio	Tip effU	Advance	Prop	Cp	Ct	Blade Angle	E X
100.0%	2071.0-207.1		1762.	-675932.	0.486	-0.001	1007.5	0.73	2.0243	0.904	0.1975	0.0882	41.90	3
95.0%	1967.4-196.7		1672.	-676022.	0.498	-0.001	979.6	0.73	2.0243	0.903	0.1876	0.0837	41.70	3
90.0%	1863.9-186.4		1583.	-676111.	0.508	-0.001	947.1	0.73	2.0243	0.903	0.1777	0.0793	41.49	3
80.0%	1656.8-165.7		1400.	-676294.	0.528	-0.001	874.2	0.73	2.0243	0.898	0.1580	0.0701	41.08	3
70.0%	1449.7-145.0		1206.	-676488.	0.551	-0.001	798.6	0.73	2.0243	0.884	0.1382	0.0604	40.65	3
60.0%	1242.6-124.3		1017.	-676678.	0.583	-0.001	725.0	0.73	2.0243	0.869	0.1185	0.0509	40.21	3
50.0%	1035.5-103.6		792.	-676902.	0.631	-0.001	653.5	0.73	2.0243	0.813	0.0987	0.0397	39.79	3

Mach Number = 0.47 Altitude = 29500. Maximum RPM = 2700.

Percent Power	HP/Eng Loss	Gear	ThrustU	ThrustI	Bsfc	TsfcI Mach	FFLOW Ratio	Tip effU	Advance	Prop	Cp	Ct	Blade Angle	E X

Power	Loss						Mach	Ratio	effU			Angle	X	
100.0%	2071.0	-207.1	1763.	-204498.	0.486	-0.005	1007.5	0.82	1.8077	0.808	0.5174	0.2313	46.72	0
95.0%	1967.4	-196.7	1693.	-204569.	0.498	-0.005	979.6	0.82	1.8077	0.816	0.4915	0.2221	46.17	0
90.0%	1863.9	-186.4	1622.	-204639.	0.508	-0.005	947.1	0.82	1.8077	0.826	0.4657	0.2128	45.62	0
80.0%	1656.8	-165.7	1473.	-204788.	0.528	-0.004	874.2	0.82	1.8077	0.844	0.4139	0.1933	44.48	0
70.0%	1449.7	-145.0	1319.	-204942.	0.551	-0.004	798.6	0.82	1.8077	0.863	0.3622	0.1730	43.31	0
60.0%	1242.6	-124.3	1156.	-205105.	0.583	-0.004	725.0	0.82	1.8077	0.883	0.3104	0.1517	42.13	0
50.0%	1035.5	-103.6	978.	-205283.	0.631	-0.003	653.5	0.82	1.8077	0.896	0.2587	0.1283	40.93	0

Mach Number = 0.57 Altitude = 29500. Maximum RPM = 2700.

Percent Power	HP/Eng Loss		Gear	ThrustU	ThrustI	Bsfc	TsfcI	FFLOW	Tip Mach	Advance Ratio	Prop effU	Cp	Ct	Blade Angle	E X
100.0%	2071.0	-207.1	1549.	-301821.	0.486	-0.003	1007.5	0.82	2.1923	0.861	0.5174	0.2032	49.26	0	
95.0%	1967.4	-196.7	1482.	-301887.	0.498	-0.003	979.6	0.82	2.1923	0.867	0.4915	0.1945	48.82	0	
90.0%	1863.9	-186.4	1416.	-301954.	0.508	-0.003	947.1	0.82	2.1923	0.874	0.4657	0.1858	48.36	0	
80.0%	1656.8	-165.7	1272.	-302098.	0.528	-0.003	874.2	0.82	2.1923	0.884	0.4139	0.1669	47.44	0	
70.0%	1449.7	-145.0	1115.	-302255.	0.551	-0.003	798.6	0.82	2.1923	0.885	0.3622	0.1463	46.49	0	
60.0%	1242.6	-124.3	961.	-302408.	0.583	-0.002	725.0	0.82	2.1923	0.890	0.3104	0.1261	45.59	0	
50.0%	1035.5	-103.6	807.	-302563.	0.631	-0.002	653.5	0.82	2.1923	0.896	0.2587	0.1058	44.69	0	

Mach Number = 0.50 Altitude = 40000. Maximum RPM = 2700.

Percent Power	HP/Eng Loss		Gear	ThrustU	ThrustI	Bsfc	TsfcI	FFLOW	Tip Mach	Advance Ratio	Prop effU	Cp	Ct	Blade Angle	E X
100.0%	2071.0	-207.1	1497.	-140982.	0.486	-0.007	1007.5	0.84	1.8673	0.709	0.7992	0.3034	52.76	0	
95.0%	1967.4	-196.7	1457.	-141023.	0.498	-0.007	979.6	0.84	1.8673	0.726	0.7593	0.2952	51.91	0	
90.0%	1863.9	-186.4	1411.	-141068.	0.508	-0.007	947.1	0.84	1.8673	0.742	0.7193	0.2860	51.09	0	
80.0%	1656.8	-165.7	1308.	-141171.	0.528	-0.006	874.2	0.84	1.8673	0.774	0.6394	0.2651	49.53	0	
70.0%	1449.7	-145.0	1188.	-141291.	0.551	-0.006	798.6	0.84	1.8673	0.803	0.5595	0.2408	47.97	0	
60.0%	1242.6	-124.3	1053.	-141427.	0.583	-0.005	725.0	0.84	1.8673	0.830	0.4795	0.2133	46.35	0	
50.0%	1035.5	-103.6	906.	-141574.	0.631	-0.005	653.5	0.84	1.8673	0.857	0.3996	0.1835	44.64	0	

Propulsion was called 24 times.
Engin routine was called 59 times.

Output for Module # 11 –> SUMMARY OUTPUT
****

SUMMARY --- ACSYNT OUTPUT: p208A

GENERAL		FUSELAGE		WING	HTAIL	VTAIL
WG	11134.	LENGTH	26.4	AREA	204.5	38.4	0.0
W/S	0.0	DIAMETER	4.2	WETTED AREA	386.5	73.1	0.0
T/W	0.00	VOLUME	200.5	SPAN	31.2	11.2	0.0
N(Z) ULT	9.0	WETTED AREA	387.8	L.E. SWEEP	30.0	30.1	90.0
CREW	1.	FINENESS RATIO	6.2	C/4 SWEEP	30.0	23.3	0.0
PASENGERS	0.			ASPECT RATIO	4.75	3.24	0.00
				TAPER RATIO	0.99	0.35	0.00
ENGINE		WEIGHTS		T/C ROOT	0.18	0.10	0.00
				T/C TIP	0.12	0.10	0.00
NUMBER	1.	W	WG	ROOT CHORD	6.6	5.1	0.0
LENGTH	8.4	STRUCT.	3340.	30.0 TIP CHORD	6.5	1.8	0.0
DIAM.	3.2	PROPUL.	3891.	35.0 M.A. CHORD	6.6	3.7	0.0
WEIGHT	3002.4	FIX. EQ.	1153.	10.4 LOC. OF L.E.	7.5	24.0	0.0
TSLS	4959.	FUEL	1323.	11.9			
SFCSLS	0.00	PAYLOAD	1019.	9.1			
ESF	0.000	OPER IT	0.	0.0			

MISSION SUMMARY

PHASE	MACH	ALT	FUEL	TIME	DIST	L/D	THRUST	SFC	Q
TAKEOFF	0.00	0.	29.	6.0	1349.6				
CLIMB	0.00	0.	0.	0.0	0.0	0.00	0.0	0.000	0.0
LANDING				0.0					

Block Time = 0.100 hr
Block Range = 0.0 nm
1 PROGRAM CALLS TO ANALIZ

ICALC	CALLS
1	1
2	1
3	1

Finished at:

Fri Mar 8 15:35:51 PST 2002

Output for Module:

Output for Module # 1 –> GEOMETRY
Output for Module # 2 –> TRAJECTORY
Output for Module # 3 –> AERODYNAMICS
Output for Module # 4 –> PROPULSION
Output for Module # 6 –> WEIGHTS
Output for Module # 11 –> SUMMARY OUTPUT

Warnings and Errors:

INITIAL DISTRIBUTION LIST

1. Defense Technical Information Center
   8725 John J. Kingman Rd., STE 0944
   Ft. Belvoir, VA 22060-6218

2. Dudley Knox Library
   Naval Postgraduate School
   411 Dyer Rd.
   Monterey, CA 93943-5000

3. Dr. Max F. Platzer, AA/PL
   Naval Postgraduate School
   Monterey, CA 93943-5106

4. LT Kurt W. Muller
   7787 C Street
   Chesapeake Beach, MD 20732

5. Dr. Conrad F. Newberry
   AA/Ne
   Naval Postgraduate School
   Monterey, CA 93943-5106

6. Dr. Richard M. Howard
   AA/Ho
   Naval Postgraduate School
   Monterey, CA 93943-5106

7. Dr. Louis V. Schmidt
   AA/Sc
   Naval Postgraduate School
   Monterey, CA 93943-5106

8. Mr. Andrew S. Hahn
   Systems Analysis Branch
   MS 237-11
   NASA Ames Research Center
   Moffett Field, CA 94035-1000

9. Dr. J.A.C. Kentfield
Department of Mechanical Engineering
The University of Calgry
Calgary, Alberta, Canada T2N 1N4

10. Mr. Paul Gelhausen
System Analysis Branch
MS 348
NASA Langley Research Center
Hampton, VA 23681-2199